Electronic Supplementary Material (ESI) for Organic & Biomolecular Chemistry.

Efficient one-step amide formation using amino porphyrins

Supporting Information

Kyle D.W. Vollett [1,2], Hai-Ling Margaret Cheng [1-3 *]

[1] Institute of Biomedical Engineering, University of Toronto, Canada

[2] Translational Biology & Engineering Program, Ted Rogers Centre for Heart Research, Toronto, Canada

[3] The Edward S. Rogers Sr. Department of Electrical & Computer Engineering, University of Toronto, Canada

Corresponding Author: Hai-Ling Margaret Cheng, 661 University Avenue, Room 1433, Toronto, Ontario, Canada M5G 1M1; (tel) 1-416-978-4095; (email) hailing.cheng@utoronto.ca

Table of Contents

EXPERIMENTAL PROCEDURES 6

Materials 6

Characterization of compounds 6

Synthesis of manganese porphyrin [1B] 7

Synthesis of manganese porphyrin isothiocyanate [1B] 8

Synthesis of porphyrin isothiocyanate [2B] 8

Synthesis of MITC conjugated to fatty acids (MITC-FA) 8

Synthesis of porphyrin isothiocyanate conjugated to fatty acids ($TPPS_3$-FA) 9

Synthesis of MITC conjugated to deoxycholic acid [1E] (MITC-Deox) 10

Synthesis of porphyrin isothiocyanate conjugated to deoxycholic acid [2E] ($TPPS_3$-Deox) 14

Synthesis of FITC conjugated to deoxycholic acid [3E] (FITC-Deox) 15

Synthesis of MITC conjugated to 3,5-dihydroxycyclohexanecarboxylic [1F] (MITC-Hex) 16

Synthesis of porphyrin isothiocyanate conjugated to 3,5-dihydroxycyclohexane-carboxylic acid [2F] ($TPPS_3$-Hex). 18

Synthesis of FITC conjugated to 3,5-dihydroxycyclohexanecarboxylic acid [3F] (FITC-Hex) 19

EDC coupling of $MnTPPS_3NH_2$ 19

Synthesis of MITC conjugated to hydroxyl of deoxycholic acid [2G] (MITC-S-Deox) 20

Synthesis of porphyrin isothiocyanate conjugated to hydroxyl of deoxycholic acid [2G] ($TPPS_3$-S-Deox) 21

Synthesis of MITC conjugated to hydroxyl of 3,5-dihydroxycyclohexanecarboxylic [1I] (MITC-S-Hex) 22

Synthesis of porphyrin isothiocyanate conjugated to hydroxyl of 3,5-dihydroxycyclohexanecarboxylic acid [2I] ($TPPS_3$-S-Hex). 24

Synthesis of porphyrin amides from thiocarbamate-linked porphyrins. 25

Preparation of MITC-Deox for in-vivo study 26

In-vivo MRI of mice injected with MITC-Deox 26

REFERENCES 28

SUPPLEMENTARY FIGURES 29

Figure s1a. Manganese Porphyrin Structures pt.1 29

Figure s1b. Manganese Porphyrin Structures pt.2 30

Figure s1c. Porphyrin Structures pt.1 31

Figure s1d. Porphyrin Structures pt.2 32

Figure s1e. Fluoresceine Structures pt.1 33

Figure s2. Reaction of MITC or $TPPS_3$-NCS with deoxycholic acid 33

Figure s3. Reaction of MITC or $TPPS_3$-NCS with 3,5-dihydroxycyclohexanecarboxylic acid 34

Figure s4. Reaction of MITC or $TPPS_3$-NCS with palmitic acid or stearic acid produces amide-linked products MITC-Palm and $TPPS_3$-Palm, or MITC-Stearic and $TPPS_3$Stearic, respectively. 34

Figure s5. Reaction of FITC with deoxycholic acid 35

Figure s6. Reaction of FITC with deoxycholic acid produces amide-linked product FITC-Hex. 35

Figure s7. Formation of MITC or $TPPS_3$-NCS with deoxycholic acid in the absence of base 36

Figure s8. Reaction of MITC or $TPPS_3$-NCS with 3,5-dihydroxycyclohexanecarboxylic acid in the absence of base 37

Figure s9. Thiocarbamate MITC-S-Deox react with deoxycholate acid in the presence of DIPEA to form amide product. 38

Figure s10. Thiocarbamates MITC-S-Deox and $TPPS_3$-S-Deox react with 3,5-dihydroxycyclohexanecarboxylic acid to form amide products. 38

Figure s11. Relaxivity measurements of MITC-Deox contrast agent. 39

Figure s12. MRI of healthy adult mouse injected i.v. with control MnTPPS4 contrast agent. 40

Figure s13. UHPLC-MS spectra of MITC-Fatty acid conjugates (MITC-FA) which includes MITC conjugates of Stearic and Palmitic acid (MITC-Stearic [**1D]** and MITC-Palm[**1C**]) .41

Figure s14. Mass spectrum obtained for MITC-Fatty acid conjugates 42

Figure s15. Fourier transform infrared spectroscopy (FTIR-ATR, Thermo Scientific Nicolet iS50) of MITC-FA. 43

Figure s16. Fourier transform infrared spectroscopy (FTIR-ATR, Thermo Scientific Nicolet iS50) of MITC-FA and $MnTPPS_3NH_2$ precursor. 43

Figure s17. 1H NMR spectrum of MITC-FA 44

Figure s18. 13C NMR spectrum of MITC-FA 45

Figure s19. UHPLC-MS of $TPPS_3$-Fatty acid conjugates (MITC-FA) which includes $TPPS_3$NCS conjugates of Stearic and Palmitic acid ($TPPS_3$-Stearic and $TPPS_3$-Palm) 46

Figure s20. Mass spectrum obtained for $TPPS_3$-FA 47

Figure s21. Fourier transform infrared spectroscopy (FTIR-ATR, Thermo Scientific Nicolet iS50) of $TPPS_3$-FA. 48

Figure s22. ^{1}H NMR spectrum of $TPPS_3$-FA 48

Figure s23. 13CNMR(500 MHz, DMSO-d6) TPPS3-FA 49
Figure s24. UHPLC-MS spectra of MITC-Deox 50
Figure s25. Mass spectrum obtained for MITC-Deox....51
Figure s26. Fourier transform infrared spectroscopy (FTIR-ATR, Thermo Scientific Nicolet iS50) of MITC-Deox. 52
Figure s27. Fourier transform infrared spectroscopy (FTIR-ATR, Thermo Scientific Nicolet iS50) of MITC-Deox and $MnTPPS_3NH_2$ 52
Figure s28. Fourier transform infrared spectroscopy (FTIR-ATR, Thermo Scientific Nicolet iS50) of deoxycholic acid. 53
Figure s29. 1H NMR spectrum of MITC-Deox 53
Figure s30. 13C NMR spectrum of MITC-Deox 54
Figure s31. UHPLC-MS spectra of $TPPS_3$-Deox....55
Figure s32. Mass spectrum obtained for $TPPS_3$-Deox 56
Figure s33. Fourier transform infrared spectroscopy (FTIR-ATR, Thermo Scientific Nicolet iS50) of $TPPS_3$-Deox....57
Figure s34. ^{1}H NMR spectrum of $TPPS_3$-Deox 57
Figure s35. ^{13}C NMR spectrum of $TPPS_3$-Deox 58
Figure s36. ^{1}H NMR spectrum of sodium deoxycholate....59
Figure s37. UHPLC-MS spectra of FITC-Deox....60
Figure s38. Mass spectrum obtained for FITC-Deox....61
Figure s39. ^{1}H NMR spectrum of FITC-Deox 62
Figure s40. UHPLC-MS spectra of MITC-Hex 63
Figure s41. Mass spectrum obtained for MITC-Hex....64
Figure s42. Fourier transform infrared spectroscopy (FTIR-ATR, Thermo Scientific Nicolet iS50) of MITC-Hex. 65
Figure s43. Fourier transform infrared spectroscopy (FTIR-ATR, Thermo Scientific Nicolet iS50) of MITC-Hex and $MnTPPS_3NH_2$ 65
Figure s44. Fourier transform infrared spectroscopy (FTIR-ATR, Thermo Scientific Nicolet iS50) of 3,5-dihydroxycyclohexanecarboxylic acid. 66
Figure s45 ^{1}H NMR spectrum of MITC-Hex....66
Figure s46. ^{13}C NMR spectrum of MITC-Hex....67
Figure s47. UHPLC-MS spectra of $TPPS_3$-Hex....68
Figure s48. Mass spectrum obtained for $TPPS_3$-Hex 69

Figure s49. Fourier transform infrared spectroscopy (FTIR-ATR, Thermo Scientific Nicolet iS50) of $TPPS_3$-Hex.....70

Figure s50. ^{1}H NMR spectrum of $TPPS_3$-Hex 70

Figure s51. ^{13}C NMR spectrum of $TPPS_3$-Hex 71

Figure s52. ^{1}H NMR spectrum of 3,5-dihydroxycyclohexanecarboxylic acid 72

Figure s53. UHPLC-MS spectra of FITC-Deox recorded.....73

Figure s54. Mass spectrum obtained for FITC-Hex 74

Figure s55. ^{1}H NMR spectrum of FITC-Hex 75

Figure s56. UHPLC-MS spectra of MITC-S-Deox.....76

Figure s57. Fourier transform infrared spectroscopy (FTIR-ATR, Thermo Scientific Nicolet iS50) of MITC-S-Deox. 76

Figure s58. Mass spectrum obtained for MITC-S-Deox 77

Figure s59. ^{1}H NMR spectrum of MITC-S-Deox 78

Figure s60. Mass Spectrum obtained for $TPPS_3$-S-Deox 79

Figure s61. Mass Spectrum obtained for $TPPS_3$-S-Deox 80

Figure s62. Fourier transform infrared spectroscopy (FTIR-ATR, Thermo Scientific Nicolet iS50) of $TPPS_3$-S-Deox. 81

Figure s63. ^{1}H NMR spectrum of $TPPS_3$-S-Deox.....81

Figure s64. UHPLC-MS spectra of MITC-S-Hex.....82

Figure s65. Mass Spectrum obtained for MITC-S-Hex 83

Figure s66. Fourier transform infrared spectroscopy (FTIR-ATR, Thermo Scientific Nicolet iS50) of MITC-S-Hex. 84

Figure s67. ^{1}H NMR spectrum of MITC-S-Hex 84

Figure s68. (a) Mass Spectrum obtained for $TPPS_3$-S-Hex 85

Figure s69. Mass Spectrum obtained for $TPPS_3$-S-Hex.....86

Figure s70. Mass Spectrum obtained for carbamate $TPPS_3$-O-Hex.....87

Figure s71. Fourier transform infrared spectroscopy (FTIR-ATR, Thermo Scientific Nicolet iS50) of $TPPS_3$-S-Hex. 88

Figure s72. ^{1}H NMR spectrum of $TPPS_3$-S-Hex.....88

Figure s73. ^{1}H NMR spectrum of crude $TPPS_3$-O-Hex with some $TPPS_3$-S-Hex.....89

Figure s74. a) UHPLC-MS spectra of deoxycholic acid reaction with the Thiocarbamate MITC-S-Deox in the presence of base 90

Figure s75. UHPLC-MS spectra of 3,5-dihydroxycyclohexanecarboxylic acid reaction with the thiocarbamate MITC-S-Hex.....91

Figure s76. UHPLC-MS spectra of reaction between 92
Figure s77. ^{1}H NMR spectrum of crude $TPPS_3$-Hex obtained from reaction of $TPPS_3$-S-Hex 92

EXPERIMENTAL PROCEDURES

Materials

N,N-diisopropylethylamine (DIPEA), manganese chloride ($MnCl_2$), dimethylformamide (DMF), anhydrous DMF, 1,8-diazabicyclo(5.4.0)undec-7-ene (DBU), acetonitrile (ACN), dimethylacetamide (DMAc), anhydrous DMAc, diethyl ether, acetone, ethyl acetate, phosphate-buffered saline (PBS), palmitic acid, 1-ethyl-3-(3-dimethylaminopropyl)carbodiimide hydrochloride (EDC), 4A molecular sieves, 4-dimethylaminopyridine (DMAP), hydroxybenzotriazole (HOBt), ammonium acetate (NH_4OAc), nitric acid 70% (HNO_3), 3,5-dihydroxycyclohexanecarboxylic acid, deoxycholic acid, fluorescein isothiocyanate (FITC), and manganese (Mn) standard for ICP were purchased from Sigma Aldrich (Steinheim, Germany). Pre-treated regenerated cellulose dialysis tubing (MWCO: 1kD and MWCO: 50kD) was purchased from Spectrum Labs (Cincinnati, Ohio, USA). Ion-exchange resin (amberlite IR120, H form) was purchased from ACROS Organics (Geel, Belgium). C-18 silica gel spherical (0.7-0.9 cm^3/g pore volume, Supelco) was purchased from Sigma Aldrich. The porphyrins Mn(III)tetra(4-sulfonatophenyl) porphyrin and ammonium 5-(4-aminophenyl)-10,15,20-(tri-4-sulfonatophenyl)porphyrin [**2B**] was purchased from PorphyChem (Dijon, France). All chemicals were of proper analytical grade and were used without further purification except for anhydrous DMSO and anhydrous DMAc, which were both stored over 4A molecular sieves at least 24 hours before use.

Characterization of compounds

The identity and purity of compounds was determined by ultra-high performance liquid chromatography-mass spectrometry (UHPLC-MS), inductively coupled plasma-optical emission spectroscopy (ICP-OES), infrared spectroscopy (IR), mass spectroscopy (MS), and ^{1}H nuclear

magnetic resonance (NMR). UV-VIS absorption was recorded in plastic cuvettes on Beckman Coulter DU 800 UV-VIS spectrophotometer (Brea, California, USA). UHPLC spectra and MS in ESI MS positive mode were recorded using a Waters ACQUITY H-class UHPLC system with photo diode array (PDA) detector with wavelength scanning between 200 and 600 nm while also fixed scanning at 419, 467, and 490 nm using a gradient from 10 mM NH_4OAc buffer in 10%-100% ACN. A Supelco Supercosil LC-18 column with dimensions 25cm × 4.6 mm and 5-µm beads were used at the University of Toronto Department of Chemistry ANALEST facility. The purity of Mn compounds was determined by Thermo Scientific iCAP Pro ICP-OES (Madison, Wisconsin, USA), measuring absorption at 257.610 nm and 213.856 nm, at the University of Toronto Department of Chemistry ANALEST facility. Mass spectroscopy was performed on samples dissolved in 1 % formic acid with an Agilent 6538 Q-TOF (Santa Clara, California, USA) in ESI MS Negative or Positive modes at the University of Toronto Department of Chemistry AIMS Mass Spectrometry Laboratory. Fourier transform infrared spectroscopy (FTIR-ATR, Thermo Scientific Nicolet iS50, Madison, Wisconsin, USA) was performed on a Bruker US 500 MHz system (Santa Clara, California, USA) at the University of Toronto Department of Chemistry CSICOMP NMR facility.

Synthesis of manganese porphyrin [1B]

The procedure for insertion of manganese (III) into 5-(4-aminophenyl)-10,15,20-(tri-4-sulfonatophenyl)porphyrin [**2B**] and characterization is outlined in our previous publication[1]. In brief 1 g (1.03 Mmol) of ammonium 5-(4-aminophenyl)-10,15,20-(tri-4-sulfonatophenyl)porphyrin [**2B**] ($TPPS_3NH_2$) and 8g (40 Mmol) $MnCl{\cdot}H_2O$ was dissolved in 58 mL of dimethylformamide with stirring. Following this, 6 mL N,N-Diisopropylethylamine (DIPEA) was added to reaction solution before put under reflux at 135 ^oC for 3 hours and then cooled overnight. The resulting manganese (III) 5-(4-aminophenyl)-10,15,20-(tri-4-sulfonatophenyl) chloride porphyrin [**1B**] ($MnTPPS_3NH_2$) product was dried by roto evaporation before being redissolved in water and desalted by retaining porphyrin in C18 column rinsed with 10 column volumes of deionized water. $MnTPPS_3NH_2$ [**1B**] was then eluted with 50 % methanol and dried again by roto evaporation before being redissolved in deionized water and subjected to sodium exchange on an amberlite IR120 resin column. Eluted product was then dried and stored as final sodium $MnTPPS_3NH_2$ [**1B**] product.

Synthesis of manganese porphyrin isothiocyanate [1A] (MITC)

This procedure and product characterization was described in our previous publication[1]. In brief sodium manganese (III) 5-(4-aminophenyl)-10,15,20-(tri-4-sulfonatophenyl) chloride porphyrin [**1B**] ($MnTPPS_3NH_2$) (300 mg, 0.3 mmol) was dissolved in deionized 37 mL of water with stirring. A solution of thiophosgene (276 µL, 3.6 mmol) dissolved in 3.5 mL chloroform was slowly added dropwise to this solution. The reaction proceeded for 5 hours and then washed 6 times with 100 mL of chloroform to remove thiophosgene from aqueous phase which contained product. This aqueous solution was dried by lyophilization and stored as powered sodium Manganese(III) 5-(4-phenylisothiocyanate)-10,15,20-(tri-4-sulfonatophenyl)porphyrin [**1A**] (MITC).

Synthesis of porphyrin isothiocyanate [2B]

Synthesis procedure was identical to above converting the amine of sodium 5-(4-aminophenyl)-10,15,20-(tri-4-sulfonatophenyl) [**2B**] to the isothiocyanate functionalized 5-(4-phenylisothiocyanate)-10,15,20-(tri-4-sulfonatophenyl)porphyrin [**2A**] ($TPPS_3$-NCS).

Synthesis of MITC conjugated to fatty acids (MITC-FA)

The isothiocyanate-functionalized Mn porphyrin 5-(4-phenylisothiocyanate)-10,15,20-(tri-4-sulfonatophenyl)porphyrin – **MITC** – [**1A**] (10.1 mg, 9.47 µmol, 1 eq) was added to a stirring solution of DMSO (0.5 mL) with dissolved fatty acids at 80 ^{o}C (palmitic and stearic acid) (12.1 mg, 47 mmol, 5 eq). DBU (7 mL, 5 eq) was added dropwise to the reaction solution. The reaction process was monitored by thin layer chromatography (TLC Silica Gel 60 416 F254, Millipore, Darmstadt, Germany) using a chloroform:methanol:water ratio of 6:3:1 mobile phase with 1% v/v of 1 N hydrochloric acid. The reaction was stopped at 1 hour and the reaction solution was added dropwise to a stirring solution of diethyl ether with 1% acetic acid (5 mL). The precipitate was dried and redissolved in methanol (1mL) before being reprecipitated in diethyl ether (10 mL). This precipitation procedure was repeated three times before the solid was dissolved in water and run through sodium exchange column. Eluted product was dried overnight in a vacuum oven. The reaction scheme is shown in **Figure s4.** The fatty acid reactant was a blend of palmitic and stearic acid and consequently produced two amide products, MITC-Palm [**1C**] and MITC-Stearic [**1D**], respectively, with a combined product weight of 12.0 mg, 98.3 % yield (estimated using ratio of

palmitic and stearic acid ratios determined by UHPLC). Λ_{max} = 467 mn. UHPLC-MS spectra for MITC-FA is shown in **Figure s13**. For MITC-Palm [**1C**], elution occurred at 2.679 minutes. MS (ESI) m/z calculated for $[M]^+$ $C_{60}H_{59}MnN_5O_{10}S_3$: 1160.28. Found: 1160.64. For MITC-Stearic, elution occurred at 2.901 minutes. MS (ESI) m/z calculated for $[M]^+$ $C_{62}H_{63}MnN_5O_{10}S_3$: 1188.31. Found: 1188.69. The purity of amide fatty acid conjugates was 93.9 % according to the peak area, with estimated fraction of 61 % MITC-Palm and 39 % MITC-Stearic. Mn concentration measured by ICP-OES was 87%. Results from Agilent 6538 Q-TOF system in ESI MS negative mode are shown in **Figure s14** for MITC-Palm, $[M]^-C_{60}H_{57}MnN_5O_{10}S_3^-$: 1159.27. Found: 1159.27. $[M_2 - 6H]^{-2}$ $(C_{60}H_{56}MnN_5O_{10}S_3)_2^{-4}$ 578.63 Found 578.63. MITC-Palm $[M]^-$ $C_{62}H_{62}MnN_5O_{10}S_3^-$: 1187.30. Found: 1187.30. $[M_2 - 6H]^{-2}$ $(C_{62}H_{60}MnN_5O_{10}S_3)_2^{-4}$ 592.6447 Found 592.6464. FTIR spectra for these fatty acid conjugated products are shown in **Figure s15.** Supplementary **Figure s16** highlights the change in spectrum from the unfunctionalized $MnTPPS_3NH_2$ precursor [**1B**], where unique alkane bands are observed at 2922 and 2851 cm^{-1} (C-H stretch), and the characteristic amide II signal [2,3] at 1519 cm^{-1} (N-H in plane bend) that is not found for $MnTPPS_3NH_2$. ^1H NMR and ^{13}C NMR spectrums of MITC-FA acquired on Bruker US 500 MHz system are in **Figure s17** and **Figure s18**. ^{1}HNMR(500 MHz, DMSO-d_6) δ: 10.24 (b, 1H), 8.82 (m, 8H), 7.76 (m, 16-18H), 2.35 (m, 2H), 1.62 (b, 1H), 1.21 (m, 26H), 0.81 (m, 3H). ^{13}CNMR(500 MHz, DMSO-d_6) δ: Not observed (45 C, manganese tri-4-sulfonatophenyl)porphyrin) 36.29, 30.97, 28.72 to 28.67 board unresolved collection of peaks, 28.59, 28.47, 28.38, 28.34, 24.77, 21.79, 13.69 (16 to 18 C, Steric and Palmic acid). Paramagnetic Mn^{3+} broadened and supressed nearby proton and carbon signals.

Synthesis of porphyrin isothiocyanate conjugated to fatty acids ($TPPS_3$-FA)

The unmetalated 5-(4-isocyanatophenyl)-10,15,20-(tri-4-sulfonatophenyl)porphyrin [**2A**] ($TPPS_3$-NCS) (5.0 mg, 5.1 μmol, 1 eq) was used to conjugate to a fatty acid blend containing palmitic acid [**2C**] ($TPPS_3$-Palm) and stearic acid (6.6 mg, 26 mmol, 5 eq) [**2D**] ($TPPS_3$-Stearic), with DBU (3.8 mL, 5 eq) producing products that could be characterized on ^1H NMR to help support the identity of the metalated analogues produced from MITC. Synthesis was nearly identical to that for fatty acid conjugation by MITC. Resulting product was 8.9 mg, 99 % yield (estimated using ratio of palmitic and stearic acid ratios determined by UHPLC). Λ_{max} = 417 mn. UHPLC-MS spectra for $TPPS_3$-Palm and $TPPS_3$-Stearic are shown in **Figure s19**. For $TPPS_3$-Palm, elution occurred at 2.442 minutes. MS (ESI) m/z calculated for $[M]^+$ $C_{60}H_{62}N_5O_{10}S_3$: 1108.37. Found: 1108.75 For

$TPPS_3$-Steric, elution occurred at 2.613 minutes. MS (ESI) m/z calculated for $[M]^+$ $C_{62}H_{66}N_5O_{10}S_3$: 1136.40. Found: 1136.78. The purity of amide fatty acid conjugates was determined to be 93.9 % by peak area, with an estimated fraction of 64 % $TPPS_3$-Palm and 36 % $TPPS_3$-Stearic. Results from Agilent 6538 Q-TOF system in ESI MS negative mode are included in **Figure 20**, with MS (ESI) m/z calculated for $TPPS_3$-Palm MS (ESI) m/z calculated for $[M]^-$ $C_{60}H_{60}N_5O_{10}S_3^-$: 1106.35 Found 1106.35. calculated for $[M]^{-2}$ $C_{60}H_{59}N_5O_{10}S_3^{-2}$: 552.6718 Found 552.6711. Calculated for $TPPS_3$-Stearic $[M]^{-2}$ $C_{62}H_{63}N_5O_{10}S_3^{-2}$: 566.69 Found 566.69. FTIR spectra for $TPPS_3$-Palm is included in **Figure s21**, where unique alkane bands are observed at 2922 and 2852 cm^{-1} (C-H stretch), and the characteristic amide II signal at 1522 cm^{-1} (N-H in plane bend). ^1H NMR and ^{13}C NMR spectrums of $TPPS_3$-FA acquired on a Bruker US 500 MHz system and in included in **Figure s22** and **Figure s23**. ^1H NMR (500 MHz, DMSO-d_6) δ (ppm) 10.34 (s, 1H), 8.85 (m, 8H, β-pyrrole), 8.14 (m , 16H), 2.62 (m, 6H), 1.87 (m 6H), 1.72 (sex, 2H), 1.57 (m, 18H), 1.29 (m, 24H), 0.80 (m, 3H). Downfield signal at 10.34 ppm is consistent with an N-aryl amide in DMSO [4]. ^{13}CNMR(500 MHz, DMSO-d_6) $TPPS_3$-Palm acquired on Bruker US 500 MHz system δ: 161.24 (1 C, DBU), 147.94, 141.26, 133.70, 124.18, 119.63, 117.41, 117.41, (45 C, tri-4-sulfonatophenyl)porphyrin) 53.32, 47.84, 37.68 (4 C, DBU), 36.67, 31.66, 31.27, 29.08 to 28.25 broad unresolved collection of peaks, 25.98, 25.25, 23.40, 22.06, 22.03, 18.94, 13.92 (16 to 18 C, Steric and Palmic acid).

Synthesis of MITC conjugated to deoxycholic acid [1E] (MITC-Deox)

The generalized procedure is as follows: for anhydrous conditions, the reaction was done under dry argon using anhydrous solvents. Solid reagents were dried overnight under vacuum at 100°C before use. The isothiocyanate functionalized Mn porphyrin, MITC [**1A**] (1 eq), was added to a stirring solution of either DMAc or DMSO with dissolved deoxycholic acid (2 eq). DBU, DMAP or DIPEA (5 eq) was added dropwise to the reaction solution. At endpoint, the reaction solution was added dropwise to a stirring solution of diethyl ether with 1% acetic acid (10x reaction volume). The precipitate was dried and redissolved in minimal methanol before being reprecipitated in diethyl ether (10x methanol volume mL). For reactions performed in DMSO, precipitation solution was a 1:1 mix of diethyl ether and acetone. This precipitation procedure was repeated three times before the solid was recovered and dried overnight in a vacuum oven. The reaction scheme is shown in **Figure s2**.

Entry 1a: Following general procedure, MITC (1.2 mg, 1.1 μmol) and deoxycholic acid (0.88 mg, 2.3 μmol) was added to a small glass vial with DMSO (0.1 mL). 0.8 μL DBU was added to reaction with Hamilton syringe and reaction was placed in oil bath for 1 hour at 80 °C. Product was purified with precipitation procedure and dried as a MITC-Deox DBU-**H**$^+$ salt with weight of 1.5 mg, 74% yield.

Entry 2a: Following general procedure, MITC (0.9 mg, 0.8 μmol) and deoxycholic acid (0.66 mg, 1.6 μmol) was added to a small glass vial with stir stick and sealed with septum. Solid reagents were dried overnight under vacuum at 100 °C and flushed with dry argon before DMSO (0.1 mL) was added. Then 0.6 μL DBU was added to reaction with Hamilton syringe and reaction was placed in oil bath for 1 hour at 80 °C. Product was purified with precipitation procedure and dried as a MITC-Deox DBU-H$^+$ salt with weight of 1.0 mg, 65% yield.

Entry 3a: Following general procedure, MITC (1.3 mg, 1.2 μmol) and deoxycholic acid (0.96 mg, 2.4 μmol) was added to a small glass vial with stir stick with DMAc (0.1 mL). Then 0.9 μL DBU was added to reaction with Hamilton syringe and reaction was placed in oil bath for 1 hour at 80 °C. Product was purified with precipitation procedure and dried as a MITC-Deox DBU-H$^+$ salt with weight of 1.3mg, 59% yield.

Entry 4a: Following general procedure, MITC (1.0 mg, 0.94 μmol) and deoxycholic acid (0.74 mg, 1.9 μmol) was added to a small glass vial with stir stick and sealed with septum. Solid reagents were dried overnight under vacuum at 100 °C and flushed with dry argon before DMAc (0.1 mL) was added. Then 0.7 μL DBU was added to reaction with Hamilton syringe and reaction was placed in oil bath for 1 hour at 80 °C. Product was purified with precipitation procedure and dried as a MITC-Deox DBU-H$^+$ salt with weight of 1.4 mg, 82% yield.

Entry 5a: Following general procedure, MITC (1.4 mg, 1.3 μmol) and deoxycholic acid (1.0 mg, 2.6 μmol) was added to a small glass vial with stir stick and DMSO (0.1 mL). Then 0.8 mg DMAP was added to reaction and placed in oil bath for 1 hour at 80 °C. Product was purified with precipitation procedure and dried as a MITC-Deox 4-dimethylamminopyridinium salt with weight of 1.4 mg, 62% yield.

Entry 6a: Following general procedure, MITC (1.3 mg, 1.2 μmol) and deoxycholic acid (0.96 mg, 2.4 μmol) was added to a small glass vial with stir stick and DMSO (0.1 mL). Then 0.7 mg was added to reaction and stirred for 1 hour. Product was purified with precipitation procedure and dried as a MITC-Deox 4-dimethylamminopyridinium salt with weight of 1.4 mg, 67% yield.

Entry 7a: Following general procedure, MITC (1.5 mg, 1.4 μmol) and deoxycholic acid (1.1 mg, 2.8 μmol) was added to a small glass vial with stir stick and DMSO (0.1 mL). Then 0.9 μL 4-dimethylamminopyridinium was added to reaction with Hamilton syringe and reaction was stirred for 1 hour. Product was purified with precipitation procedure and dried as a MITC-Deox 4-dimethylamminopyridinium salt with weight of 1.8 mg, 74% yield.

Entry 8a: Following general procedure, MITC (1.2 mg, 1.1 μmol) and deoxycholic acid (0.88 mg, 2.3 μmol) was added to a small glass vial with DMAc (0.1 mL). Then 1 μL DIPEA was added to reaction with Hamilton syringe and reaction was stirred for 1 hour. Product was purified with precipitation procedure and dried as a MITC-Deox DIPEA salt with weight of 1.3 mg, 66% yield.

Bulk synthesis **entry 10a** was performed by adding MITC [**1A**] (10.0 mg, 9.4 μmol, 1 eq) to a stirring solution of DMSO (0.5 mL) with dissolved deoxycholic acid (7.4 mg, 18.8 mmol, 2 eq). DBU (7 μL, 5 eq) was added dropwise to the stirring reaction solution at room temperature. The reaction process was monitored by thin layer chromatography (TLC Silica Gel 60 416 F254, Millipore, Darmstadt, Germany) using a chloroform:methanol:water ratio of 6:3:1 mobile phase with 1% v/v of 1 N hydrochloric acid. The reaction was stopped at 1 hour and the reaction solution was added dropwise to a stirring solution of diethyl ether with 1% acetic acid (5 mL). The precipitate was dried and redissolved in methanol (1mL) before being reprecipitated in diethyl ether (10 mL). For reactions performed in DMSO, precipitation solution was a 1:1 mix of diethyl ether and acetone. This precipitation procedure was repeated three times before the solid was recovered and dried overnight in a vacuum oven. This solid was dissolved in MilliQ water and sodium exchange was performed following by lyophilization to obtain the sodium MITC-Deox [**1E**] product weight of 13.2 mg, 99.2 % yield. It should be noted that during testing of reaction conditions, deoxycholic acid sometimes precipitated after the addition of base (conditions not included). In these circumstances, reactions took 24 hours for completion or precipitate could be dissolved by briefly heating the reaction to 60 ^{o}C. Λ_{max} = 467 mn. UHPLC-MS spectra for purified MITC-Deox [**1E**] is included in **Figure s24**; MITC-Deox was found to elute at 2.008 minutes with

a MS (ESI) m/z calculated for $[M]^+$ $C_{68}H_{67}MnN_5O_{12}S_3^+$: 1296.3. Found: 1296.5. The purity of MITC-Deox was determined to be 95.0 % according to peak area; Mn concentration measured by ICP-OES was 89.0 %. Results for MITC-Deox from the Agilent 6538 Q-TOF system in ESI MS negative mode are included in **Figure s25.** m/z calculated for $[M - 2H]^-$ $C_{68}H_{67}MnN_5O_{12}S_3^{2-}$: 1296.33. found: 1296.32. Calculated for $[M_2 - 6H]^{4-}$ $(C_{68}H_{64}MnN_5O_{12}S_3^{2-})_2)^{4-}$: 646.66. found: 646.65. Calculated for $[M - 3H]^{3-}$ $C_{68}H_{64}MnN_5O_{12}S_3^{3-}$: 431.1037. found: 431.1031. Calculated for $[M - 3H + formate]^{2-}$ $C_{69}H_{66}MnN_5O_{14}S_3^{2-}$ 669.66 found 669.66. Calculated for $[M_2 - 4H + formate]^{3-}$ $C_{137}H_{131}Mn_2N_{10}O_{26}S_6^{3-}$ 878.21 found 878.21. FTIR spectra for MITC-Deox is shown in **Figure s26.** Supplementary **Figure s27** highlights the change in spectrum from the unfunctionalized $MnTPPS_3NH_2$ [**1B**] precursor, with unique bands for MITC-Deox observed at 2927 and 2863 cm^{-1} (C-H stretch). Additionally, MITC-Deox has another unique signal characteristic of amide II at 1520 cm^{-1} (N-H in plane bend) which is absent from both $MnTPPS_3NH_2$ and deoxycholic acid whose spectrum is provided in supplementary **Figure s28**. The selectivity for MITC reaction with deoxycholic acid was determined by finding the peak area of MITC-Deox at around 2.0 minutes and calculating the total percentage of combined peak areas. These significant peaks included unreacted MITC at around 1.6 minutes and $MnTPPS_3NH_2$ [**1B**] or thiourea dimer at 1.1 minutes. The resulting percentage is expected to be an underestimate, given the proportional reduction in porphyrin absorption caused by ACN concentration[5], which is consistent with our observations. ^{1}H NMR and ^{13}C NMR spectrums of MITC-Deox acquired on Bruker US 500 MHz system are in **Figure s29** and **Figure s30**. ^{1}HNMR(500 MHz, DMSO-d_6) δ: 10.15 (b, 1H), 7.68 (b, 16H), 4.46 (b, 1H), 4.15 (b, 1H), 3.73 (b, 1H), 1.98 (b, 2H), 1.73 (b, 6H), 1.53 (b, 6H), 1.27 (b, 10H), 0.98 (s, 3H), 0.91 (b, 3H), 0.75 (b, 3H), 0.53 (b, 3H). ^{13}CNMR(500 MHz, DMSO-d_6) δ: 122.54 (45 C, manganese tri-4-sulfonatophenyl)porphyrin), 70.25, 69.24, 46.68, 45.44, 45.21, 35.49, 34.86, 34.38, 34.33, 33.01, 32.86, 32.14, 30.63, 29.95, 29.46, 27.82, 26.41, 26.20, 25.34, 22.76, 22.35, 16.38, 11.74 (23 C, deoxycholic acid), 64.16, 14.41 (2 C, Acetate). Paramagnetic Mn^{3+} broadened and supressed nearby proton can carbon signals. We measured MITC-Deox to have a T_1 relaxivity of 14.4 $mM^{-1}s^{-1}$ by potting relaxation rate against concentration in **Figure s11**. T_1 of MITC-Deox solutions was determined using a two-dimensional (2D) inversion-recovery TSE sequence: inversion times (TI) = [25, 50, 75, 100, 200, 250, 500, 750, 1000, 1250, 1500, 1750, 2000, 2500] ms, repetition time (TR) = 3000 ms, echo time (TE) =

18.4 ms, field-of-view (FOV) = 60 mm, slice thickness (SL) = 2 mm, 0.4688 mm × 0.4688 mm in-plane resolution, and number of signal averages (NSA) = 1.

Synthesis of porphyrin isothiocyanate conjugated to deoxycholic acid [2E] ($TPPS_3$-Deox)

Synthesis was nearly identical to that for general synthesis of MITC-Deox. The unmetalated 5-(4-isocyanatophenyl)-10,15,20-(tri-4-sulfonatophenyl)porphyrin [**2A**] ($TPPS_3$-NCS) (1 eq) was used to conjugate to deoxycholic acid (2 eq) [**2E**] ($TPPS_3$-Deox), producing a product that could be characterized on ^{1}H NMR to identify the metalated analogue MITC-Deox [**1E**].

Entry 10a: Following general procedure, $TPPS_3$NCS (4.9 mg, 5.0 μmol, 1 eq) and deoxycholic acid (3.9 mg, 10.2 mmol, 2 eq) was added to a small glass vial with stir stick and DMSO (0.25 mL). Then 3.1 mg DMAP was added to reaction under stirring and removed upon completion. Product was purified with precipitation procedure and dried as a $TPPS_3$-Deox 4-dimethylamminopyridinium salt with weight of 7.8 mg, 97% yield.

Entry 11a: The unmetalated 5-(4-isocyanatophenyl)-10,15,20-(tri-4-sulfonatophenyl)porphyrin [**2A**] ($TPPS_3$-NCS) (10 mg, 5.0 μmol, 1 eq) was used to conjugate to deoxycholic acid (10.0 mg, 10.2 mmol, 2 eq) [**2E**] ($TPPS_3$-Deox) in DMSO with DBU (7.6 mL, 5 equ.) producing a product that could be characterized on ^{1}H NMR to identify the metalated analogue MITC-Deox [**1E**]. After sodium exchange the resulting weight was 13 mg, 98 % yield. Λ_{max} = 417 mn. UHPLC-MS spectra for $TPPS_3$-Deox are included in **Figure s31**; $TPPS_3$-Deox was found to elute at 1.987 minutes with MS (ESI) m/z calculated for $[M + H]^+$ $C_{68}H_{70}N_5O_{12}S_3^+$: 1244.42. Found: 1244.85. The purity of $TPPS_3$-Deox was determined to be 93.9 % according to peak area. Results from the Agilent 6538 Q-TOF system in ESI MS negative mode are shown in **Figure s32**, with m/z calculated for $[M – 2H]^{2-}$ $C_{68}H_{67}N_5O_{12}S_3^{2-}$: 620.6967. found: 620.6980. Calculated for $[M – 3H]^{3-}$ $C_{68}H_{66}N_5O_{12}S_3^{3-}$: 413.46. found: 413.46. FTIR spectra for $TPPS_3$-Deox is included in **Figure s33**, where unique alkane bands are observed at 2924 and 2854 cm^{-1} (C-H stretch), and the characteristic amide II signal at 1523 cm^{-1} (N-H in plane bend). ^{1}H NMR and ^{13}C NMR spectrums of $TPPS_3$-Deox acquired on a Bruker US 500 MHz system and in included in **Figure s34** and **Figure s35**. ^{1}H NMR (500 MHz, DMSO-d_6) δ (ppm) 10.44 (s, 1H), 8.84 (m, 8H, β-pyrrole), 8.21 (m , J= 7.9 Hz, 6H), 8.13 (m, 2H), 8.07 (m 8H), 4.54 (b, 1H), 4.38 (b, 1H), 3.84 (b, 1H), 1.87 (m, 7H), 1.61 (m, 4H),

1.34 (m, 8H), 1.19 (m, 2H) 1.05 (d, 3H), 0.84 (s, 3H), 0.62 (s, 3H), -2.93 (s, 2H). Downfield signal at 10.44 ppm is consistent with an N-aryl amide in DMSO [4]. ^{13}C NMR spectrum of $TPPS_3$-Deox acquired on Bruker US 500 MHz system. ^{13}CNMR(500 MHz, DMSO-d_6) δ: 147.65, 141.52, 134.76, 133.81, 124.30, 119.68, 117.55 (45 C, tri-4-sulfonatophenyl)porphyrin), 71.17, 70.07, 47.59, 46.39, 46.14, 41.70, 40.43, 36.36, 35.77, 35.23, 33.92, 33.04, 31.65, 30.44, 28.71, 26.22, 23.65, 23.19, 17.32, 12.60 (23 C, deoxycholic acid). The ^{1}H NMR spectrum of deoxycholic acid is included in **Figure s36** for reference. The selectivity for $TPPS_3$-NCS [**2A**] reaction with deoxycholic acid was determined by finding the peak area of $TPPS_3$-Deox at around 1.98 minutes and calculating the total percentage of combined peak areas. These significant peaks included unreacted $TPPS_3$-NCS [**2A**] at around 1.8 minutes, and $TPPS_3NH_2$ [**2B**] or thiourea dimer at 1.4 minutes. The resulting percentage is expected to be an underestimate, given the proportional reduction in porphyrin absorption caused by ACN concentration[6] which is consistent with our observations.

Synthesis of FITC conjugated to deoxycholic acid [3E] (FITC-Deox)

Entry 10a: FITC [**3a**] (3.6 mg, 9.4 μmol, 1 eq) was added to a stirring solution of DMSO (0.5 mL) with dissolved deoxycholic acid (7.4 mg, 18.8 mmol, 5 eq). DMAP (5 eq) was added to the reaction solution. The reaction process was monitored by TLC using a chloroform:methanol (10:1) mobile phase. The reaction scheme is shown in **Figure s5**. The UHPLC-MS spectra for FITC-Deox [**3E**] is shown in **Figure s37**; FITC-Deox was found to elute at 2.477 minutes with a MS (ESI) m/z calculated for $[M]^+$ $C_{44}H_{52}NO_8^+$: 722.37. Found: 722.45. A mass spectrum obtained for FITC-Deox with an Agilent 6538 Q-TOF system in ESI MS positive mode is shown in **Figure s38**. MS (ESI) m/z calculated for [M]+ C44H52NO8+: 722.3687. Found: 722.3680. The ^{1}H NMR spectrum of FITC-Deox acquired on Bruker US 500 MHz system is shown in **Figure s39**. ^{1}H NMR (500 MHz, DMSO-d_6) δ (ppm) 10.32 (s, 1H), 7.81 (d, 1H), 7.16 (dd, 1H), 6.59 (m, 6H), 4.47 (s, 1H), 4.22 (d, 1H), 3.81 (m, 1H), 1.80 (m, 6H), 1.63 (m, 6H), 1.38 (m, 10H), 0.98 (d, 3H), 0.84 (s, 3H), 0.62 (s, 3H). The downfield signal at 10.32 ppm is consistent with aryl-N amides in DMSO[4]. The selectivity for FITC reaction with deoxycholic acid was determined by finding the peak area of FITC-Deox at around 1.98 minutes and calculating the total percentage of combined peak areas. These significant peaks included unreacted FITC at around 1.7 minutes and amino-fluorescein [**3B**] at around 1.1 minutes. The resulting percentage is expected to be an underestimate, given the

proportional reduction in fluorescein absorption caused by ACN concentration[5], which is consistent with our observations.

Synthesis of MITC conjugated to 3,5-dihydroxycyclohexanecarboxylic [1F] (MITC-Hex)

The generalized procedure is as follows: The isothiocyanate functionalized Mn porphyrin, MITC [**1A**] (1 eq), was added to a stirring solution of DMSO with dissolved 3,5-dihydroxycyclohexanecarboxylic acid (2 eq). DMAP, DIPEA or DBU (5 eq) was added dropwise to the reaction solution. The reaction was stopped at 1 hour and the reaction solution was added dropwise to a stirring solution of 50:50 diethyl ether and acetone with 1% acetic acid (10x reaction volume). The precipitate was dried and redissolved in minimal methanol before being reprecipitated in 1:1 acetone: diethyl ether. This precipitation procedure was repeated three times before the resulting solid was recovered and dried overnight in a vacuum oven. The reaction scheme is shown in **Figure s6**.

Entry 1b: Following general procedure, MITC (4.0 mg, 3.8 μmol) and 3,5-dihydroxycyclohexanecarboxylic acid (1.2 mg, 7.5 μmol) was added to a small glass vial with stir stick and DMSO (0.2 mL). Then 2.3 mg DMAP was added to reaction with Hamilton syringe and reaction was stirred for 1 hour. Product was purified with precipitation procedure and dried as a 4-dimethylamminopyridinium MITC-Hex salt with weight of 4.3 mg, 76% yield.

Entry 2b: Following general procedure, MITC (3.8 mg, 3.6 μmol) and 3,5-dihydroxycyclohexanecarboxylic acid (1.1 mg, 7.1 μmol) was added to a small glass vial with stir stick and DMSO (0.2 mL). Then 3.1 μL DIPEA was added to reaction with Hamilton syringe and reaction was stirred for 1 hour. Product was purified with precipitation procedure and dried as a MITC-Hex pyridinium salt with weight of 4.7 mg, 87% yield.

Entry 3b: synthesis was performed by adding MITC [**1A**] (10.0 mg, 9.4 μmol, 1 eq) to a stirring solution of DMSO (0.5 mL) with dissolved 3,5-dihydroxycyclohexanecarboxylic acid (3.0 mg, 19 μmol, 2 eq). DBU (7μL, 5 eq) was added dropwise to the reaction solution. The reaction process was monitored by TLC using a chloroform:methanol:water (6:3:1) mobile phase with 1% v/v of 1 N hydrochloric acid. The reaction was stopped at 1 hour and the reaction solution was added dropwise to a stirring solution of 50:50 diethyl ether and acetone with 1% acetic acid (5 mL). The

precipitate was dried and redissolved in methanol (1mL) before being reprecipitated in 1:1 acetone: diethyl ether (10 mL). This precipitation procedure was repeated three times before the resulting solid was recovered and dried overnight in a vacuum oven. The dry solid was redissolved in MilliQ water and underwent sodium exchange before being dried again by lyophilization. The resulting sodium MITC-Hex [**1F**] product weighed 10.9 mg, 97.3% yield. Λ_{max} = 467 mn. UHPLC-MS spectra for MITC-Hex [**1F**] is shown in **Figure s40**; MITC-Hex was found to elute at 1.082 minutes with MS (ESI) m/z calculated for $[M]^+$ $C_{68}H_{67}MnN_5O_{12}S_3^+$: 1064.11. Found: 1064.52. The purity of MITC-Hex was determined to be 94.2 % according to peak area; Mn concentration was measured by ICP-OES to be 88.6%. The results from an Agilent 6538 Q-TOF system in ESI MS negative mode are included in **Figure s41** – m/z calculated for $[M\text{-}1H]^{1-}$ $C_{51}H_{38}MnN_5O_{12}S_3^-$: 1063.11. Found 1063.11. MS (ESI) m/z calculated for $[M_2\text{-}6H]^{4-}$ $((C_{51}H_{36}MnN_5O_{12}S_3)_2)^{4-}$: 530.5457. Found: 530.5451. MS (ESI) m/z calculated for [M - 2H + acetate]$^{2-}$ $(C_{53}H_{40}MnN_5O_{14}S_3)^{2-}$: 560.56. Found: 560.56. The FTIR spectra for MITC-Hex is shown in **Figure s42**. **Figure s43** highlights the change in spectrum from the unfunctionalized $MnTPPS_3NH_2$ [**1B**] precursor, with unique alkane bands observed at 2949 cm^{-1} (C-H stretch) for MITC-Hex. Additionally, MITC-Hex has another unique signal characteristic of amide II at 1517 cm^{-1} (N-H in plane bend), which is absent from both $MnTPPS_3NH_2$ [**1B**] and 3,5-dihydroxycyclohexanecarboxylic acid whose spectrum is shown in **Figure s44.** The selectivity for MITC reaction with 3,5-dihydroxycyclohexanecarboxylic acid was determined by finding the peak area of MITC-Hex at around 1.0 minutes and calculating the total percentage of combined peak areas. These significant peaks included unreacted MITC [**1A**] at around 1.6 minutes, and $MnTPPS_3NH_2$ [**1B**] or thiourea dimer at 1.1 minutes. ^{1}H NMR and ^{13}C NMR spectrums of MITC-Hex acquired on Bruker US 500 MHz system are in **Figure s45** and **Figure s46**. ^{1}HNMR(500 MHz, DMSO-d_6) δ: 10.19 (b, 1H), 7.71 (b, 16H), 4.67 (b, 2H), 1.99 to 1.90 (m, 3H), 1.19 (b, 1H), 1.00 (b, 3H). ^{13}C NMR spectrum of MITC-Hex acquired on Bruker US 500 MHz system. ^{13}CNMR(500 MHz, DMSO-d_6) δ: 122.71 (45 C, manganese tri-4-sulfonatophenyl)porphyrin), 66.03, 44.32, 37.19, 30.16 (6 C, cyclohexanediol), 64.37, 14.62 (2 C, Acetate). Paramagnetic Mn^{3+} broadened and supressed nearby proton and carbon signals.

Synthesis of porphyrin isothiocyanate conjugated to 3,5-dihydroxycyclohexane-carboxylic acid [2F] ($TPPS_3$-Hex).

Synthesis was nearly identical to that for general synthesis of MITC-Hex. The unmetalated 5-(4-isocyanatophenyl)-10,15,20-(tri-4-sulfonatophenyl)porphyrin [**2A**] ($TPPS_3$-NCS) was used to conjugate to 3,5-dihydroxycyclohexanecarboxylic acid to create [**2F**] ($TPPS_3$-Hex), producing a product which could be characterized by ^{1}H NMR to indirectly identify the metalated analogue MITC-Hex [**1F**].

Entry 4b: Following general procedure, $TPPS_3$NCS (4.2 mg, 4.3 μmol, 1 eq) and 3,5-dihydroxycyclohexanecarboxylic acid (1.4 mg, 8.6 μmol, 2 eq) was added to a small glass vial with stir stick and DMSO (0.25 mL). Then 2.6 mg DMAP was added to reaction under stirring and removed upon completion. Product was purified with precipitation procedure and dried as a $TPPS_3$-Hex 4-dimethylamminopyridinium salt with weight of 5.3 mg, 90% yield.

Entry 5b: Following general procedure, $TPPS_3$NCS (10 mg, 10.2 μmol, 1 eq) and 3,5-dihydroxycyclohexanecarboxylic acid (3.3 mg, 20.5 μmol, 2 eq) was added to a small glass vial with stir stick and DMSO (0.5 mL). Then 7.6 μL DBU was added to reaction under stirring and removed after 1 hour. Product was purified with precipitation procedure and underwent sodium exchange before lyophilization to powdered $TPPS_3$-Hex with weight of 10.8 mg, 98% yield. Λ_{max} = 416 mn. UHPLC-MS spectra for $TPPS_3$-Hex [**2F**] is included in **Figure s47**; $TPPS_3$-Hex was found to elute at 1.309 minutes with a MS (ESI) m/z calculated for $[M+H]^+$ $C_{51}H_{42}N_5O_{12}S_3^+$: 1012.20. Found: 1012.60. The purity of $TPPS_3$-Hex was determined to be 95.9 % according to peak area. The results from an Agilent 6538 Q-TOF system in ESI MS negative mode are included in **Figure s48** – m/z calculated for $[M-2H]^{2-}$ $C_{51}H_{39}N_5O_{12}S_3^{2-}$: 504.5884. Found: 504.5873. Calcd for $[M-3H]^{3-}$ $C_{51}H_{38}N_5O_{12}S_3^{3-}$: 336.06. Found: 336.06. Calcd for $[M]^-$ $C_{51}H_{40}N_5O_{12}S_3^-$: 1010.18. Found: 1010.19. The FTIR spectra for $TPPS_3$-Hex is shown in **Figure s49**, where unique amide II signal is observed at 1524 cm^{-1} (N-H in plane bend). ^{1}H NMR and ^{13}C NMR spectrums of $TPPS_3$-Hex acquired on a Bruker US 500 MHz system and in included in **Figure s50** and **Figure s51**. (500 MHz, DMSO-d_6) δ (ppm) 10.52 (s, 1H), 8.86 (m, 8H, β-pyrrole), 8.13 (m, 16H), 4.87 (s, 2H), 3.57 (m 2H), 2.60 (d, 1H), 2.16 (m, 1H), 2.08 (m, 2H), 1.37 (m, 2H), 1.15 (m, 1H). Downfield signal at 10.52 ppm is consistent with an N-aryl amide in DMSO-d_6 [4].The ^{1}H NMR spectrum of 3,5-dihydroxycyclohexanecarboxylic acid is included in **Figure s52** for reference. ^{13}CNMR(500

MHz, DMSO-d_6) δ: 173.73, 147.58, 141.57, 139.57, 135.71, 134.75, 133.83, 124.32, 120.35, 119.69, 117.66 (45 C, tri-4-sulfonatophenyl)porphyrin), 66.75, 40.43, 37.99 (6 C, cyclohexanediol). The selectivity for $TPPS_3$-NCS [**2A**] reaction with 3,5-dihydroxycyclohexanecarboxylic acid was determined by finding the peak area of $TPPS_3$-Hex at around 1.3 minutes and calculating the total percentage of combined peak areas. These significant peaks included unreacted $TPPS_3$-NCS [**2A**] at around 1.8 minutes, and $TPPS_3NH_2$ [**2B**] or thiourea dimer at 1.4 minutes.

Synthesis of FITC conjugated to 3,5-dihydroxycyclohexanecarboxylic acid [3F] (FITC-Hex)

Entry 4b: FITC [**3A**] (3.6 mg, 9.4 μmol, 1 eq) was added to a stirring solution of DMSO (0.5 mL) with dissolved 3,5-dihydroxycyclohexanecarboxylic acid (3.0 mg, 18.8 μmol, 2 eq). DMAP (5 eq) was added dropwise to the reaction solution. The reaction process was monitored by TLC using a chloroform:methanol (10:1) mobile phase. The reaction scheme is shown in **Figure s6**. UHPLC-MS spectra for FITC-Deox [**3F**] is shown in **Figure s53**; FITC-Deox was found to elute at 0.990 minutes with a MS (ESI) m/z calculated for $[M]^+$ $C_{27}H_{24}NO_8^+$: 490.15. Found: 490.25. Mass spectrum obtained for FITC-Hex is shown in **Figure s54**. MS (ESI) m/z calculated for [M]+ C44H52NO8+: 490.1496. Found: 490.1488. The ^{1}H NMR spectrum of FITC-Hex is shown in **Figure s55**: (500 MHz, DMSO-d_6) δ (ppm) 10.32 (s, 1H), 8.13 (d, 1H), 7.8 (dd, 1H), 6.96 (d, 1H), 6.62 (dd, 2H), 6.12 (m, 4H), 4.72 (b, 1H), 4.50 (b, 2H), 2.36 (m, 1H), 2.06 (m, 1H), 1.98 (m, 2H), 1.26 (m, 2H), 1.15ff (m, 1H). Large downfield signal at 10.32 ppm is consistent with an N-aryl amide in DMSO-d_6 [4]. The selectivity for FITC reaction with 3,5-dihydroxycyclohexanecarboxylic acid was determined by finding the peak area of FITC-Hex at around 1.0 minutes and calculating the total percentage of combined peak areas. These significant peaks included unreacted FITC at around 1.7 minutes and amino-fluorescein at around 1.1 minutes.

EDC coupling of $MnTPPS_3NH_2$ [1B]

To a flask was added the amine functionalized porphyrin 5-(4-phenylamino)-10,15,20-(tri-4-sulfonatophenyl)porphyrin [**1B**] ($MnTPPS_3NH_2$) (10 mg, 9.8 μmol, 1.0 eq), along with deoxycholic acid (7.7 mg, 19.6 μmol, 2 eq) or 3,5-dihydroxycyclohexanecarboxylatic acid (3.1 mg, 19.6 μmol, 2 eq), EDCl (3.8 mg, 19.6 μmol, 2.0 eq), HOBt (0.5 mg, 3.92 μmol, 0.2 eq), DMAP

(2.4 mg, 19.6 μmol, 2.0 eq). The flask was sealed and evacuated with vacuum before being filled with argon before the addition of DMAc (0.5 mL). Solution was then stirred vigorously as DIPEA (19 μmol, 5.0 eq) was added dropwise at either 23°C or 60°C. The reaction process was monitored by TLC using a chloroform:methanol:water (6:3:1) mobile phase with 1% v/v of 1 N hydrochloric acid. At 6, 24, or 48 hours, a fraction of reaction solution was added dropwise to a stirring solution of diethyl ether with 1% acetic acid (10 mL). The precipitate was dried and redissolved in methanol (1mL) before being reprecipitated to diethyl ether (10 mL). This precipitation procedure was repeated three times before being dried overnight in a vacuum oven. Samples were tested on UHPLC-MS to determine % conversion for tables. Conversion of $MnTPPS_3NH_2$ to an amide product was determined by finding the peak areas associated with the amide products of either deoxycholic acid [**1E**] (MITC-Deox) (2.0 minutes) or 3,5-dihydroxycyclohexanecarboxylatic acid [**1F**] (MITC-Hex) (1.0 minute) and finding its percentage compared to $MnTPPS_3NH_2$ [**1B**] (1.1 minutes).

Synthesis of MITC conjugated to hydroxyl of deoxycholic acid [1G] (MITC-S-Deox)

Entry 1e: The isothiocyanate functionalized Mn porphyrin, MITC [**1A**] (10.0 mg, 9.4 μmol, 1 eq), was added to deoxycholic acid (19 mg, 48 mmol, 5 eq) in a flask with stir-bar and sealed with septum. A needle was placed into septum and the reaction flask was dried under vacuum overnight at 80°C. The next morning, the flask was purged with dry argon before 0.5 mL of anhydrous DMSO was added to the stirring reaction flask submerged in an oil bath at 60°C. The reaction process was monitored by thin layer chromatography (TLC Silica Gel 60 416 F254, Millipore, Darmstadt, Germany) using a chloroform:methanol:water ratio of 6:3:1 mobile phase with 1% v/v of 1 N hydrochloric acid. Reaction was tested at 6, 24, 48, and 72 hours to characterize reaction progression. The reaction scheme is shown in **Figure s7.** Upon completion, 40 μL of reaction solution was set aside for use in entry 1g and the rest was added dropwise to a stirring solution solution of 1:1 diethyl ether and acetone. Precipitate was re-dissolved in methanol before precipitation procedure was repeated. This precipitation procedure was repeated 2 times before the solid was recovered and dried overnight in a vacuum oven. The MITC-S-Deox [**1G**] (48 hrs) product was weighed to be 11.0 mg, 79.7 % yield. This fraction was assessed by UHPLC for conversion, with product eluting at 2.117 minutes. For characterization, the remaining products were consolidated and purified further by flash chromatography on a BUCHI C-810

(Flawil,Liechtenstein) with C18 column using a continuous ramping protocol with a mobile phase gradient ranging from 10% ACN in 25 mM NH_4OAc buffer to 100% ACN. Elution of product was monitored by UV-Vis absorption at λ = 467 nm. Product was frozen immediately and lyophilized overnight on Labconco Freezone (Labconco, Kansas City, USA). This purified MITC-S-Deox was assessed by UHPLC and shown in **Figure s56**; MITC-S-Deox was found to elute at 2.471 minutes with a MS (ESI) m/z calcd for [M]+ $C_{69}H_{67}MnN_5O_{13}S_4^+$: 1356.30. Found: 1356.87. Trace signal for carbamate product MITC-O-Deox [**1H**] was found earlier at around 2.0 minutes with MS (ESI) m/z calcd for $[M]^+$ $C_{69}H_{67}MnN_5O_{14}S_3^+$: 1340.32. Found: 1340.70. UV-Vis found unique peak at 284.6 nm likely associated with n-π* transitions of aryl-NH thiocarbamate [7–9]. The FTIR spectra for MITC-S-Deox is shown in **Figure s57**, where thiocarbamate signal is observed at 1519 cm^{-1} (N-H in plane bend)[10]. A unique signal attributed to MITC-S-Deox which is distinct from amide products is observed at 1701 cm^{-1} associated with carboxylate C=O stretching[11]. MITC-S-Deox was also characterized on an Agilent 6538 Q-TOF system in ESI MS negative mode; results are shown in **Figure s58**: where MS (ESI) m/z calculated for $[M2\text{-}6H]^{4-}$ $((C_{69}H_{64}MnN_5O_{13}S_4)_2)^{4-}$: 676.6387 Found: 676.6392. MS (ESI) m/z calculated for $[M2\text{-}8H]^{6-}$ $((C_{69}H_{63}MnN_5O_{13}S_4)_2)^{6-}$: 450.76. Found: 450.76. Carbamate product MITC-O-Deox [**1H**] could be found at MS (ESI) m/z calculated for $[M2\text{-}6H]^{4-}$ $((C69H66MnN5O14S3)2)^{4-}$: 669.66. Found: 669.66. ^1H NMR spectrum of MITC-S-Hex [**1I**] was acquired on Bruker US 500 MHz system is included in **Figure s59**. ^{1}HNMR(500 MHz, DMSO-d_6) δ: 11.28 (b, 1H), 8.85 (b, 8H), 7.76 (b, 16H), 5.34 (b, 1H), 4.24 (b, 1H), 0.90 (b, 3H), 0.94 (b, 3H), 0.59 (b, 3H). Signal associated with N-aryl thiocarbamate at δ (ppm) 11.28 [12,13]. Paramagnetic Mn^{3+} broadened and supressed nearby proton signals.

Synthesis of porphyrin isothiocyanate conjugated to hydroxyl of deoxycholic acid [2G] ($TPPS_3$-S-Deox)

Entry 2e: The unmetalated 5-(4-isocyanatophenyl)-10,15,20-(tri-4-sulfonatophenyl)porphyrin [**2A**] ($TPPS_3$-NCS) (10.2 mg, 10.4 μmol) was used to conjugate to the hydroxyl of deoxycholic acid (20 mg, 51 μmol) [**2G**] ($TPPS_3$-S-Deox), producing a product that could be characterized on ^1H NMR to identify the metalated analogue MITC-S-Deox [**1G**]. Methods of synthesis and characterization were nearly identical to those for MITC-S-Deox. Product was weighed as 11.6 mg, 80.9 % yield. Crude product was assessed for conversion via UHPLC monitoring at 419 nm

eluting at 2.091 minutes. UHPLC-MS spectra for flash purified $TPPS_3$-S-Deox [**2G**] is shown in **Figure s60**; $TPPS_3$-S-Deox was found to elute at 2.284 minutes with a MS (ESI) m/z calculated for $[M+H]^+$ $C_{69}H_{70}N_5O_{13}S_4^+$: 1304.38. Found: 1304.70. Trace signal for minor carbamate product $TPPS_3$-O-Deox [**2H**] was found earlier at around 2.284 minutes MS (ESI) m/z calculated for $[M]^+$ $C_{69}H_{70}MnN_5O_{14}S_3^+$: 1288.41. Found: 1288.8. The results for $TPPS_3$-S-Deox from an Agilent 6538 Q-TOF system in ESI MS negative mode are shown in **Figure s61**: m/z calculated for $[M-2H]^{2-}$ $C_{69}H_{67}N_5O_{13}S_4^{2-}$: 650.6815. Found: 650.6807. Calcd for $[M-3H]^{3-}$ $C_{52}H_{38}N_5O_{13}S_4^{3-}$: 356.05. Found: 356.05. Calcd for $[M]^-$ $C_{52}H_{40}N_5O_{13}S_4^-$: 1070.15. Found: 1070.15. Sample for NMR and IR was dialyzed briefly for 6 hours at 4°C using cellulose dialysis tubing (MWCO: 1kD) to remove remaining NH_4OAc while minimizing product breakdown. The FTIR spectra for $TPPS_3$-S-Deox is shown in **Figure s62**, where thiocarbamate signal is observed at 1520 cm^{-1} (N-H in plane bend)[10]. A unique signal attributed to $TPPS_3$-S-Deox which is distinct from amide products is observed at 1701 cm^{-1} associated with carboxylate C=O stretching[11]. ^1H NMR spectrum of $TPPS_3$-S-Deox is shown in **Figure s63**: (500 MHz, DMSO-d_6) δ (ppm) 11.49 (b, 1H), 8.86 (m, 8H, β-pyrrole), 8.20 (m , J= 7.9 Hz, 8H), 8.06 (m 8H), 5.43 (s, 1H), 4.76 (d, 1H), 3.85 (t, 1H), 1.87 (m, 6H), 1.22 (d, 3H), 0.94 (s, 3H), 0.62 (s, 3H), -2.91 (s, 2H). Large downfield signal at 11.49 ppm is consistent with an N-aryl thiocarbamate in DMSO-d_6 [12,13] Signal associated with carbamate nitrogen from $TPPS_3$-O-Deox [**2H**] is found at δ (ppm) 10.06 (s, 1H).

Synthesis of MITC conjugated to hydroxyl of 3,5-dihydroxycyclohexanecarboxylic [1I] (MITC-S-Hex)

Entry 3f: The isothiocyanate functionalized Mn porphyrin, MITC [**1A**] (10.3 mg, 9.6 μmol, 1 eq), was added to 3,5-dihydroxycyclohexanecarboxylic acid (7.5 mg, 47 μmol, 5 eq) in a flask with stir-bar and sealed with septum. A needle was placed into septum and the reaction flask was dried under vacuum overnight at 80°C. The next morning, the flask was purged with dry argon before 0.5 mL of anhydrous DMSO was added to the stirring reaction flask submerged in an oil bath at 60°C. The reaction process was monitored by thin layer chromatography (TLC Silica Gel 60 416 F254, Millipore, Darmstadt, Germany) using a chloroform:methanol:water ratio of 6:3:1 mobile phase with 1% v/v of 1 N hydrochloric acid. Reaction was tested at 6, 24, 48, and 72 hours to characterize reaction progression. The reaction scheme is shown in **Figure s8**. Upon completion, reaction solution was added dropwise to a stirring solution of 50:50 diethyl ether and acetone. The

precipitate was dried and redissolved in methanol (1mL) before being reprecipitated in 50:50 diethyl ether and acetone (10 mL). This precipitation procedure was repeated three times before the solid was recovered and dried overnight in a vacuum oven. The resulting product was 10.2 mg, 85.7 % yield. This fraction was assessed by UHPLC to determine conversion, eluting at 1.161 minutes. The remaining product was consolidated and purified further by flash chromatography on a BUCHI C-810 (Flawil,Liechtenstein) with C18 column using a continuous ramping protocol with a mobile phase gradient ranging from 10% ACN in 25 mM NH_4OAc buffer to 100% ACN. Elution of product was monitored by UV-Vis absorption at $\lambda = 467$ nm. The eluted product was frozen immediately and lyophilized overnight on Labconco Freezone (Labconco, Kansas City, USA). This purified MITC-S-Hex [**1I**] was assessed by UHPLC. Results are shown in **Figure s64**; MITC-S-Hex was found to elute at 1.518 minutes with MS (ESI) m/z calcd for $[M]^+$ $C_{52}H_{39}MnN_5O_{13}S_4^+$: 1124.08. Found: 1124.47. UV-Vis found unique peak at 284.6 nm likely associated with n-π^* transitions of aryl-NH thiocarbamate [7–9]. Carbamate product MITC-O-Hex [**1J**] could be found at MS (ESI) m/z calcd for $[M]^+$ $C_{52}H_{39}MnN_5O_{14}S_3^+$: 1108.10. Found: 1108.54. The results for MITC-S-Hex from an Agilent 6538 Q-TOF system in ESI MS negative mode are shown in **Figure s65**: where MS (ESI) m/z calculated for $[M\text{-}H]^-$ $C_{52}H_{38}MnN_5O_{13}S_4^-$: 1123.07 Found: 1123.07. MS (ESI) m/z calcd for $[M_2\text{-}6H]^{4-}$ $((C_{52}H_{36}MnN_5O_{13}S_4)_2)^{4-}$: 560.5292 Found: 560.5284 MS (ESI) m/z calculated for $[M_2\text{-}8H]^{6-}$ $((C_{52}H_{35}MnN_5O_{13}S_4)_2)^{6-}$: 373.35. Found: 373.35. MS (ESI) m/z calculated for $[M\text{-}3H]^{3-}$ $C_{63}H_{44}MnN_5O_{11}S_3^{3-}$: 399.05. Found 399.05. MS (ESI) m/z calculated for $[M_2\text{-}4H]^{3-}$ $((C_{52}H_{36}N_5O_{13}S_4Mn)_2)^{3-}$: Calculated 748.04. Found 748.04. Carbamate product MITC-O-Hex could be found at MS (ESI) m/z calculated for $[M - 3H]^{-2}$ $(C_{52}H_{36}MnH_5O_{14}S_3)^{2-}$: calculated 552.54, found 552.5395. The FTIR spectra for MITC-S-Hex is shown in **Figure s66**, where thiocarbamate signal is observed at 1519 cm^{-1} (N-H in plane bend)[10]. A unique signal attributed to MITC-S-Hex which is distinct from amide products is observed as a shoulder at approximately 1703 cm^{-1} associated with carboxylate C=O stretching[11]. ^1H NMR spectrum of MITC-S-Hex acquired on Bruker US 500 MHz system **Figure 67**. ^{1}HNMR(500 MHz, DMSO-d_6) δ: 11.29 (b, 1H), 7.73k (b, 16H), 5.35 (b, 1H) 4.93 (b, 1H), 2.23 to 2.06 (m, 3H), 1.21(b, 1H), 1.12 (b, 1H) 1.01 (b, 1H) Signal associated with N-aryl thiocarbamate at δ (ppm) 11.29 [12,13]. Paramagnetic Mn^{3+} broadened and supressed nearby proton signals.

Synthesis of porphyrin isothiocyanate conjugated to hydroxyl of 3,5-dihydroxycyclohexanecarboxylic acid [2I] ($TPPS_3$-S-Hex).

Entry 4f: The unmetalated 5-(4-isocyanatophenyl)-10,15,20-(tri-4-sulfonatophenyl)porphyrin [**2A**] ($TPPS_3$-NCS) (10.0 mg, 10.2 μmol) was used to conjugate to the hydroxyl of 3,5-dihydroxycyclohexanecarboxylic acid ($TPPS_3$-S-Hex) [**2I**], producing a product that could be characterized on ^{1}H NMR to identify the metalated analogue MITC-S-Hex [**1I**]. Synthesis and characterization methods were nearly identical to those for MITC-S-Hex. After precipitation procedure, crude product was assessed for conversion by UHPLC monitoring at 419 nm, eluting at 1.317 minutes. The resulting product was 10.4 mg, 88.1 % yield. UHPLC-MS spectra for flash-purified $TPPS_3$-S-Hex [**2I**] are shown in **Figure s68** and was found to elute at 1.519 minutes with a MS (ESI) m/z calculated for MS (ESI) m/z calcd for $[M+H]^+$ $C_{52}H_{42}MnN_5O_{13}S_4^+$: 1072.17. Found: 1072.45. The results for $TPPS_3$-S-Hex from an Agilent 6538 Q-TOF system in ESI MS negative mode are shown in **Figure s69**: MS (ESI) m/z calcd for $[M-2H]^{2-}$ $C_{52}H_{39}N_5O_{13}S_4^{2-}$: 534.5719. Found: 534.5715. Calcd for $[M-3H]^{3-}$ $C_{52}H_{38}N_5O_{13}S_4^{3-}$: 356.05. Found: 356.05. Calcd for $[M]^-$ $C_{52}H_{40}N_5O_{13}S_4^-$: 1070.15. Found: 1070.15. A larger proportion of carbamate product $TPPS_3$-O-Hex [**2J**] was isolated for one reaction with mass spectrum, as shown in **Figure s70**: MS (ESI) m/z calcd for $[M-2H]^{2-}$ $C_{52}H_{39}N_5O_{14}S_3^{2-}$: 526.5833. Found: 526.5835. Calcd for $[M-3H]^{3-}$ $C_{52}H_{38}N_5O_{14}S_3^{3-}$: 350.72. Found: 350.72. Calcd for $[M]^-$ $C_{52}H_{40}N_5O_{14}S_3^-$: 1054.17. Found: 1054.17. Sample for FTIR and NMR was dialyzed briefly for 6 hours at 4°C using cellulose dialysis tubing (MWCO: 1kD) to remove remaining NH_4OAc while minimizing product breakdown. The FTIR spectra for $TPPS_3$-S-Hex is shown in **Figure s71**, where thiocarbamate signal is observed at 1523 cm^{-1} (N-H in plane bend)[10]. A unique signal attributed to $TPPS_3$-S-Hex which is distinct from amide products is observed as a shoulder at approximately 1699 cm^{-1} associated with carboxylate C=O stretching[11]. The ^{1}H NMR spectrum of $TPPS_3$-S-Hex is shown in **Figure s72**: (500 MHz, DMSO-d_6) δ (ppm) 11.55 (b, 1H), 8.84 (m, 8H, β-pyrrole), 8.20 (m, 16H), 5.46 (s, 1H), 4.81 (m 1H), 3.66 (d, 1H), 2.54 (m, 1H), 2.23 (m, 2H), 2.11 (m, 2H), 1.49 (m, 2H), 1.14 (m, 1H). Large downfield signal at 11.55 ppm is consistent with an N-aryl thiocarbamate in DMSO-d_6 [12,13]. An example of the generation of carbamate product $TPPS_3$-O-Hex [**2J**] over time from $TPPS_3$-S-Hex is shown in Figure s51, with associated unpurified ^{1}H NMR for $TPPS_3$-O-Hex included in **Figure s73**.

Synthesis of porphyrin amides from thiocarbamate-linked porphyrins.

Entry 2g: Thiocarbamates used in these reactions were isolated as crude products from precipitation procedures described above. Solid precipitate was dried overnight in vacuum oven and afterward stored at -20°C before use. The scheme for MITC-S-Deox [**1G**] reaction with deoxycholic acid is shown in **Figure s9**. Deoxycholic acid was added at approximately 5 equivalence to crude thiocarbamate and dissolved in DMSO stirring at 60°C before DIPEA (5 equ) was added dropwise. After 24 hours, reaction solutions were added dropwise to a stirring solution of diethyl ether with 1 % acetic acid. The precipitate was dried and redissolved in methanol (1mL) before being reprecipitated in diethyl ether (10 mL). This precipitation procedure was repeated three times before the solid was recovered and dried overnight in a vacuum oven. This fraction was assessed by UHPLC to determine conversion to amide product. Conversion was determined in the same manner as previously by integrating peak areas associated with the amide product and finding its percentage relative to other peaks. An example of UHPLC-MS data and high-resolution mass spectrum obtained from crude MITC-Deox [**1E**] synthesized from MITC-S-Deox [**1G**] is included in **Figure s74.**

Entry 3g and **4g:** The scheme outlining the reaction of either MITC-S-Hex [**1I**] or $TPPS_3$-S-Hex [**2I**] with 3,5-dihydroxycyclohexanecarboxylic acid is shown in **Figure s10**. The acid was added at approximately 5 equivalence to crude thiocarbamate and dissolved in DMSO, stirring at 60°C before DIPEA (5 equ) was added dropwise. After 24 hours, reaction solutions were added dropwise to a stirring solution of 1:1 acetone and diethyl ether with 1 % acetic acid. The precipitate was dried and redissolved in methanol before being reprecipitated in 1:1 acetone and diethyl ether. This precipitation procedure was repeated three times before the solid was recovered and dried overnight in a vacuum oven. This fraction was assessed by UHPLC to determine conversion to amide product. An example of UHPLC-MS data obtained from crude MITC-Hex [**1F**] synthesized from MITC-S-Hex [**1I**] is shown in **Figure s75**, while crude $TPPS_3$-Hex [**2F**] synthesized from $TPPS_3$-S-Hex [**2I**] is included in **Figure s76**. Associated ^{1}H NMR spectrum from crude product is included in **Figure s77**.

Preparation of MITC-Deox [1E] for in-vivo study

For use *in-vivo*, MITC-Deox [**1E**] was purified by flash chromatography on a BUCHI C-810 (Flawil,Liechtenstein) with C18 column using a continuous ramping protocol with a mobile phase gradient ranging from 10% ACN in 25 mM NH_4OAc buffer to 100% ACN. Elution of product was monitored by UV-Vis absorption at $\lambda = 467$ nm. Acetonitrile was removed from eluted product by rotary evaporation using an IKA RV10 and S001 vacuum pump (Saufen, Germany) before dilution in distilled water and lyophilization overnight on Labconco Freezone (Labconco, Kansas City, USA). The product was dissolved in distilled water and was dialyzed for 2 days using cellulose dialysis tubing (MWCO: 1kD) to remove remaining NH_4OAc. Ammonium cations of desalted product were then exchanged with sodium using pre-loaded amberlite IR120 ion exchange resin. Eluted MITC-Deox was then lyophilized overnight and stored as a dry powder at -20°C. Resulting purity was determined with UHPLC (99%) and ICP-OES (90%). For animal experiments, MITC-Deox was prepared on the day of use by dissolving in PBS, mixed for 5 minutes, and sterile-filtered through a 0.22 μm syringe filter (MilliPore, Oakville, Ontario, Canada).

In-vivo MRI of mice injected with MITC-Deox [1E]

All animal procedures were performed in compliance with a protocol approved by the University of Toronto's Animal Care Committee (protocol number # 20012748). Furthermore, all procedures were conducted in accordance with the Canadian Council on Animal Care. Six- to eight-week-old Balbc mice (n = 9, Charles River Laboratories, Senneville, Quebec, Canada) weighing approximately 25g were utilized. Mice were anesthetized with 4% isoflurane in 100% oxygen (0.5 L/min) and maintained at 1.5 to 2.0% isoflurane during catheter insertion and the imaging session. Tail vein was cannulated with a 26-gauge angio-catheter pre-rinsed with heparin prior to being transferred to the MRI bed. Imaging was performed on a 3 Tesla pre-clinical scanner (MR Solutions, Guildford, United Kingdom). Mice were placed head-first and prone inside the whole-body mouse coil maintained at 37°C by air heating mouse holder. A pneumatic respiratory pillow was taped to the lower abdomen to provide respiratory-gated imaging. Localizer scan was first acquired to determine placement of mouse. The imaging-injection procedure consisted of (1) baseline pre-injection T_1 mapping by a variable flip angle method.[3] FA= [2°, 3°, 10°, 20°], TR=11 ms, TE = 2 ms, 4 averages, FOV = 60 mm, slice thickness 1 mm, 24 slices, 256×128) and a 3D

spoiled gradient echo (SPGR) sequence (FA = 30°, TR = 11 ms, TE = 2 ms, 4 averages, FOV = 60 mm, slice thickness 1 mm, 24 slices, 256×128). Approximately 120 μL of a solution of MITC-Deox [**1E**] was administered via the tail vein catheter at a dose of 0.02 mmol/kg followed by T_1 mapping and SPGR acquisitions at 2, 30, and 60 minutes post-contrast. Imaging was repeated the next day at the 24-hour post-contrast timepoint. MRI data were transferred to an independent workstation for quantitative analysis using in-house software developed in MATLAB (v.9.10, MathWorks). Calculations of T_1 relaxation times were performed on a pickle-by-pixel basis as described previously[14]. T_1 values were averaged over all pixels within an area of interest and reported as mean values and standard deviation.

Heart, liver, kidney, and lungs were excised at relevant timepoints and washed in PBS before being weighed and added to falcon tubes containing 10mL of 70% HNO_3 and left overnight for digestion. Samples were subsequently sonicated for 2 hours at 40°C before being diluted to 4% HNO_3 with distilled water and filtered through 0.4 μm PTFE filter (EMD Millipore-Merck). These solutions were weighed, and Mn concentration quantified by inductively coupled-plasma atomic emission spectroscopy (ICP-AES) at the university's Department of Chemistry Analest facility.

REFERENCES

1 K. D. W. Vollett, D. A. Szulc and H. L. M. Cheng, *Int J Mol Sci*, , DOI:10.3390/ijms24119532.

2 J. Alvarez, D. C. Lee, S. A. Baldwin and D. Chapman, *Journal of Biological Chemistry*, 1987, **262**, 3502–3509.

3 C. Zhang, Z. Ren, Z. Yin, H. Qian and D. Ma, *Polymer Bulletin*, 2008, **60**, 97–101.

4 R. Quintanilla-Licea, J. F. Colunga-Valladares, A. Caballero-Quintero, C. Rodríguez-Padilla, R. Tamez-Guerra, R. Gómez-Flores and N. Waksman, *molecules NMR Detection of Isomers Arising from Restricted Rotation of the C-N Amide Bond of N-Formyl-o-toluidine and N,N'-bis-Formyl-o-tolidine †*, 2002, vol. 7.

5 N. M. Barbosa Neto, D. S. Correa, L. De Boni, G. G. Parra, L. Misoguti, C. R. Mendonça, I. E. Borissevitch, S. C. Zílio and P. J. Gonçalves, *Chem Phys Lett*, 2013, **587**, 118–123.

6 L. Tang, P. Li, Y. Han, G. Yang, H. Xin, S. Zhao, R. Guan, Z. Liu and D. Cao, *J Photochem Photobiol A Chem*, , DOI:10.1016/j.jphotochem.2022.114511.

7 E. Humeres, C. Zucco, M. Nunes, N. A. Debacher and R. J. Nunes, in *Journal of Physical Organic Chemistry*, 2002, vol. 15, pp. 570–575.

8 S. Dey, L. A. S. Parolis and G. Yorath, *Transactions of the Indian Institute of Metals*, 2012, **65**, 387–392.

9 W. Arar, A. Khatyr, M. Knorr, C. Strohmann, A. Schmidt and A. Schmidt Bis, 2022, **2022**, 1381.

10 V. Sterba and V. KADERABEK jr, *Chem. Cummun.*, 1984, **49**, 1577–1591.

11 L. L. Shevchenko, *Russian Chemical Reviews*, 1963, **32**, 201–207.

12 C. A. Ellis, M. A. Miller, J. Spencer, J. Zukerman-Schpector and E. R. T. Tiekink, *CrystEngComm*, 2009, **11**, 1352–1361.

13 C. M. Levinn, A. K. Steiger and M. D. Pluth, *ACS Chem Biol*, 2019, **14**, 170–175.

14 H. L. Cheng and G. A. Wright, *Magn Reson Med*, 2006, **55**, 566–574.

15 M. J. Webb and N. Bampos, *Chem Sci*, 2012, **3**, 2351–2366.

SUPPLEMENTARY FIGURES

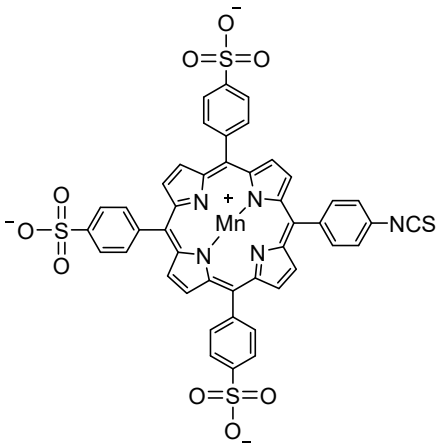

MITC [**1A**]

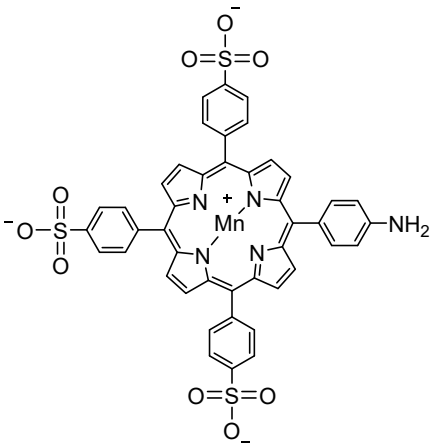

$MnTPPS_3$-NH_2 [**1B**]

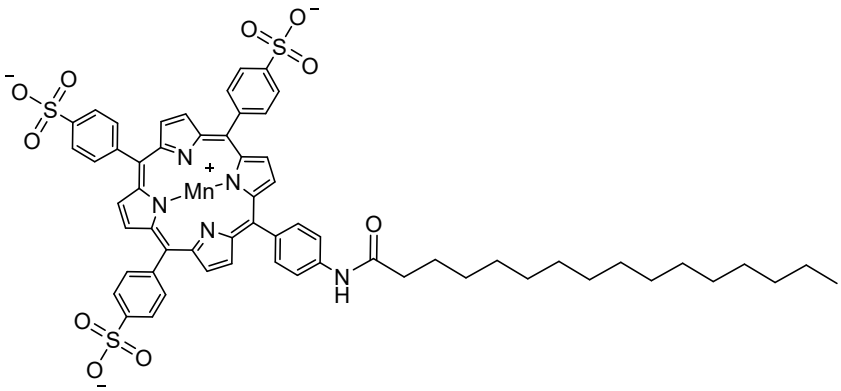

MITC-Palm [**1C**]

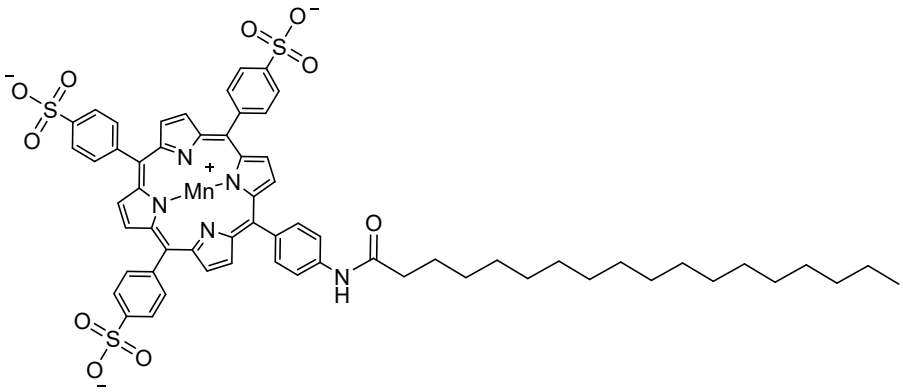

MITC-Stearic [**1D**]

Figure s1a. Manganese Porphyrin Structures pt.1

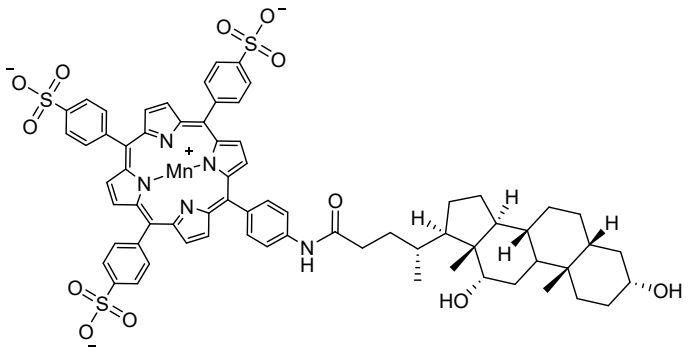

MITC-Deox [**1E**]

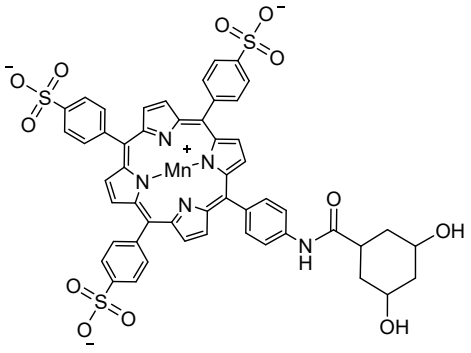

MITC-Hex [**1F**]

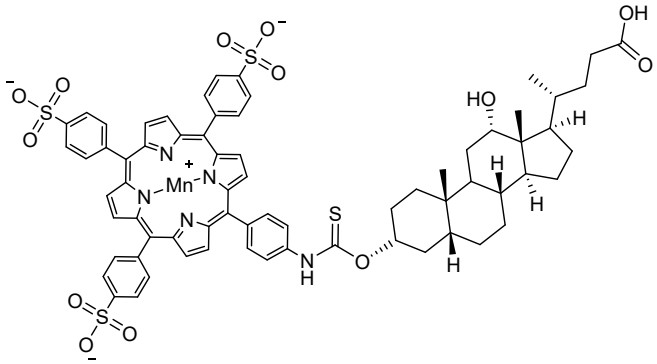

MITC-S-Deox [**1G**]

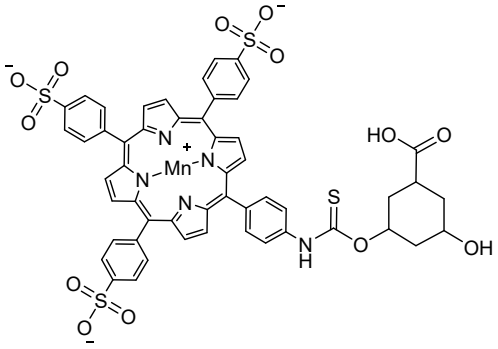

MITC-S-Hex [**1I**]

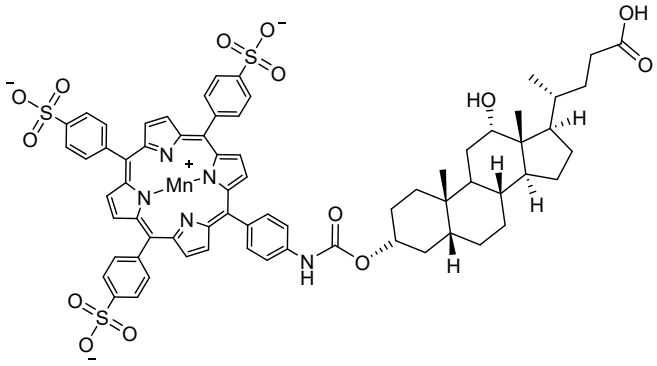

MITC-O-Deox [**1H**]

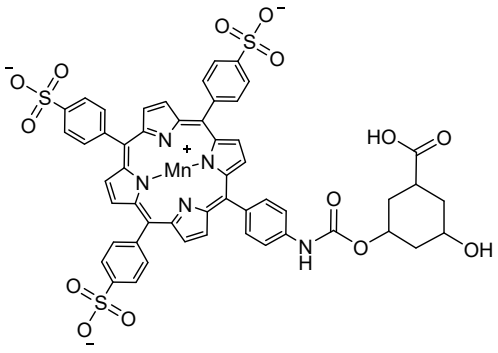

MITC-O-Hex [**1J**]

Figure s1b. Manganese Porphyrin Structures pt.2

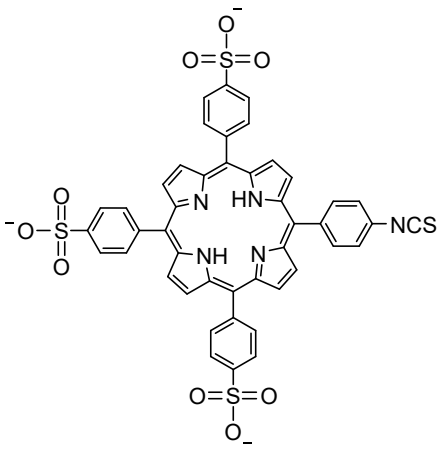

TPPS$_3$-NCS [**2A**]

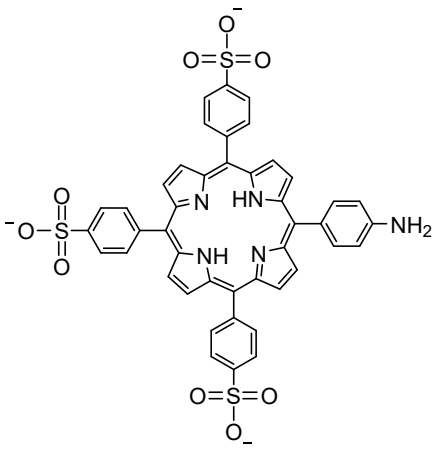

TPPS$_3$-NH$_2$ [**2B**]

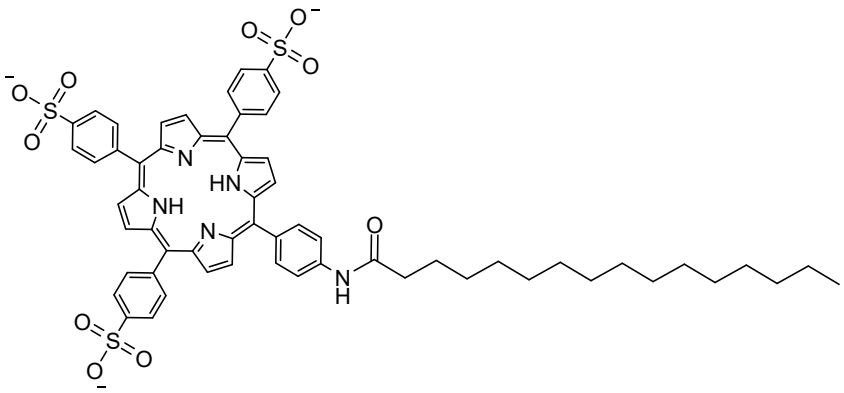

TPPS$_3$-Palm [**2C**]

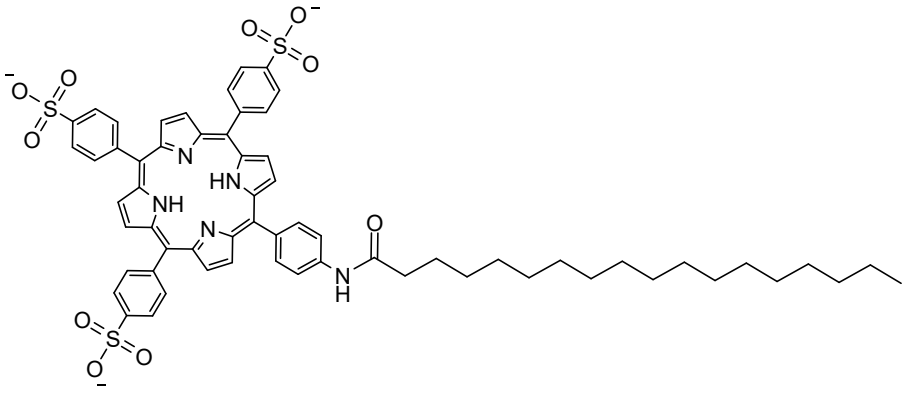

TPPS$_3$-Stearic [**2D**]

Figure s1c. Porphyrin Structures pt.1

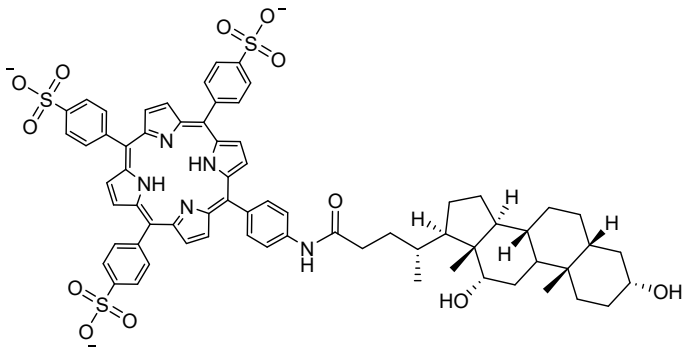

$TPPS_3$-Deox [**2E**]

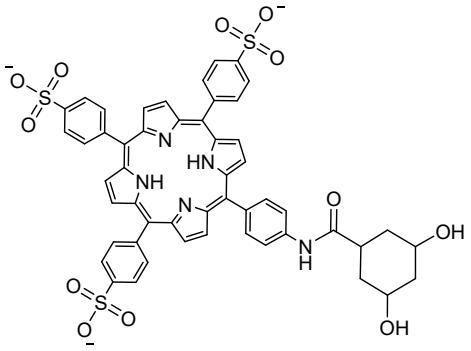

$TPPS_3$-Hex [**2F**]

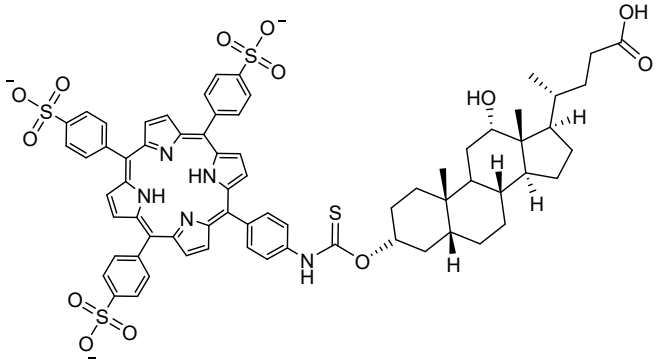

$TPPS_3$-S-Deox [**2G**]

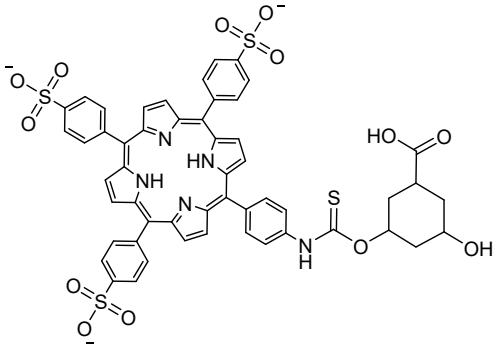

$TPPS_3$-S-Hex [**2I**]

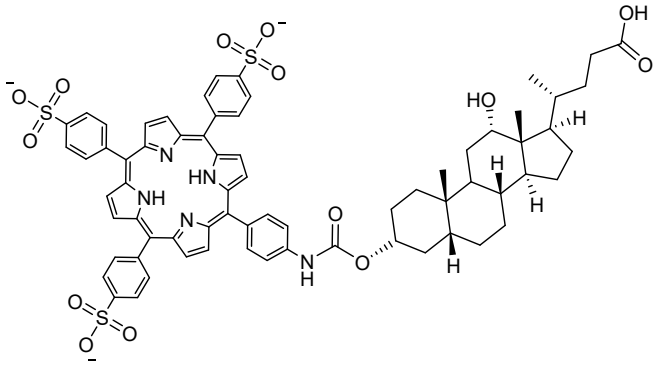

$TPPS_3$-O-Deox [**2H**]

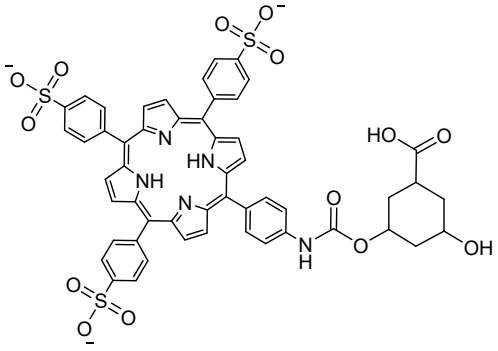

$TPPS_3$-O-Hex [**2J**]

Figure s1d. Porphyrin Structures pt.2

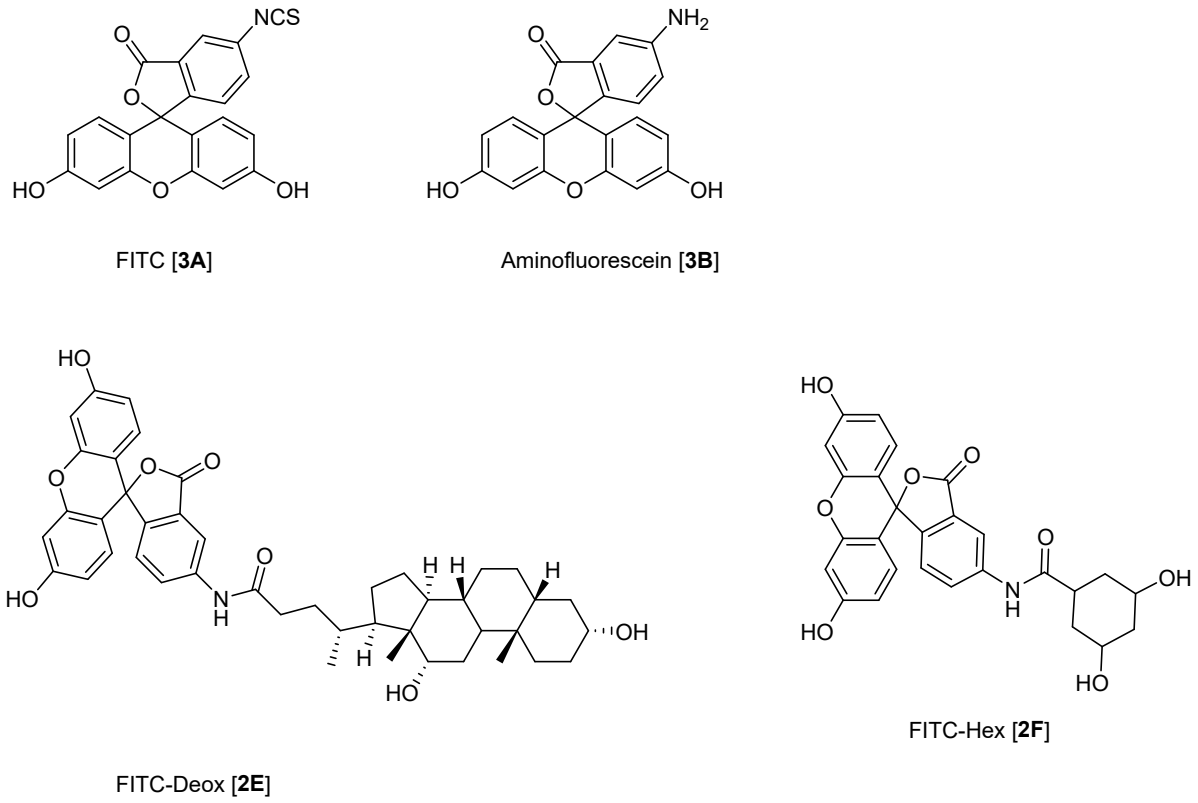

Figure s1e. Fluoresceine Structures pt.1

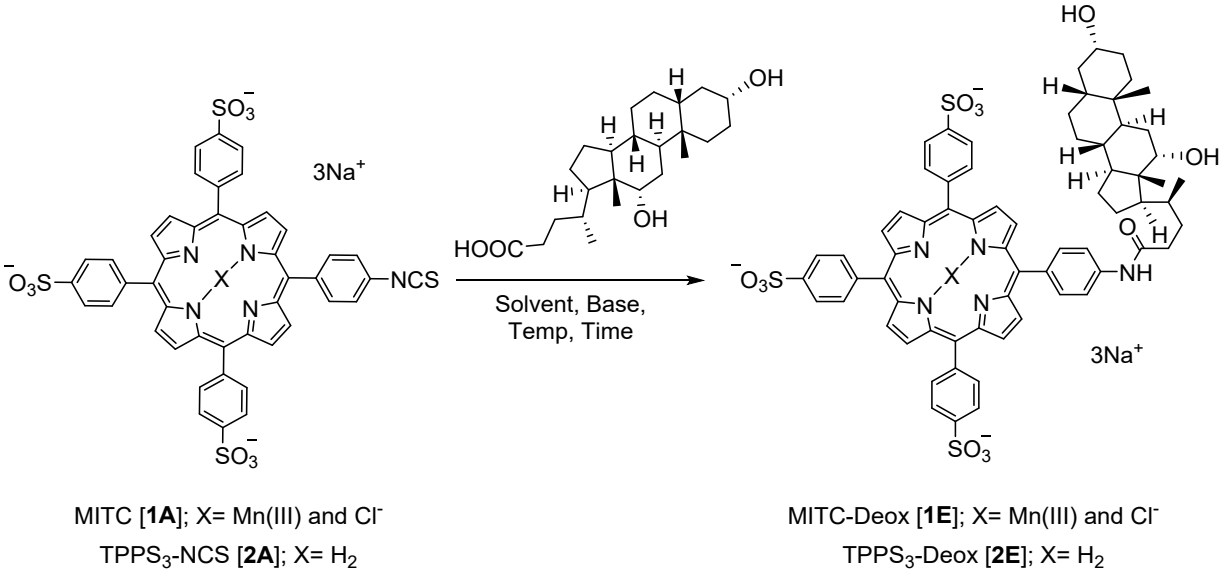

Figure s2. Reaction of MITC [**1A**] or $TPPS_3$-NCS [**2A**] with deoxycholic acid produces amide-linked products MITC-Deox [**1E**] or $TPPS_3$-Deox [**2E**], respectively.

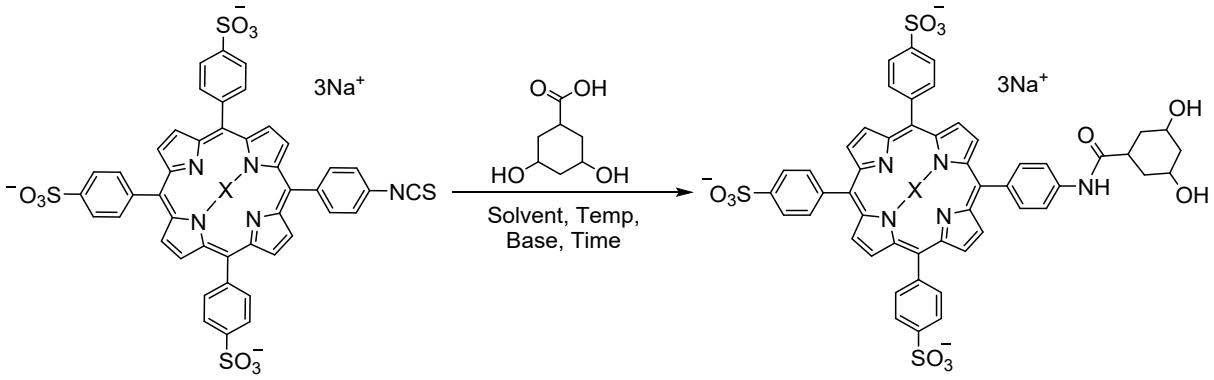

Figure s3. Reaction of MITC [**1A**] or $TPPS_3$-NCS [**2A**] with 3,5-dihydroxycyclohexanecarboxylic acid produces amide-linked products MITC-Hex [**1F**] or $TPPS_3$-Hex [**2F**], respectively.

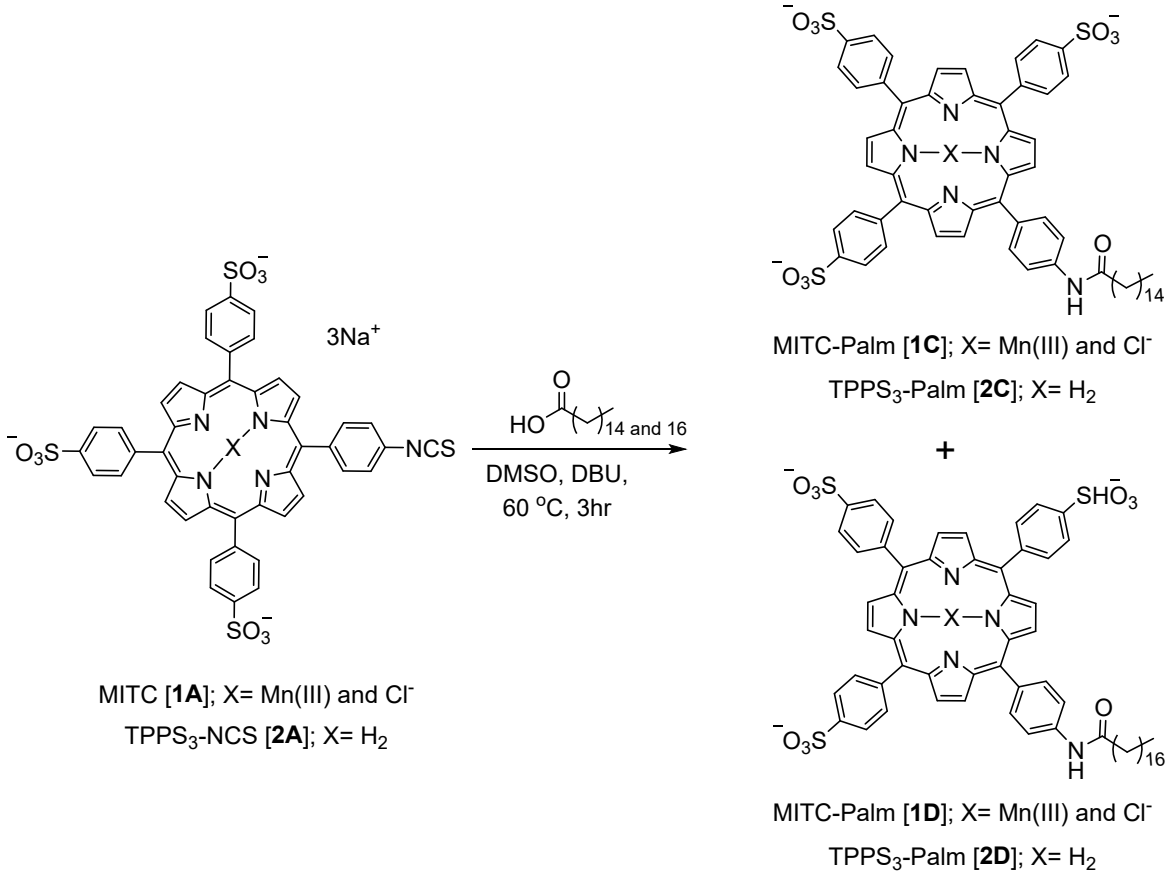

Figure s4. Reaction of MITC [**1A**] or $TPPS_3$-NCS [**2A**] fatty acid blend containing palmitic acid and stearic acid producing amide-linked products MITC-Palm [**1C**] and $TPPS_3$-Palm [**2C**], or MITC-Stearic [**1D**] and $TPPS_3$Stearic [**2D**], respectively.

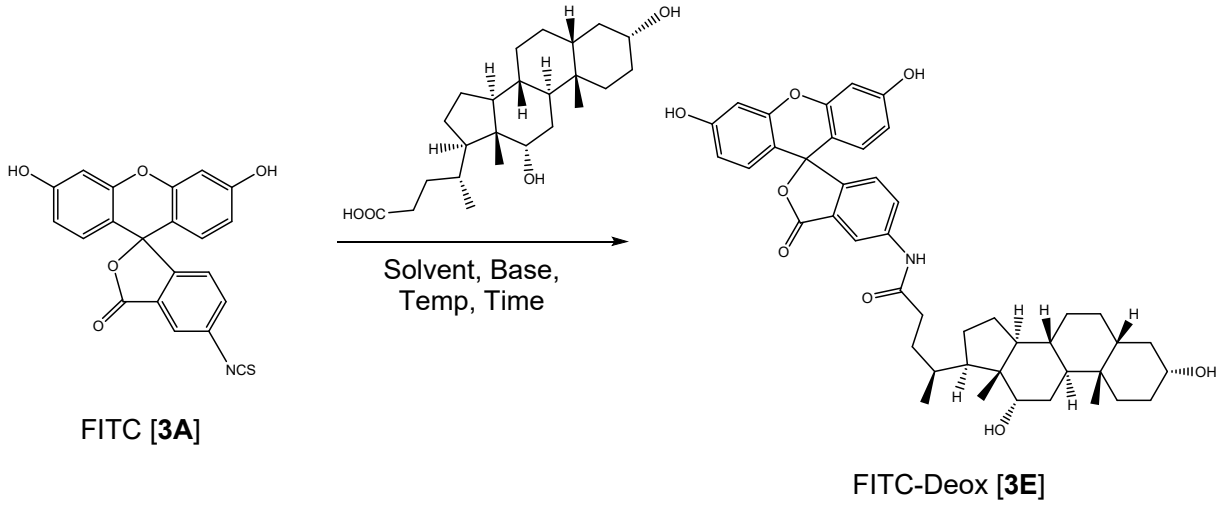

Figure s5. Reaction of FITC with deoxycholic acid produces amide-linked product FITC-Deox [**3E**].

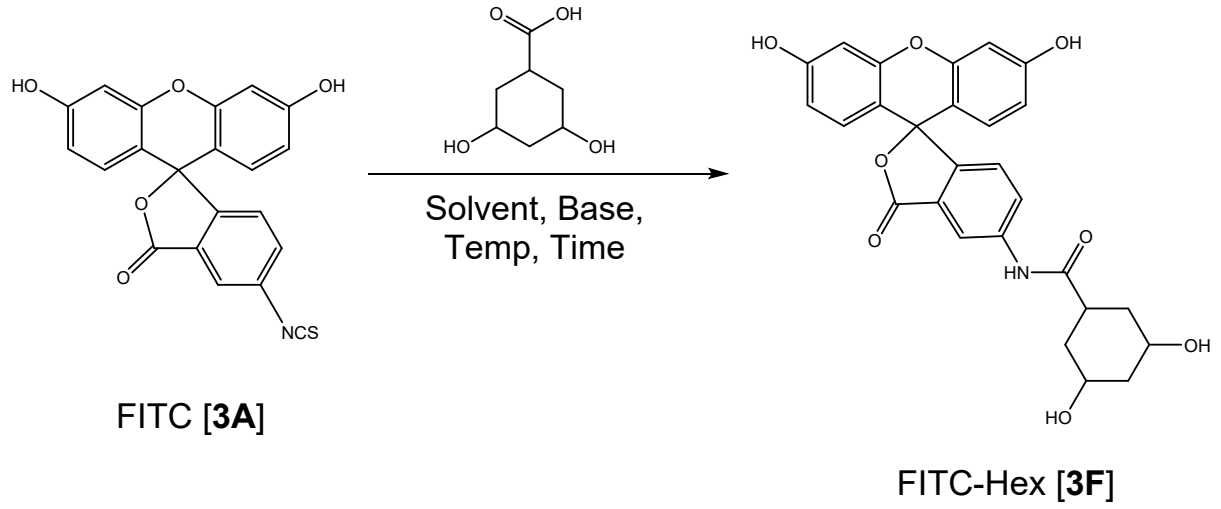

Figure s6. Reaction of FITC with deoxycholic acid produces amide-linked product FITC-Hex [**3F**].

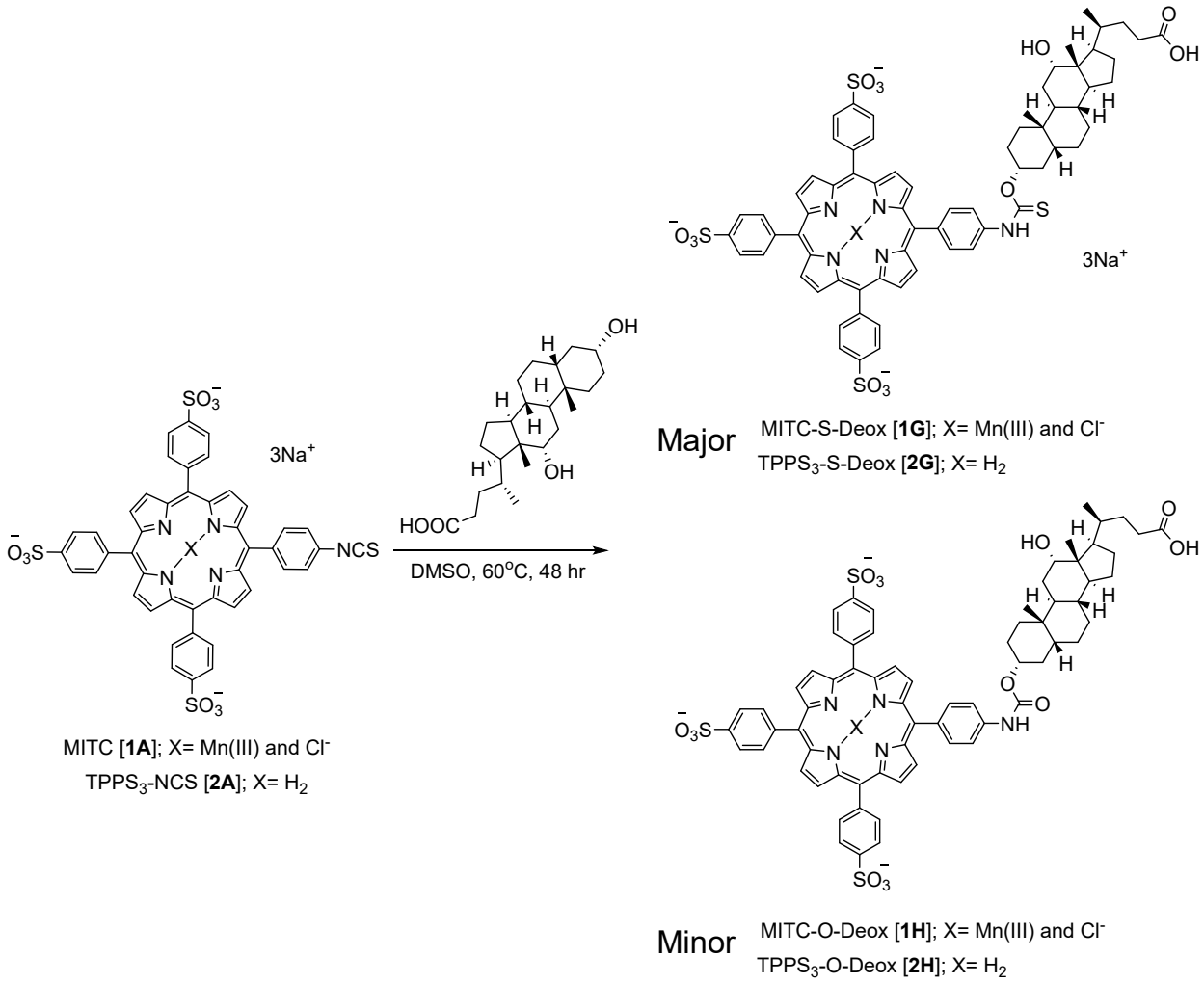

Figure s7. Formation of MITC [**1A**] or $TPPS_3$-NCS [**2A**] with deoxycholic acid in the absence of base produces thiocarbamate linked products MITC-S-Deox [**1G**] or $TPPS_3$-S-Deox [**2G**], respectively. Trace amounts of the carbamate products MITC-O-Deox [**1H**] and $TPPS_3$-O-Deox [**2H**] were also observed for each respective reaction.

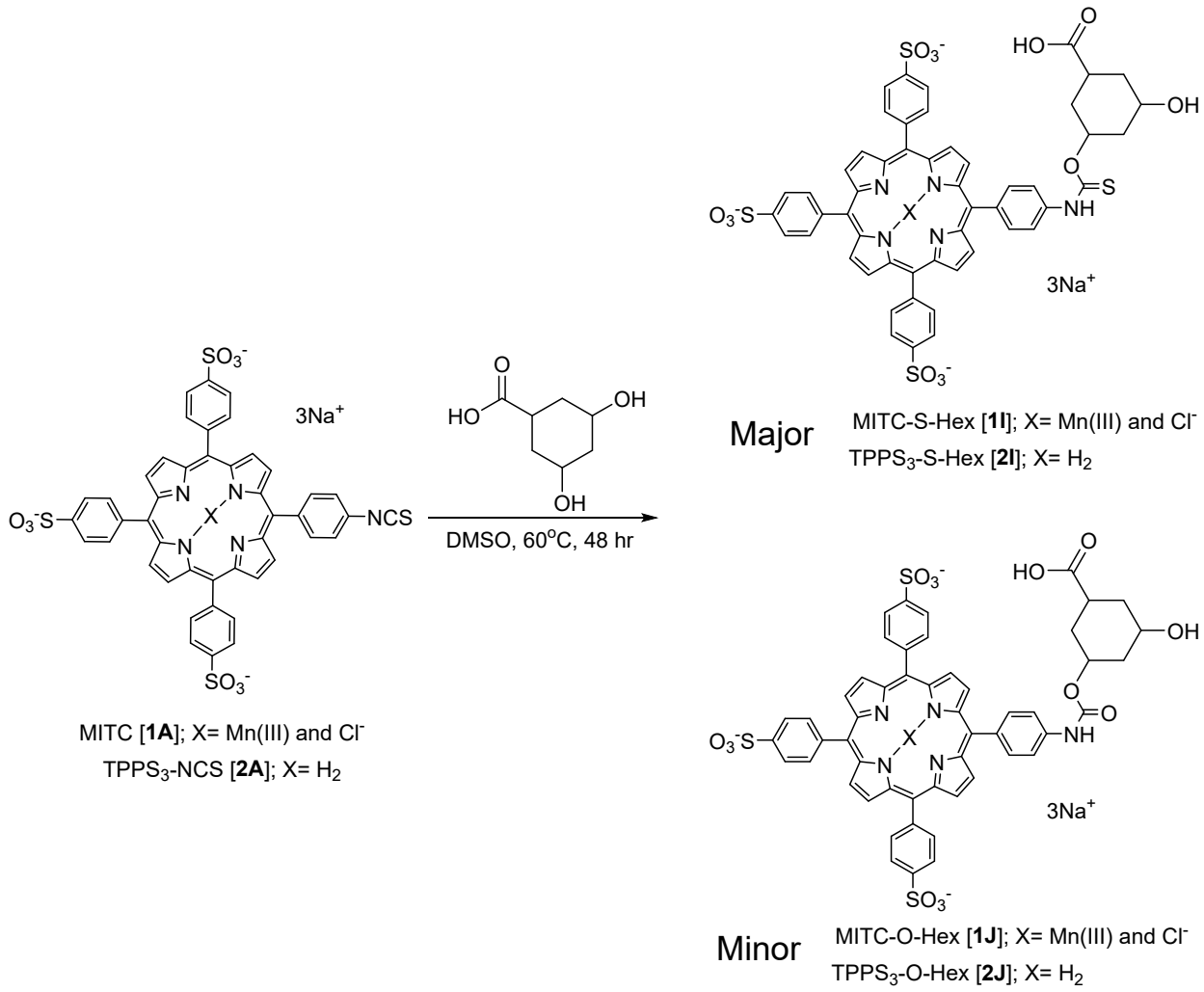

Figure s8. Reaction of MITC [**1A**] or $TPPS_3$-NCS [**2A**] with 3,5-dihydroxycyclohexanecarboxylic acid in the absence of base produces thiocarbamate-linked products MITC-S-Hex [**1I**] or $TPPS_3$-S-Hex [**2I**], respectively. Trace amounts of the carbamate products MITC-O-Hex [**1J**] and $TPPS_3$-O-Hex [**2J**] were also observed.

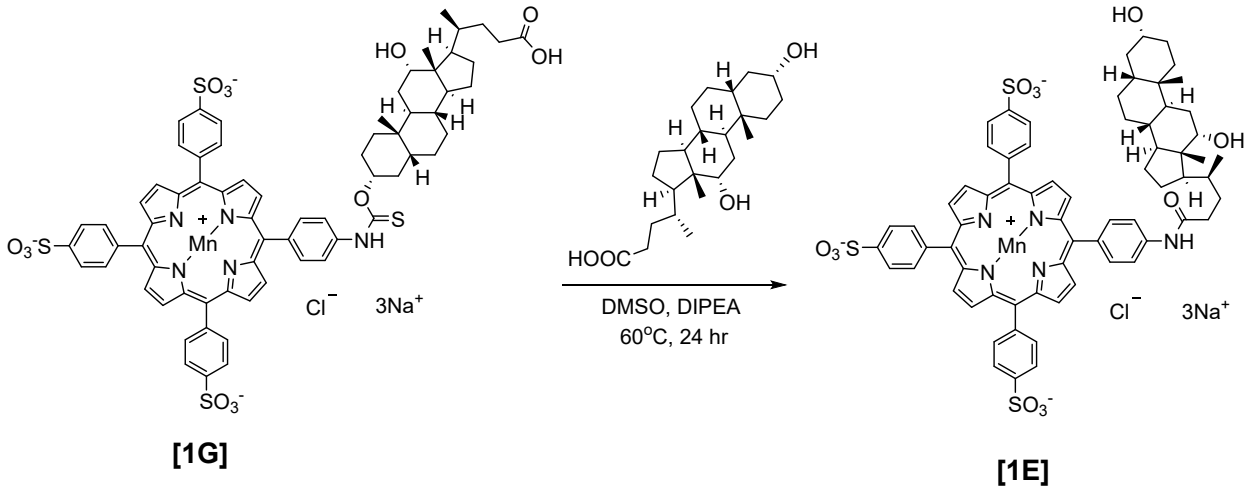

[1G] **[1E]**

Figure s9. Thiocarbamate MITC-S-Deox [**1G**] react with deoxycholate acid in the presence of DIPEA to form amide product MITC-Deox [**1E**].

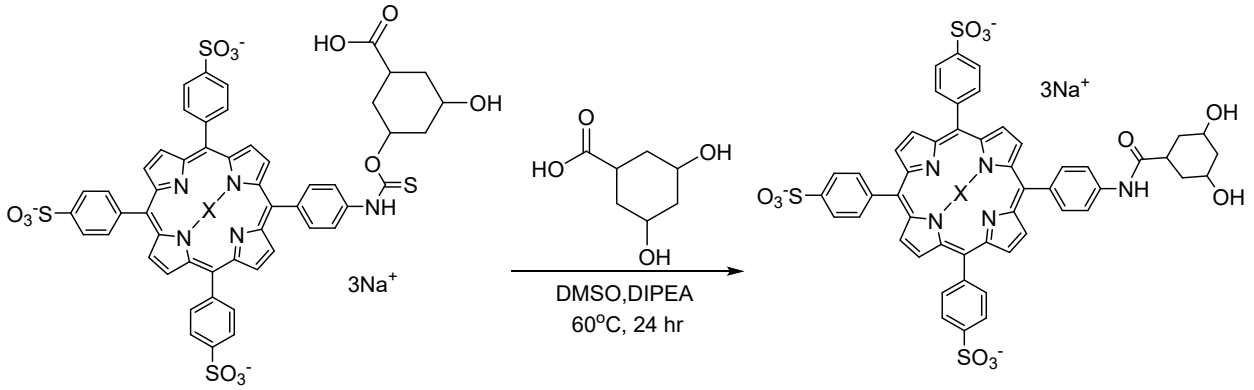

MITC [**1I**]; X= Mn(III) and Cl^-
$TPPS_3$-NCS [**2I**]; X= H_2

MITC [**1F**]; X= Mn(III) and Cl^-
$TPPS_3$-NCS [**2F**]; X= H_2

Figure s10. Thiocarbamates MITC-S-Hex [**1I**] and $TPPS_3$-S-Hex [**2I**] react with 3,5-dihydroxycyclohexanecarboxylic acid to form amide products MITC-Hex [**1F**] and $TPPS_3$-Hex [**2F**] respectively.

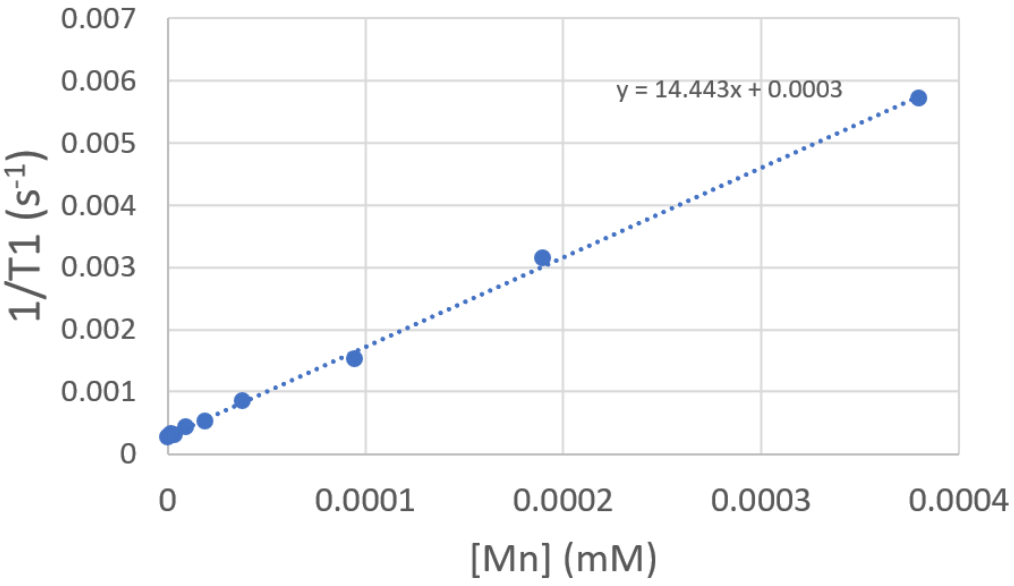

Figure s11. Relaxivity measurements of MITC-Deox [**1E**] contrast agent. The longitudinal relaxivity is equal to the slope of the line of best fit to the graph of longitudinal relaxation rate (1/T1) to manganese (Mn) concentration.

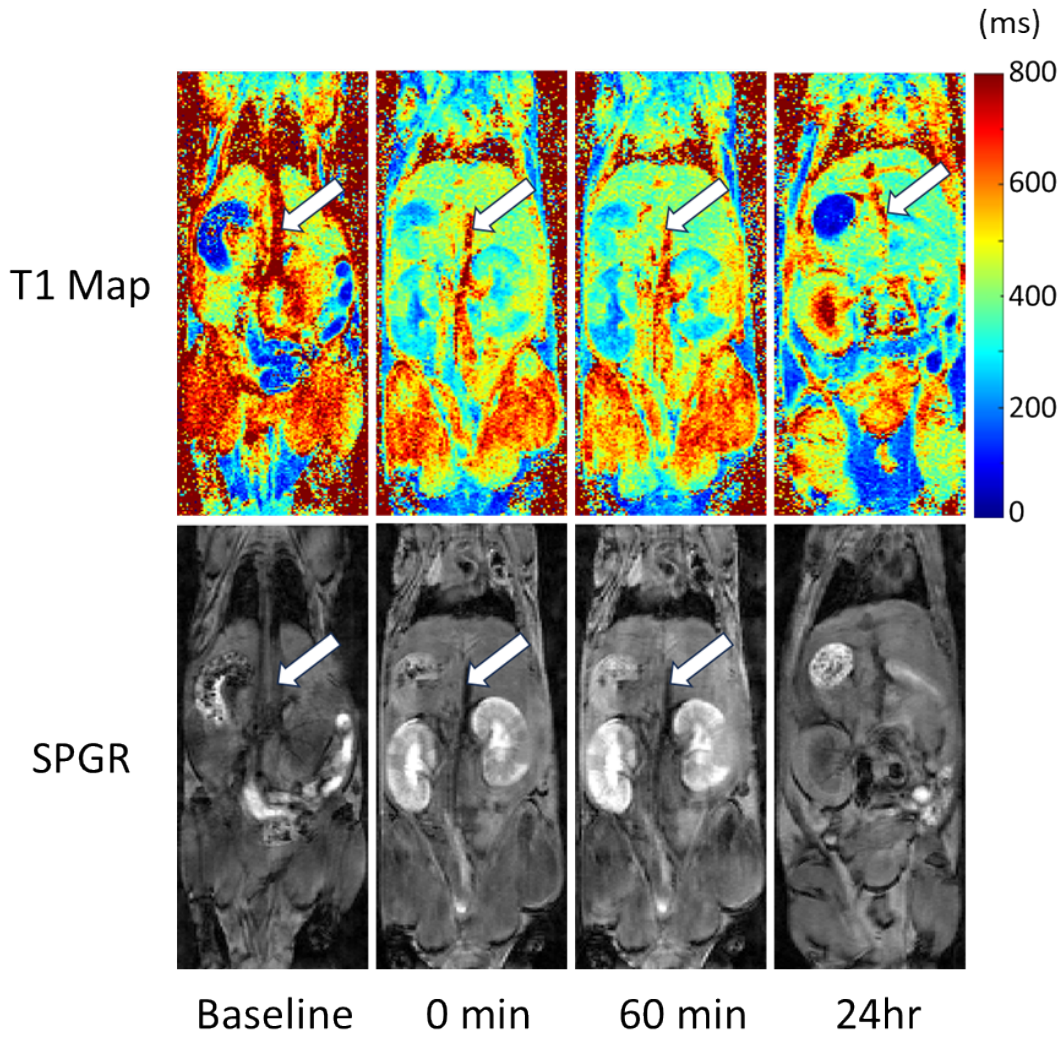

Figure s12. MRI of healthy adult mouse injected i.v. with control sodium Mn(III)tetra(4-sulfonatophenyl) porphyrin ($MnTPPS_4$) contrast agent. In-vivo maps of T_1 relaxation times (ms) (top row) and spoiled gradient echo recalled (SPGR) T_1-weighted images (bottom row) at the corresponding slice locations. Shown are baseline images before i.v. administration of unfunctionalized $MnTPPS_4$ and images at various timepoints post-contrast. White arrow highlights aorta.

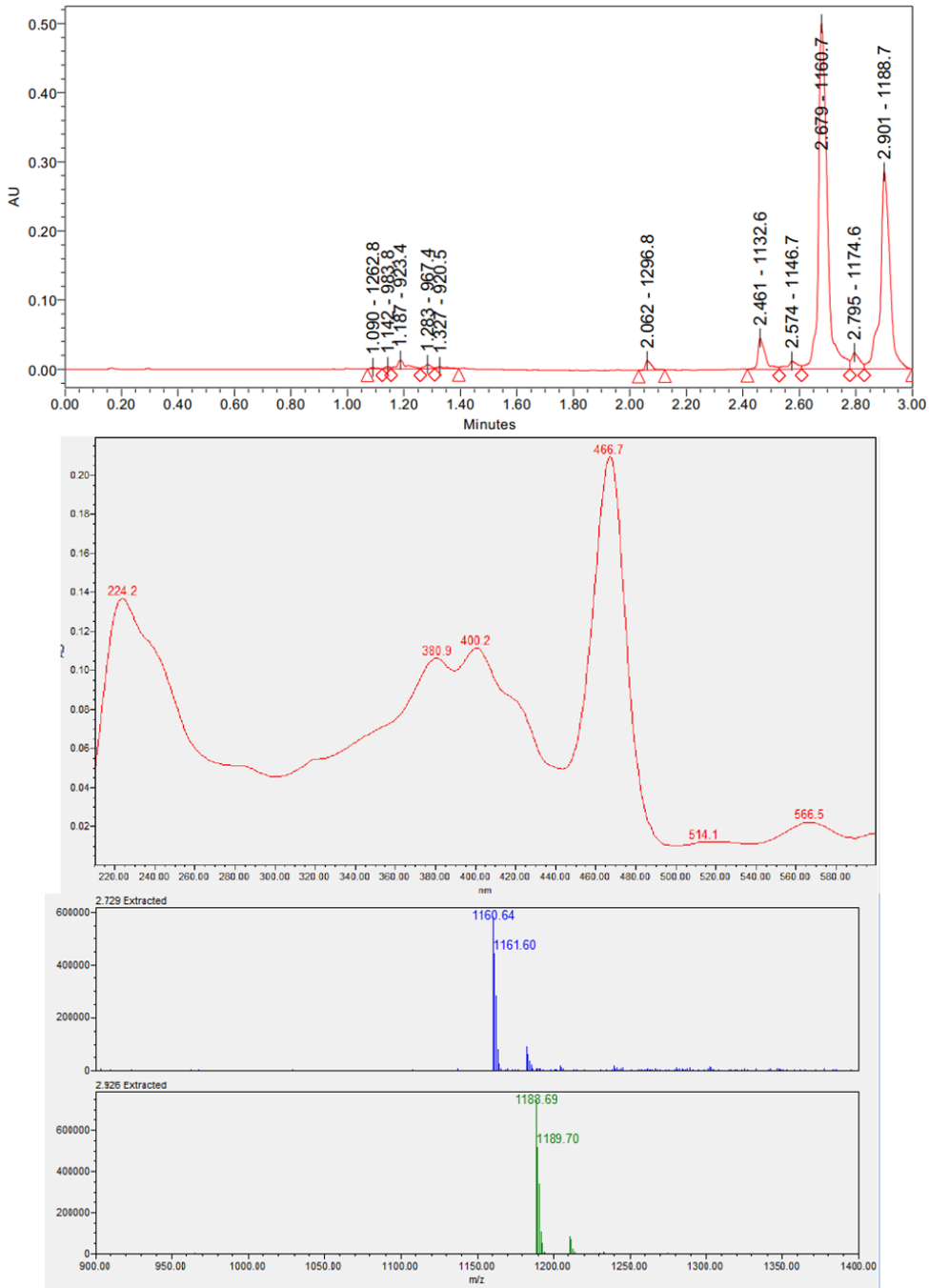

Figure s13. UHPLC-MS spectra of MITC conjugated fatty acids (MITC-Stearic [**1D]** and MITC-Palm [**1C**]) recorded with Waters ACQUITY H-class UHPLC system with PDA detector recording at 467 nm and single quadrupole MS detector in positive mode. MITC-Stearic: elution occurred at 2.901 minutes. MS (ESI) m/z calculated for $[M]^+$ $C_{62}H_{63}MnN_5O_{10}S_3$: 1188.31. Found: 1188.69. MITC-Palm: elution occurred at 2.679 minutes. MS (ESI) m/z calculated for $[M]^+$ $C_{60}H_{59}MnN_5O_{10}S_3$: 1160.28. Found: 1160.64.

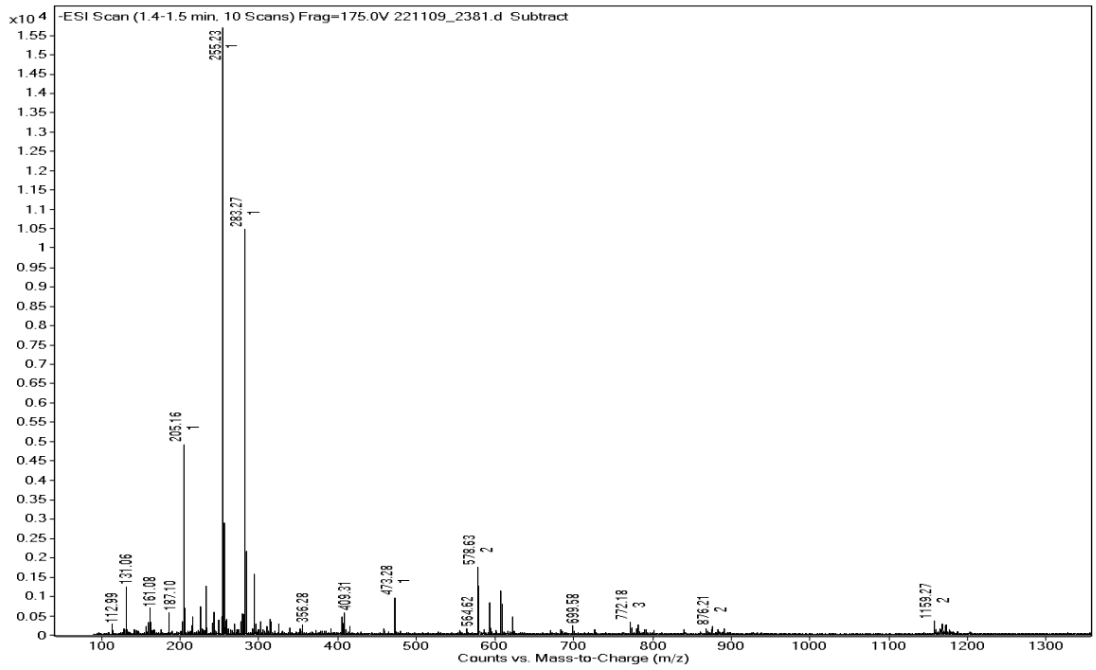

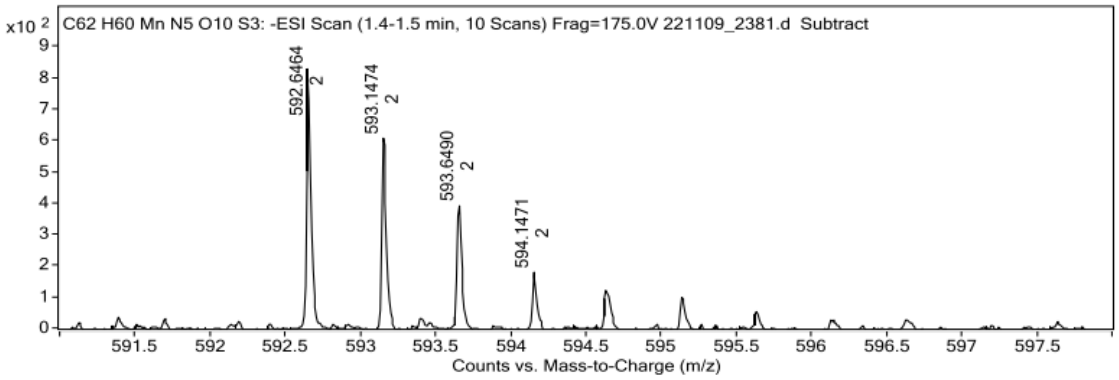

Predicted Isotope Match Table

Isotope	*m/z*	*Calc m/z*	Diff (mDa)	Abund (%)	Calc Abund (%)	+/-
1	592.6464	592.6447	1.7	100.0	100.0	0.0
2	593.1474	593.1462	1.2	75.5	72.3	-3.2
3	593.6490	593.6460	3.0	47.6	41.3	-6.3
4	594.1471	594.1463	0.8	22.4	17.1	-5.3
5	594.6309	594.6464	-15.5	15.2	5.9	-9.3
6	595.1317	595.1466	-14.9	12.5	1.7	-10.8

Figure s14. Mass spectrum obtained for MITC conjugated fatty acids (MITC-Stearic [**1D]** and MITC-Palm [**1C**]) on Agilent 6538 Q-TOF system in ESI MS Negative mode. MS (ESI) m/z calculated for palmitic acid, $[M]^-$ $C_{16}H_{31}O_2^-$: 255.23. Found: 255.23. Stearic acid, $[M]^-$ $C_{18}H_{35}O_2^-$: 283.26. Found: 283.27. MITC-Palm, $[M]^-C_{60}H_{57}MnN_5O_{10}S_3^-$: 1159.27. Found: 1159.27. $[M_2 – 6H]^{-2}$ $(C_{60}H_{56}MnN_5O_{10}S_3)_2^{-4}$ 578.63 Found 578.63. MITC-Stearic $[M]^-$ $C_{62}H_{62}MnN_5O_{10}S_3^-$: 1187.30. Found: 1187.30. $[M_2 – 6H]^{-2}$ $(C_{62}H_{60}MnN_5O_{10}S_3)_2^{-4}$ 592.6447 Found 592.6464.

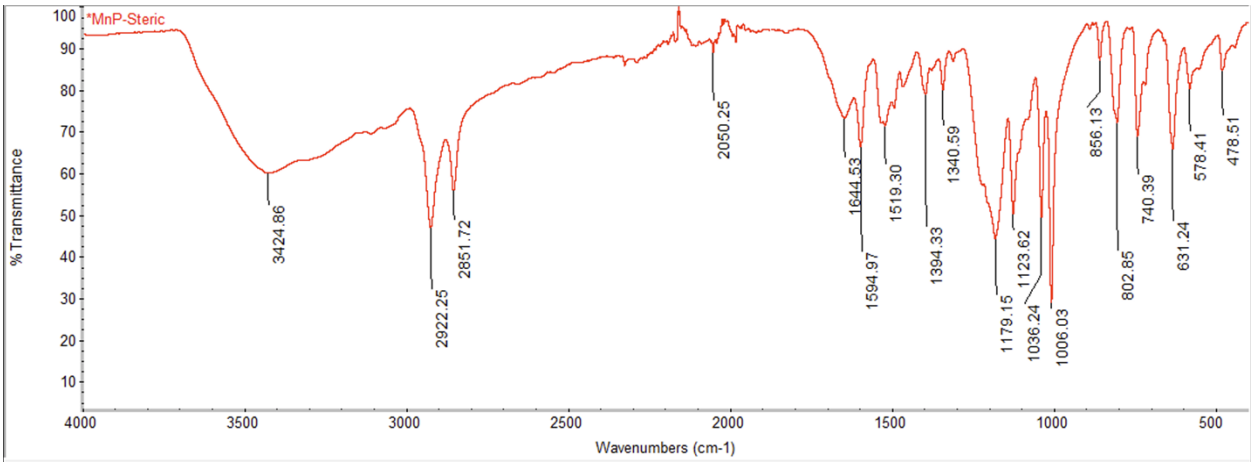

Figure s15. Fourier transform infrared spectroscopy of MITC conjugated fatty acids (MITC-Stearic [**1D]** and MITC-Palm [**1C**]) (FTIR-ATR, Thermo Scientific Nicolet iS50) of MITC-FA. FTIR: γcm^{-1}: 2922 and 2851 (C-H stretch), 1519(N-H in plane bend).

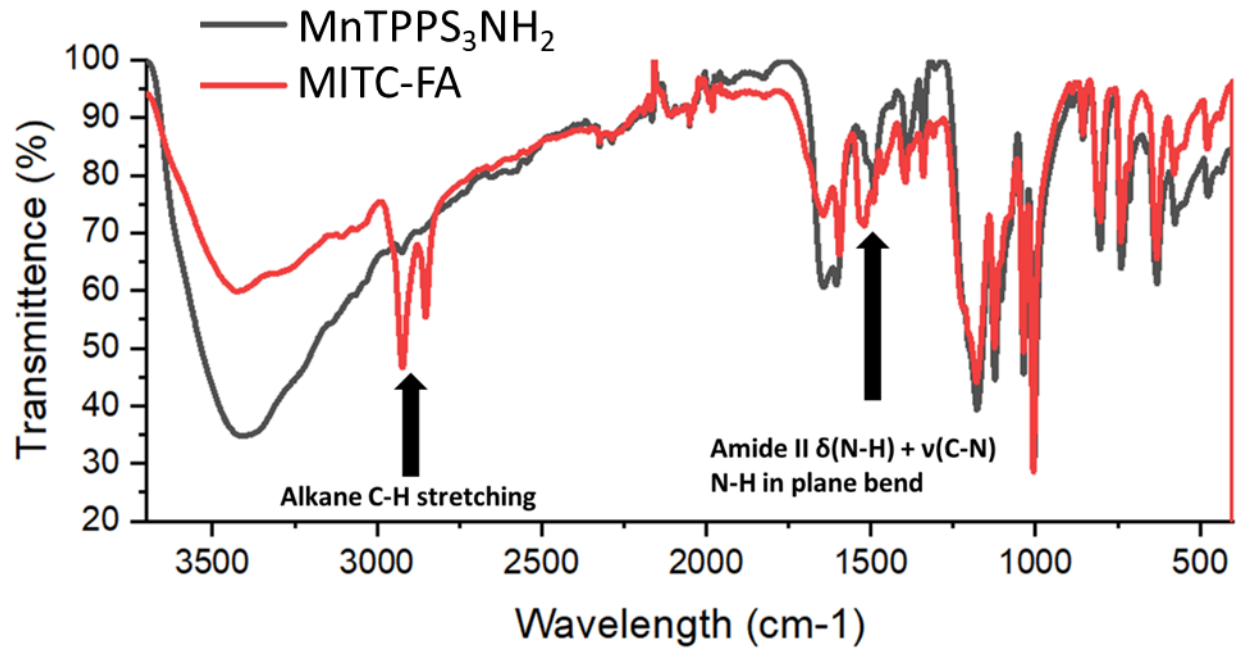

Figure s16. Fourier transform infrared spectroscopy (FTIR-ATR, Thermo Scientific Nicolet iS50) of MITC conjugated fatty acids (MITC-Stearic [**1D]** and MITC-Palm [**1C**])) and $MnTPPS_3NH_2$ [**1B**] precursor. FTIR: γcm^{-1}: 2922 and 2851 (C-H stretch), 1519 (N-H in plane bend).

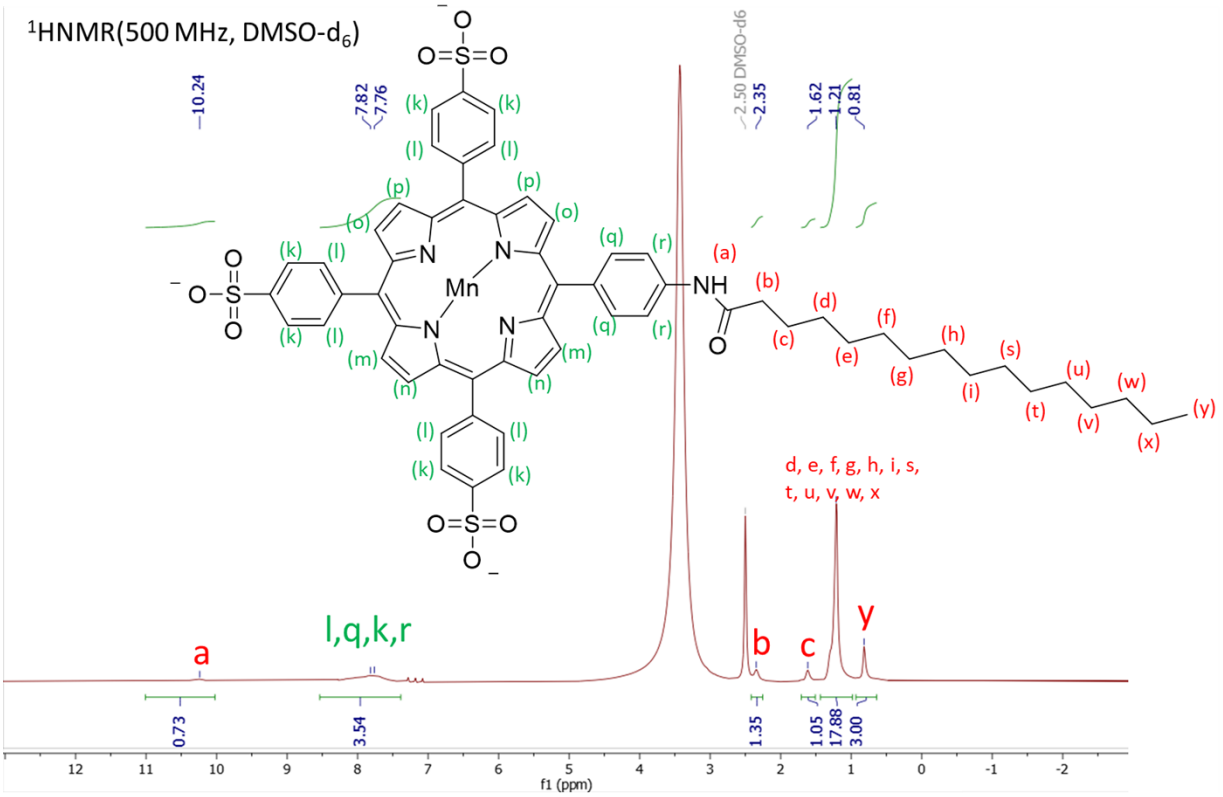

Figure s17. 1H NMR spectrum of MITC conjugated fatty acids (MITC-Stearic [**1D]** and MITC-Palm [**1C**]) acquired on Bruker US 500 MHz system. ^{1}HNMR(500 MHz, DMSO-d_6) δ: 10.24 (b, 1H), 8.82 (m, 8H), 7.76 (m, 16H), 2.35 (m, 2H), 1.62 (b, 1H), 1.21 (m, 26H), 0.81 (m, 3H). Paramagnetic Mn^{3+} broadened and supressed nearby proton signals.

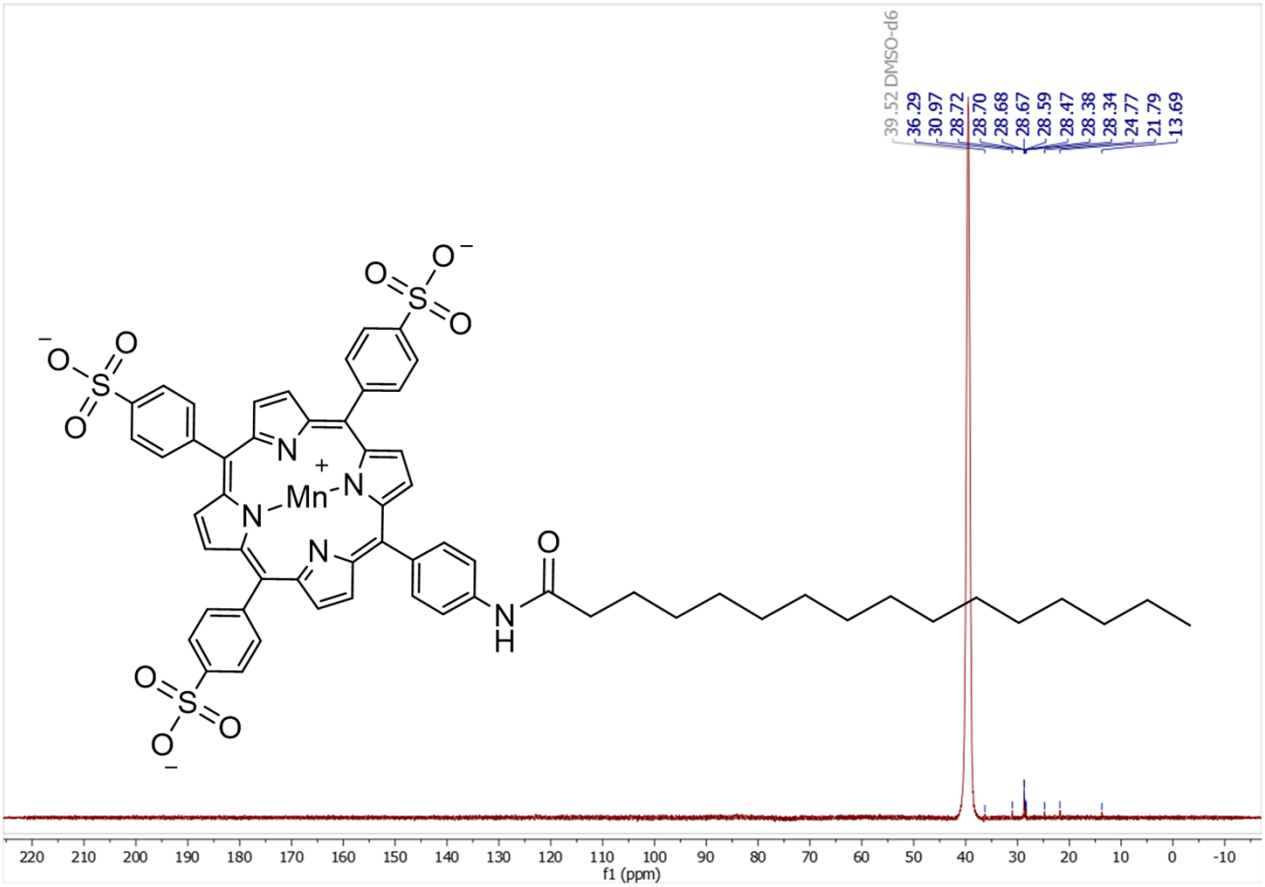

Figure s18. 13C NMR spectrum of MITC Fatty acid conjugates of stearic (MITC-Stearic [**1D]**) and palmitic acid (MITC-Palm [**1C**]) acquired on Bruker US 500 MHz system. ^{13}CNMR(500 MHz, DMSO-d_6) δ: Not observed (45 C, manganese tri-4-sulfonatophenyl)porphyrin) 36.29, 30.97, 28.72 to 28.67 unresolved collection of peaks, 28.59, 28.47, 28.38, 28.34, 24.77, 21.79, 13.69 (16 to 18 C, Steric and Palmic acid). Paramagnetic Mn^{3+} broadened and supressed nearby carbon signals.

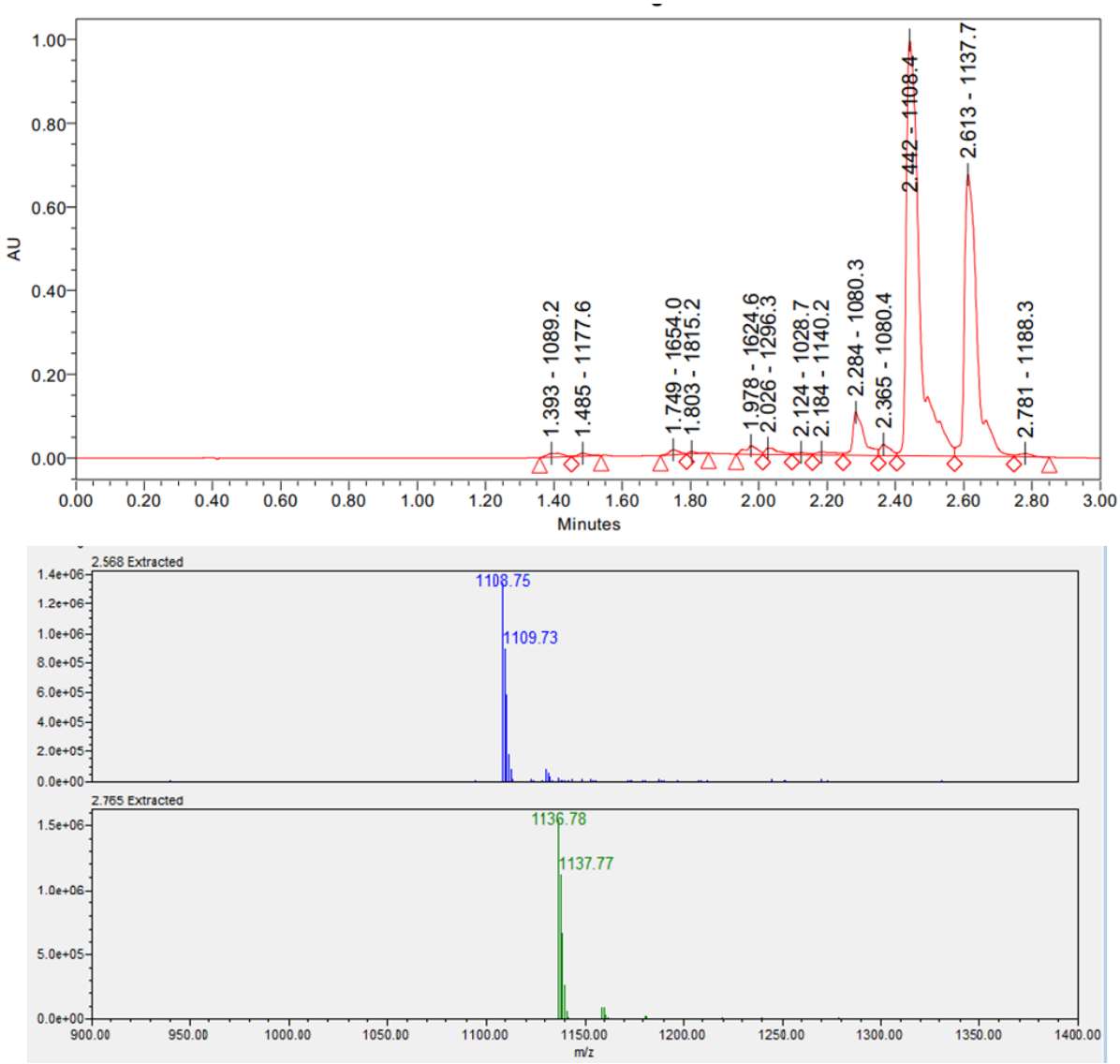

Figure s19. UHPLC-MS of $TPPS_3NCS$ conjugated fatty acids ($TPPS_3$-Stearic [**2D]** and $TPPS_3$-Palm [**2C**]) recorded with Waters ACQUITY H-class UHPLC system with PDA detector recording at 419 nm and single quadrupole MS detector in positive mode. For $TPPS_3$-Palm, elution occurred at 2.442 minutes. MS (ESI) m/z calculated for $[M]^+$ $C_{60}H_{62}N_5O_{10}S_3$: 1108.37. Found: 1108.75 For $TPPS_3$-Steric, elution occurred at 2.613 minutes. MS (ESI) m/z calculated for $[M]^+$ $C_{62}H_{66}N_5O_{10}S_3$: 1136.40. Found: 1136.78.

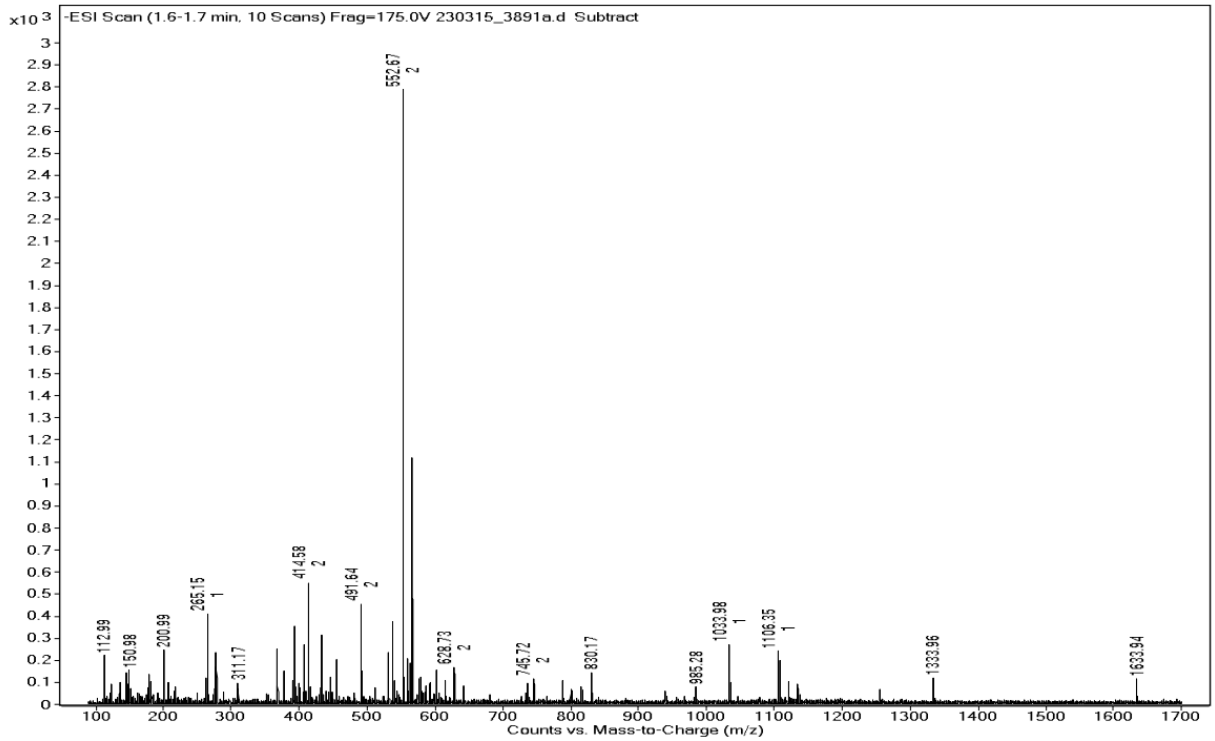

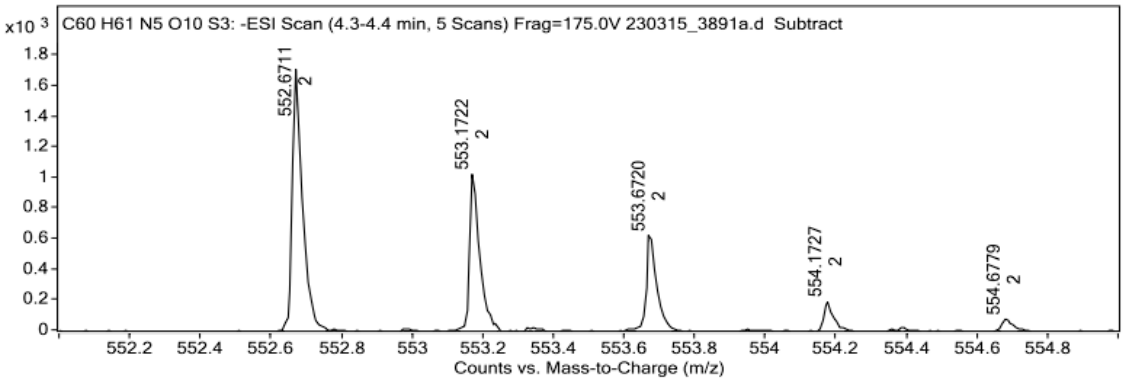

Predicted Isotope Match Table

Isotope	*m/z*	*Calc m/z*	Diff (mDa)	Abund (%)	Calc Abund (%)	+/-
1	552.6711	552.6718	-0.7	100.0	100.0	0.0
2	553.1722	553.1733	-1.1	62.1	70.1	8.0
3	553.6720	553.6730	-1.0	38.4	39.7	1.3
4	554.1727	554.1733	-0.6	11.6	16.3	4.7

Figure s20. Mass spectrum obtained for $TPPS_3$-NCS [**2A**] conjugated fatty acids ($TPPS_3$-Stearic [**2D]** and $TPPS_3$-Palm [**2C**]) on Agilent 6538 Q-TOF system in ESI MS Negative mode. MS (ESI) m/z calculated for $TPPS_3$-Palm MS (ESI) m/z calculated for $[M]^-$ $C_{60}H_{60}N_5O_{10}S_3^-$: 1106.35 Found 1106.35. calculated for $[M]^{-2}$ $C_{60}H_{59}N_5O_{10}S_3^{-2}$: 552.6718 Found 552.6711. $TPPS_3$-Stearic $[M]^{-2}$ $C_{62}H_{63}N_5O_{10}S_3^{-2}$: 566.69 Found 566.69.

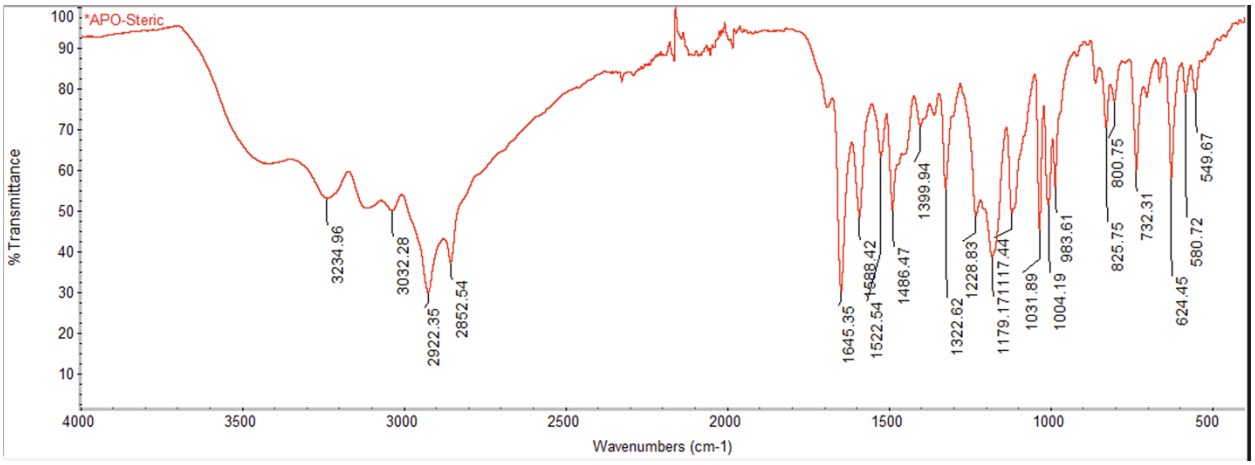

Figure s21. Fourier transform infrared spectroscopy of $TPPS_3$-NCS [**2A**] conjugated fatty acids ($TPPS_3$-Stearic [**2D]** and $TPPS_3$-Palm [**2C**]) (FTIR-ATR, Thermo Scientific Nicolet iS50) of $TPPS_3$-FA. FTIR: γcm^{-1}: 2922 and 2853 (C-H stretch), 1522 (N-H in plane bend).

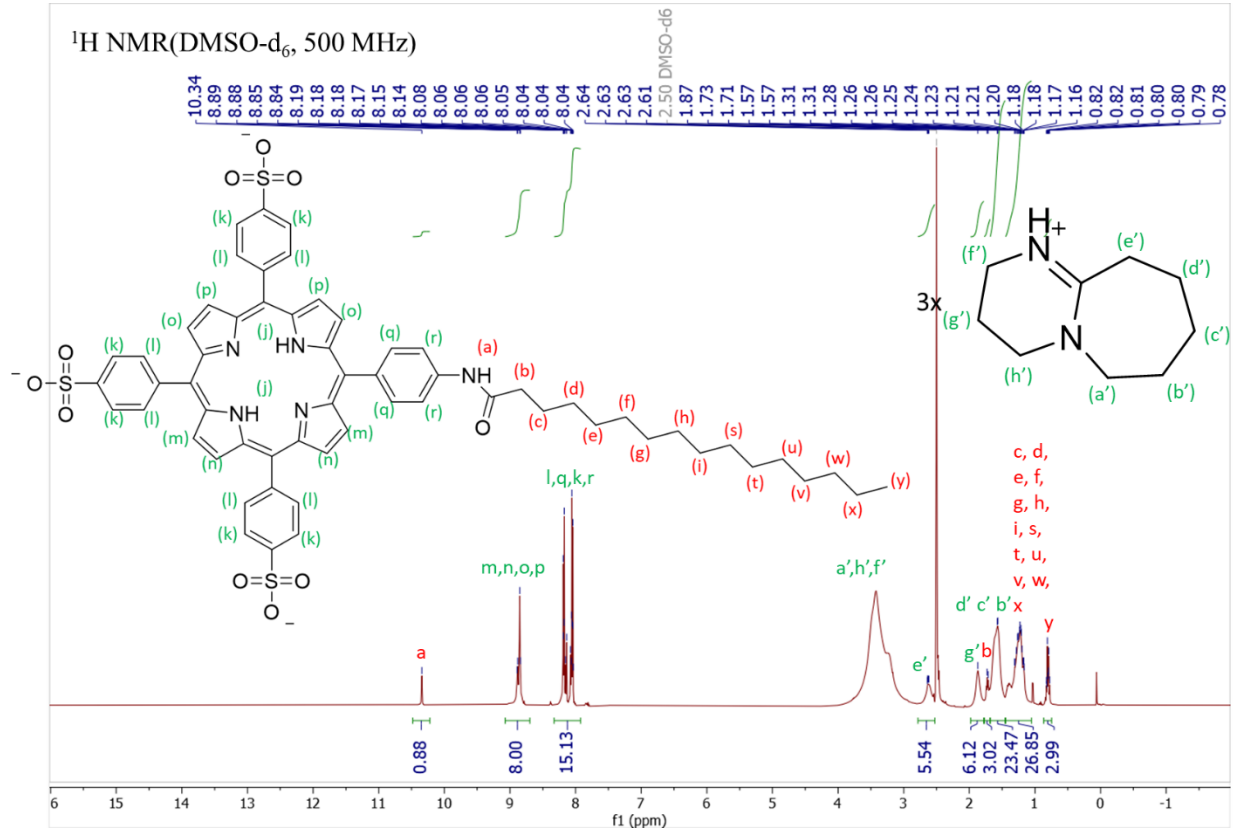

Figure s22. ^1H NMR spectrum of $TPPS_3$-NCS [**2A**] conjugated fatty acids ($TPPS_3$-Stearic [**2D]** and $TPPS_3$-Palm [**2C**]) acquired on Bruker US 500 MHz system. ^1H NMR (500 MHz, DMSO-d_6) δ (ppm) 10.34 (s, 1H), 8.85 (m, 8H, β-pyrrole), 8.14 (m, 16H), 2.62 (m, 6H), 1.87 (m 6H), 1.72 (sex, 2H), 1.57 (m, 18H), 1.29 (m, 26H), 0.80 (m, 3H)

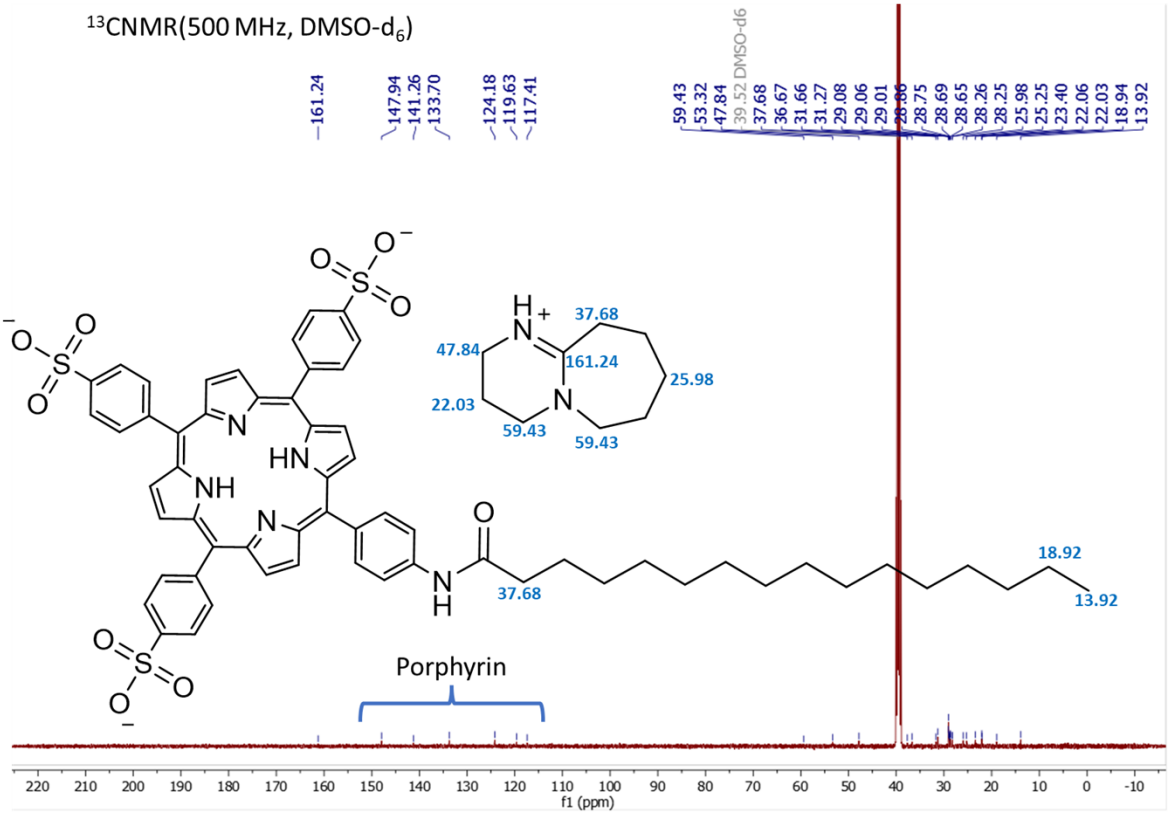

Figure s23. 13CNMR(500 MHz, DMSO-d6) $TPPS_3$-NCS [**2A**] conjugated fatty acids ($TPPS_3$-Stearic [**2D]** and $TPPS_3$-Palm [**2C**]) acquired on Bruker US 500 MHz system δ: 161.24 (1 C, DBU), 147.94, 141.26, 133.70, 124.18, 119.63, 117.41, 117.41, (45 C, tri-4-sulfonatophenyl)porphyrin) 53.32, 47.84, 37.68 (4 C, DBU), 36.67, 31.66, 31.27, 29.08 to 28.25 broad, 25.98, 25.25, 23.40, 22.06, 22.03, 18.94, 13.92 (16 to 18 C, Steric and Palmic acid).

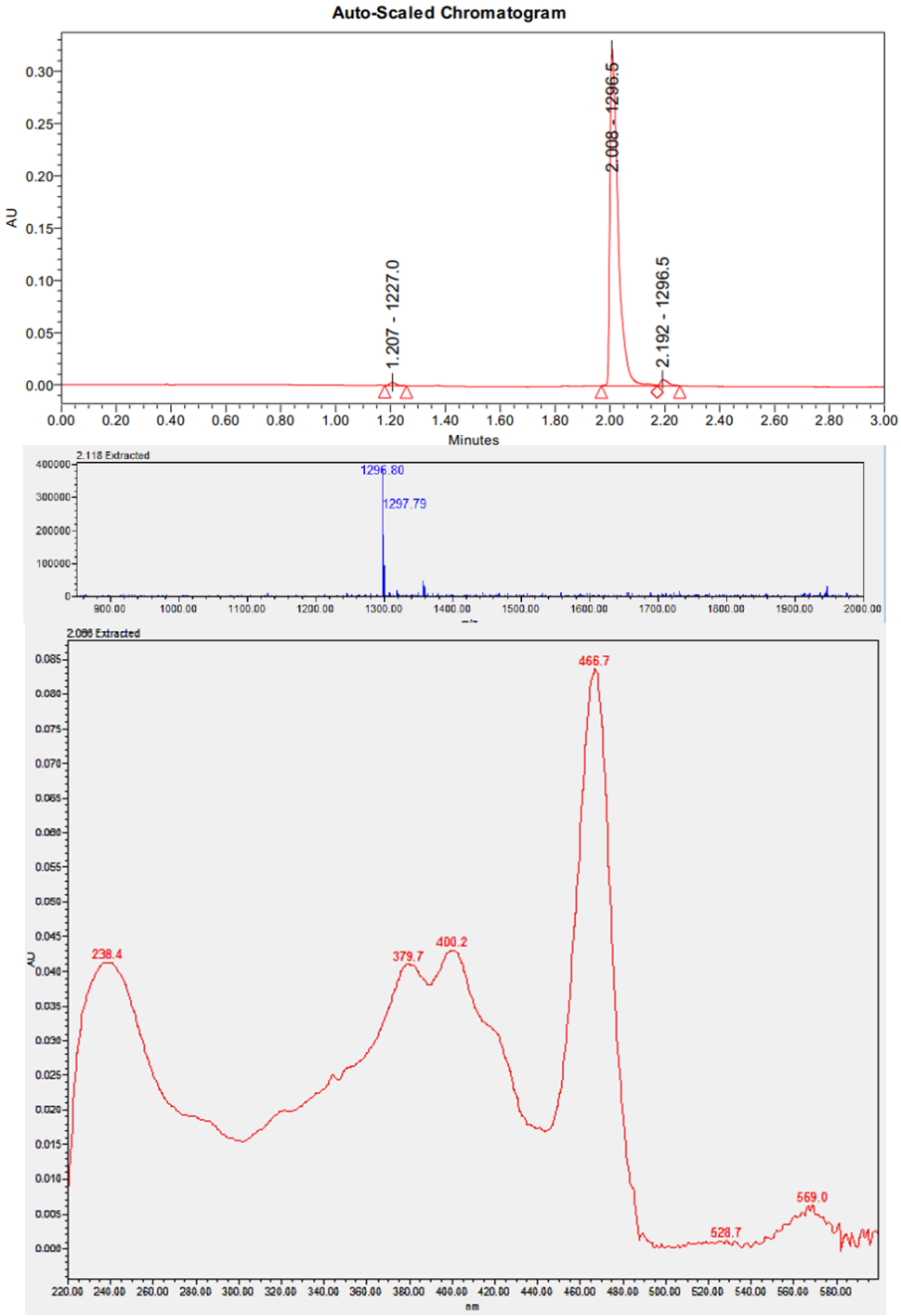

Figure s24. UHPLC-MS spectra of MITC-Deox [**1E**] recorded with Waters ACQUITY H-class UHPLC system with PDA detector recording at 467 nm and single quadrupole MS detector in positive mode. Elution occurred at 2.008 minutes. Mass spectrum obtained by MS (ESI) m/z calcd for $[M]^+$ $C_{68}H_{67}MnN_5O_{12}S_3^+$: 1296.3. Found: 1296.5. Accompanied by spectral profile found for MITC-Deox.

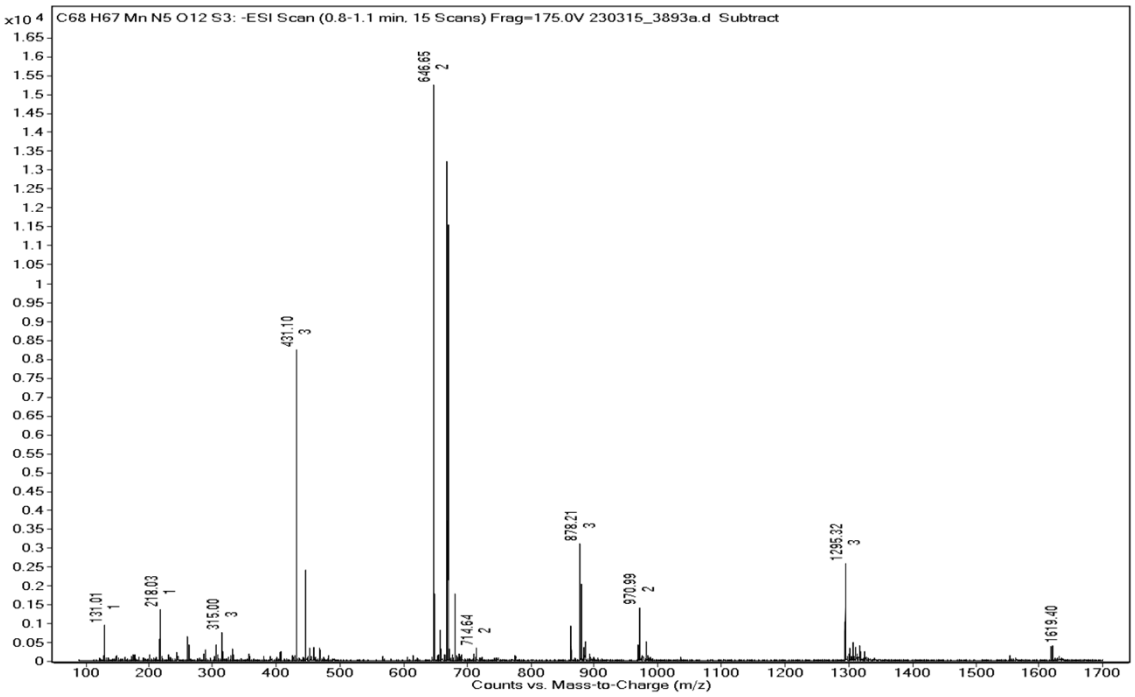

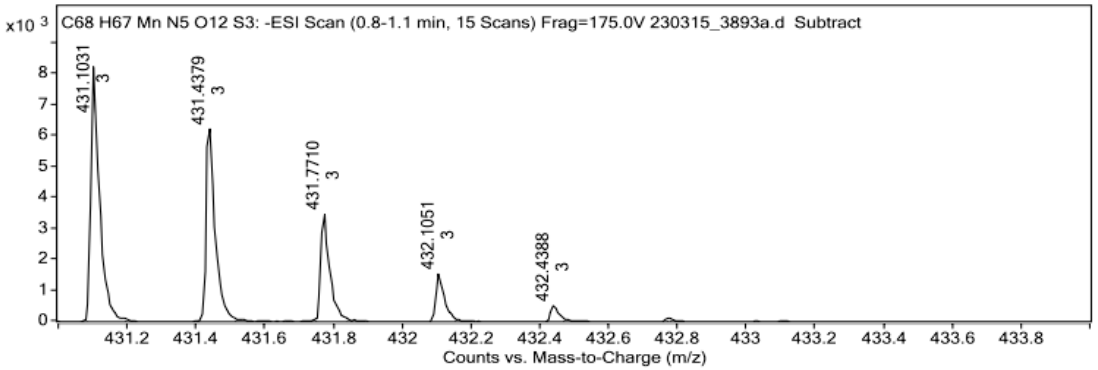

Predicted Isotope Match Table

Isotope	*m/z*	*Calc m/z*	Diff (mDa)	Abund (%)	Calc Abund (%)	+/-
1	431.1031	431.1037	-0.6	100.0	100.0	0.0
2	431.4379	431.4381	-0.2	74.3	78.9	4.6
3	431.7710	431.7714	-0.4	41.2	46.6	5.4
4	432.1051	432.1049	0.2	18.4	20.3	1.9
5	432.4388	432.4384	0.4	6.3	7.3	1.0

Figure s25. Mass spectrum obtained for MITC-Deox [**1E**] with Agilent 6538 Q-TOF system in ESI MS Negative mode. MS (ESI) m/z calculated for $[M_3 - 3H]^-$ $C_{68}H_{67}MnN_5O_{12}S_3^{2-}$: 1295.33. found: 1295.32. Calculated for $[M_2 - 6H]^{4-}$ $(C_{68}H_{64}MnN_5O_{12}S_3^{2-})_2)^{4-}$: 646.66. found: 646.65. Calculated for $[M - 3H]^{3-}$ $C_{68}H_{64}MnN_5O_{12}S_3^{3-}$: 431.1037. found: 431.1031. Calculated for [M - 3H + formate]$^{2-}$ $C_{69}H_{66}MnN_5O_{14}S_3^{2-}$ 669.66 found 669.66. Calculated for $[M_2 - 4H + formate]^{3-}$ $C_{137}H_{131}Mn_2N_{10}O_{26}S_6^{3-}$ 878.21 found 878.21.

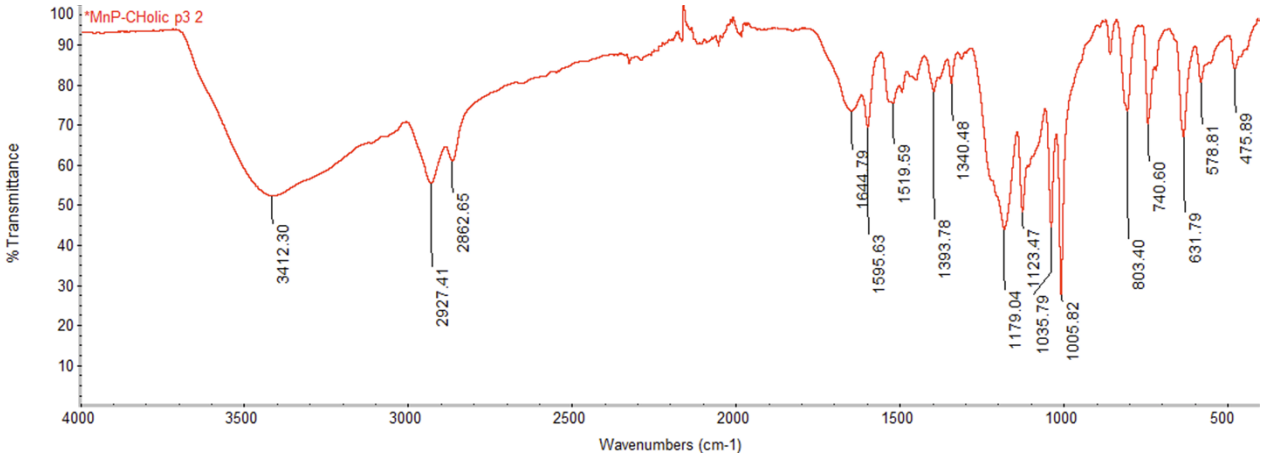

Figure s26. Fourier transform infrared spectroscopy (FTIR-ATR, Thermo Scientific Nicolet iS50) of MITC-Deox [**1E**]. FTIR: γcm^{-1}: 2927 and 2863 (C-H stretch), 1520 (N-H in plane bend).

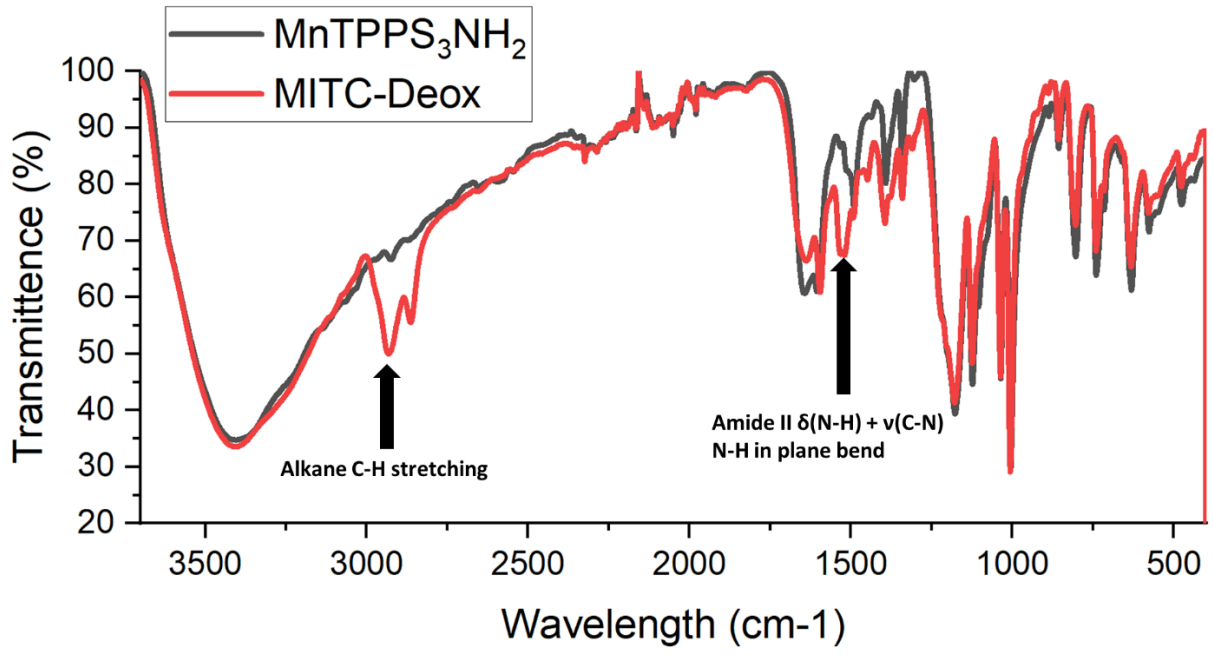

Figure s27. Fourier transform infrared spectroscopy (FTIR-ATR, Thermo Scientific Nicolet iS50) of MITC-Deox [**1E**] and $MnTPPS_3NH_2$ [**1B**] precursor. FTIR: γcm^{-1}: 2927 and 2863 (C-H stretch), 1520 (N-H in plane bend).

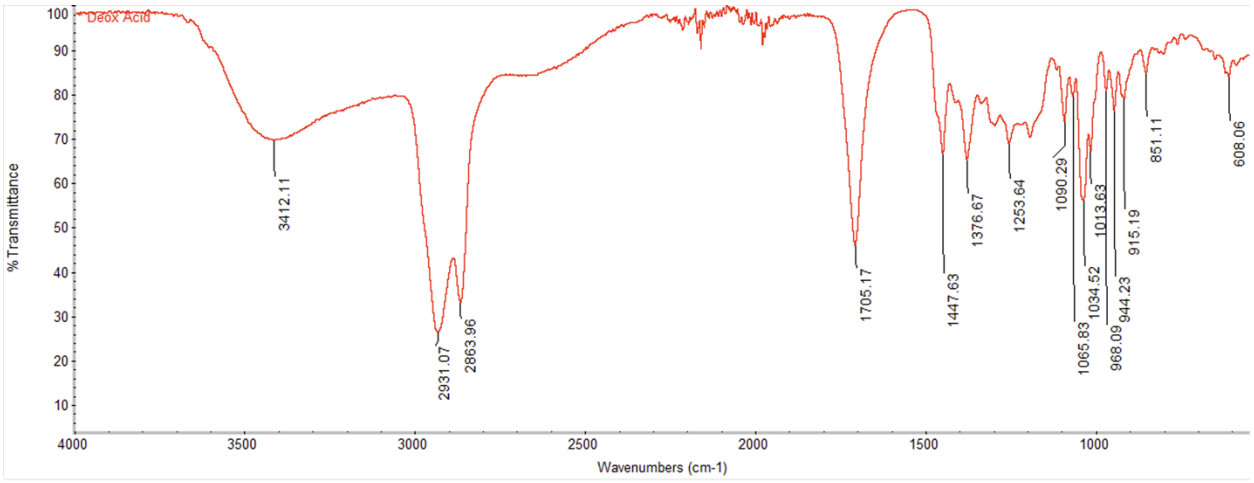

Figure s28. Fourier transform infrared spectroscopy (FTIR-ATR, Thermo Scientific Nicolet iS50) of deoxycholic acid.

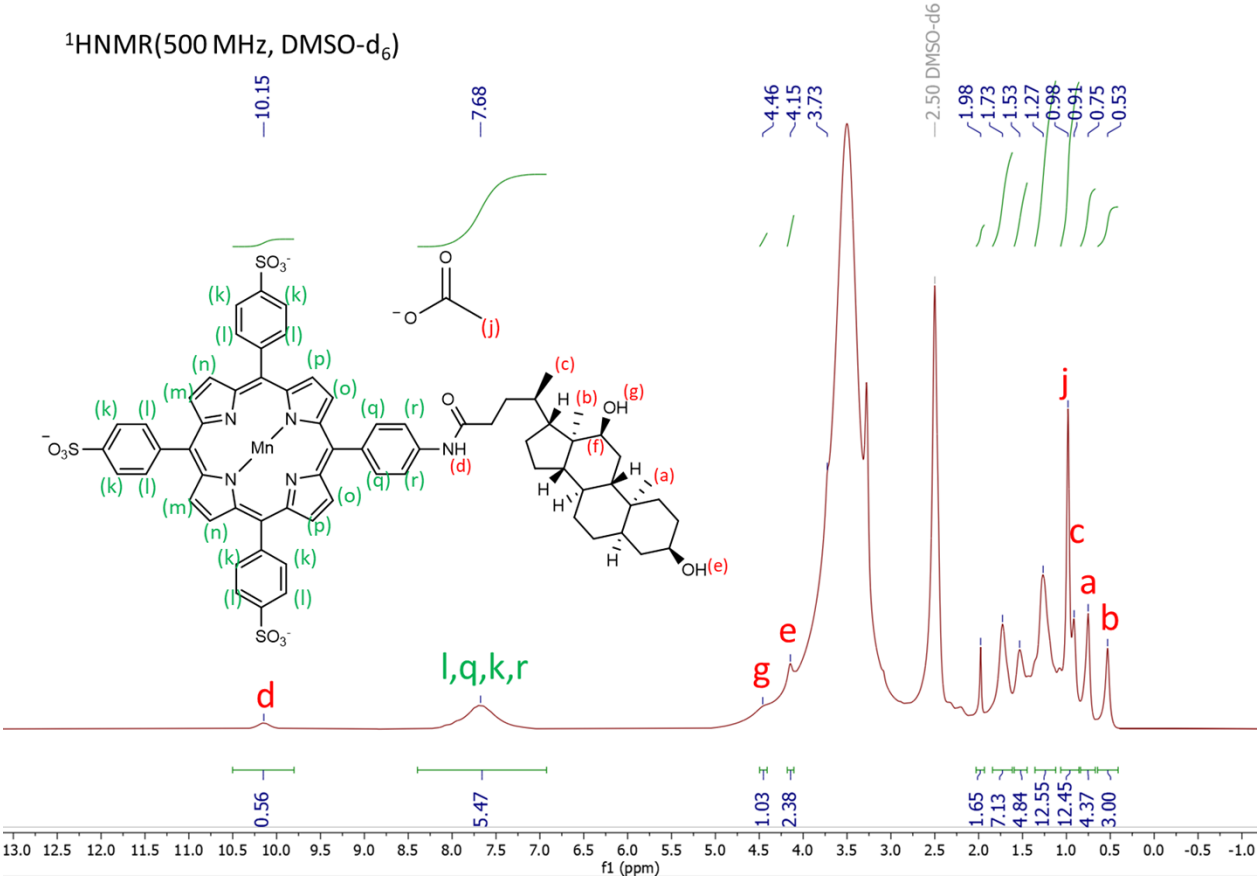

Figure s29. 1H NMR spectrum of MITC-Deox [**1E**] acquired on Bruker US 500 MHz system. ^{1}HNMR(500 MHz, DMSO-d_6) δ: 10.15 (b, 1H), 7.68 (b, 16H), 4.46 (b, 1H), 4.15 (b, 1H), 3.73 (b, 1H), 1.98 (b, 2H), 1.73 (b, 6H), 1.53 (b, 6H), 1.27 (b, 10H), 0.98 (s, 3H), 0.91 (b, 3H), 0.75 (b, 3H), 0.53 (b, 3H). Paramagnetic Mn^{3+} broadened and supressed nearby proton signals.

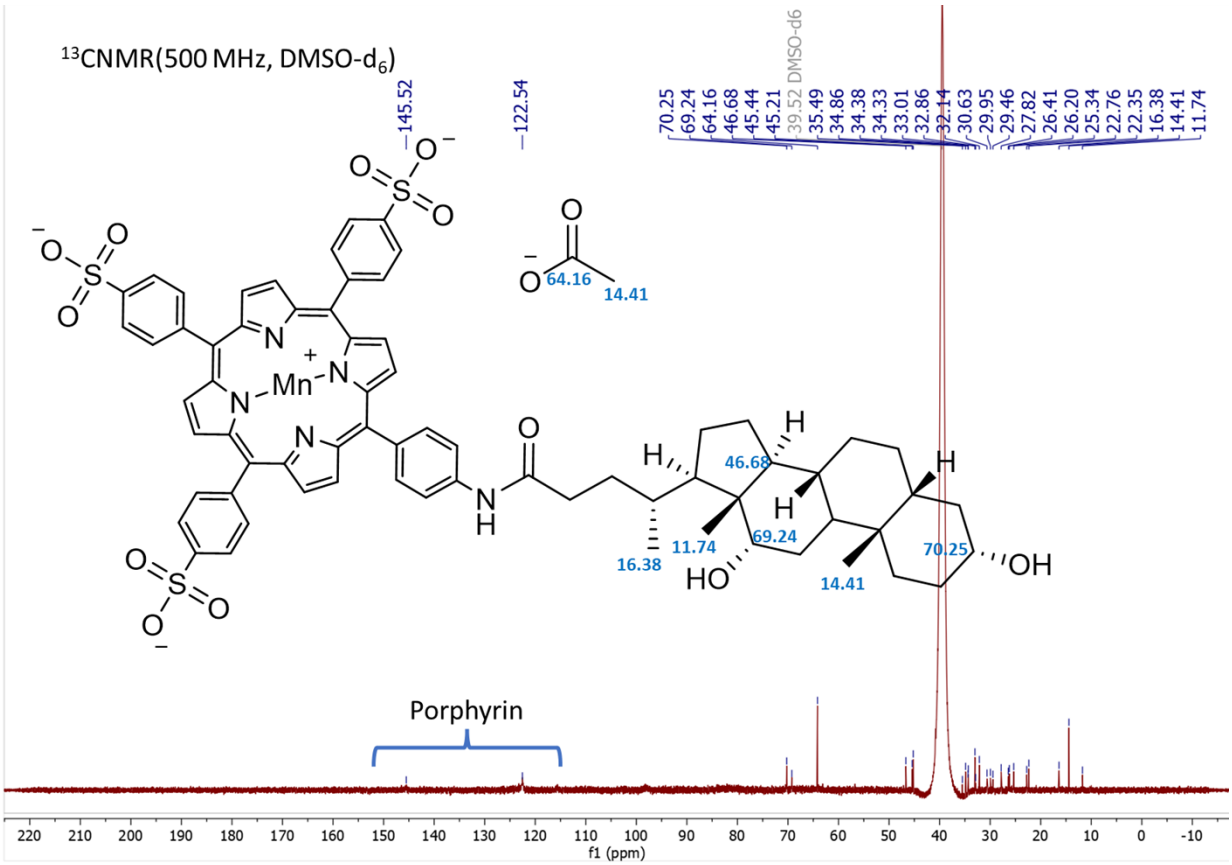

Figure s30. 13C NMR spectrum of MITC-Deox [**1E**] acquired on Bruker US 500 MHz system. ^{13}CNMR(500 MHz, DMSO-d_6) δ: 145.52, 122.54 (45 C, manganese tri-4-sulfonatophenyl)porphyrin), 70.25, 69.24, 46.68, 45.44, 45.21, 35.49, 34.86, 34.38, 34.33, 33.01, 32.86, 32.14, 30.63, 29.95, 29.46, 27.82, 26.41, 26.20, 25.34, 22.76, 22.35, 16.38, 11.74 (23 C, deoxycholic acid), 64.16, 14.41 (2 C, Acetate). Paramagnetic Mn^{3+} broadened and supressed nearby carbon signals.

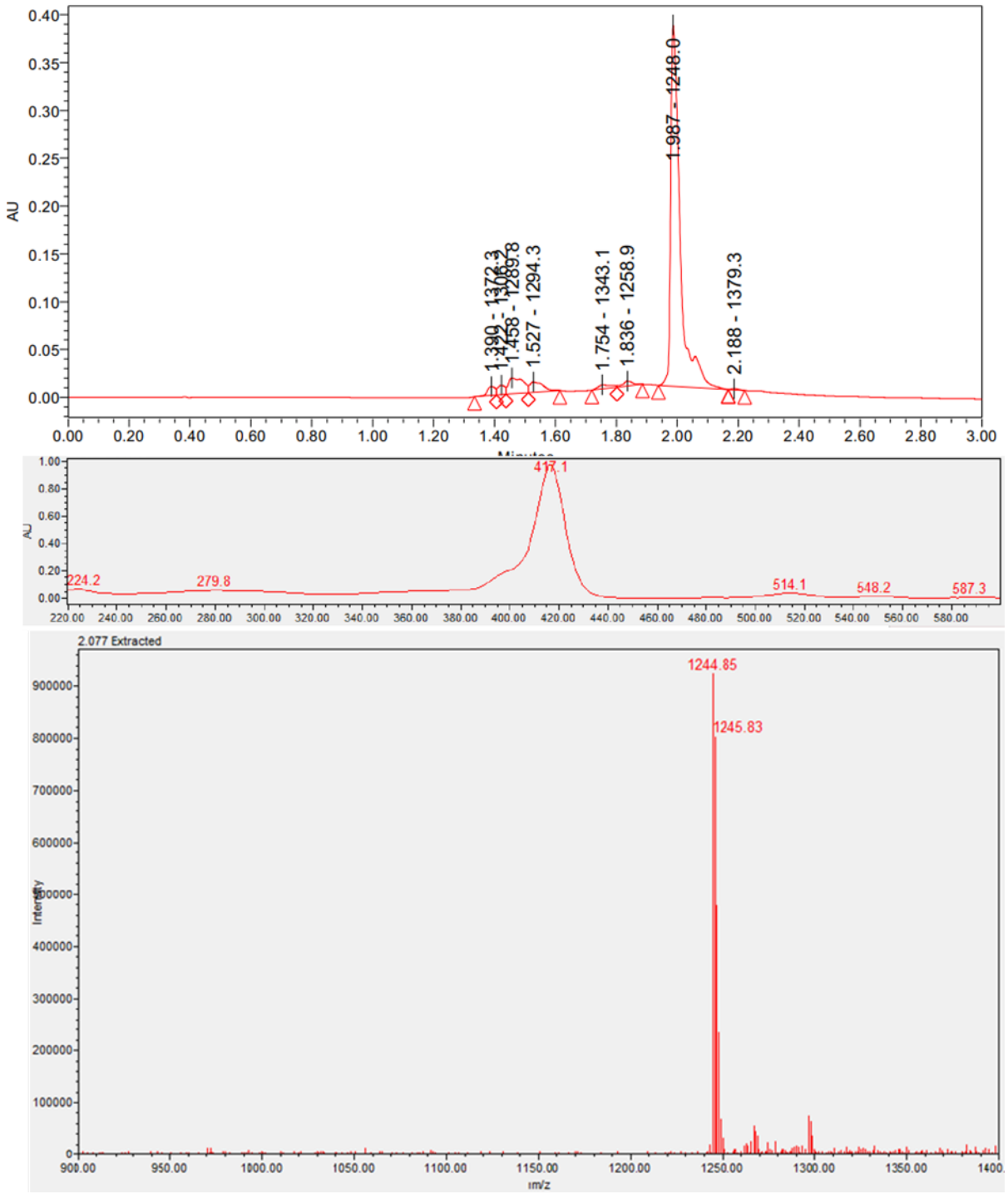

Figure s31. UHPLC-MS spectra of $TPPS_3$-Deox [**2E**] recorded Waters ACQUITY H-class UHPLC system with PDA detector recording at 419 nm and single quadrupole MS detector in positive mode. Elution occurred at 1.987 minutes. MS (ESI) m/z calculated for $[M + H]^+$ $C_{68}H_{70}N_5O_{12}S_3^+$: 1244.42. Found: 1244.85.

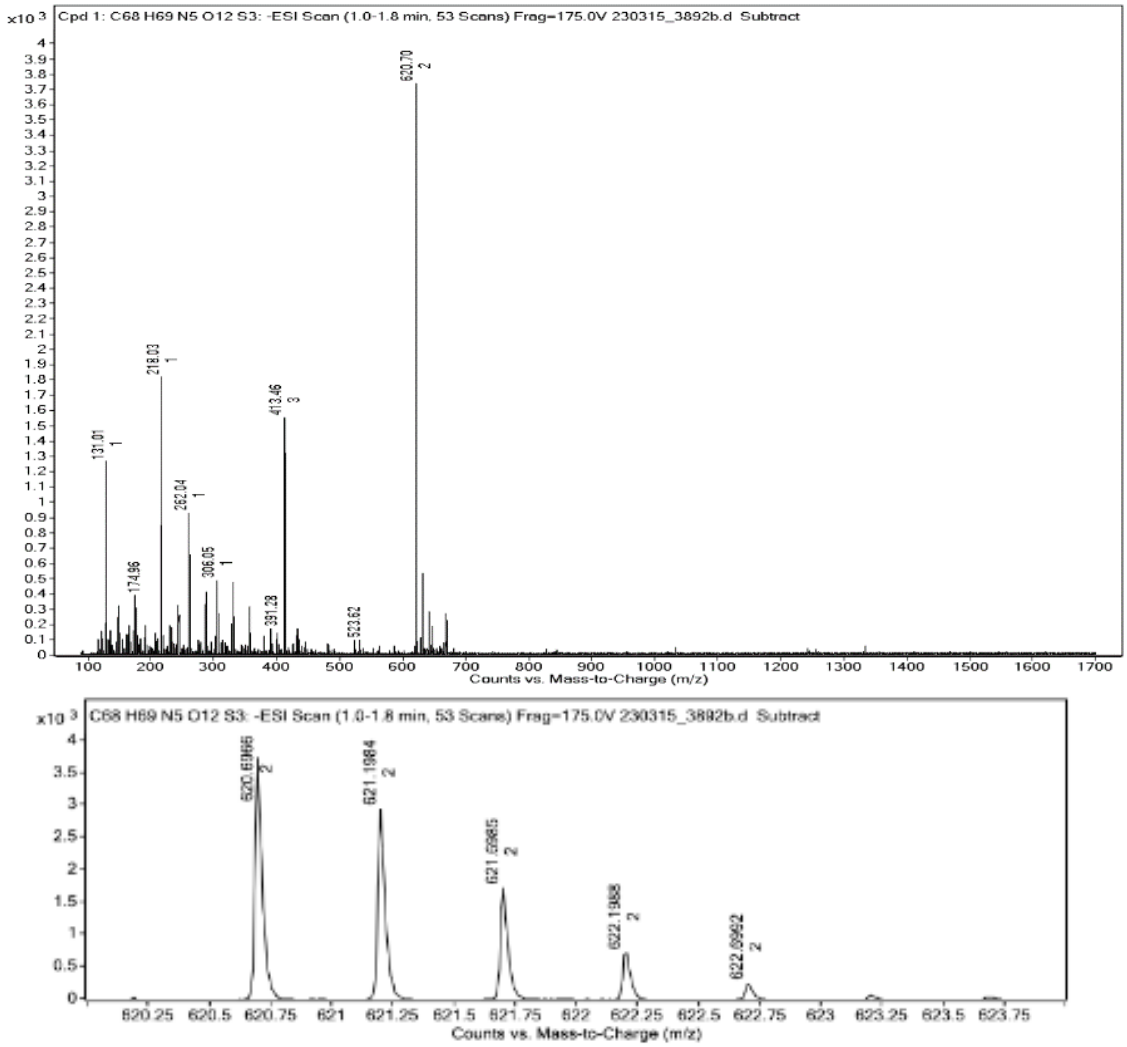

Predicted Isotope Match Table

Isotope	m/z	Calc m/z	Diff (mDa)	Abund (%)	Calc Abund (%)	+/-
1	620.6967	620.6980	-1.3	100.0	100.0	0.0
2	621.1985	621.1995	-1.0	78.2	79.0	0.8
3	621.6986	621.6995	-0.9	45.4	46.7	1.3
4	622.1989	622.1999	-1.0	19.4	20.3	0.9
5	622.6993	622.7000	-0.7	6.7	7.3	0.6

Figure s32. Mass spectrum obtained for $TPPS_3$-Deox [**2E**] with Agilent 6538 Q-TOF system in ESI MS Negative mode. MS (ESI) m/z calculated for $[M - 2H]^{2-}$ $C_{68}H_{67}N_5O_{12}S_3^{2-}$: 620.6967. found: 620.6980. Calculated for $[M - 3H]^{3-}$ $C_{68}H_{66}N_5O_{12}S_3^{3-}$: 413.46. found: 413.46.

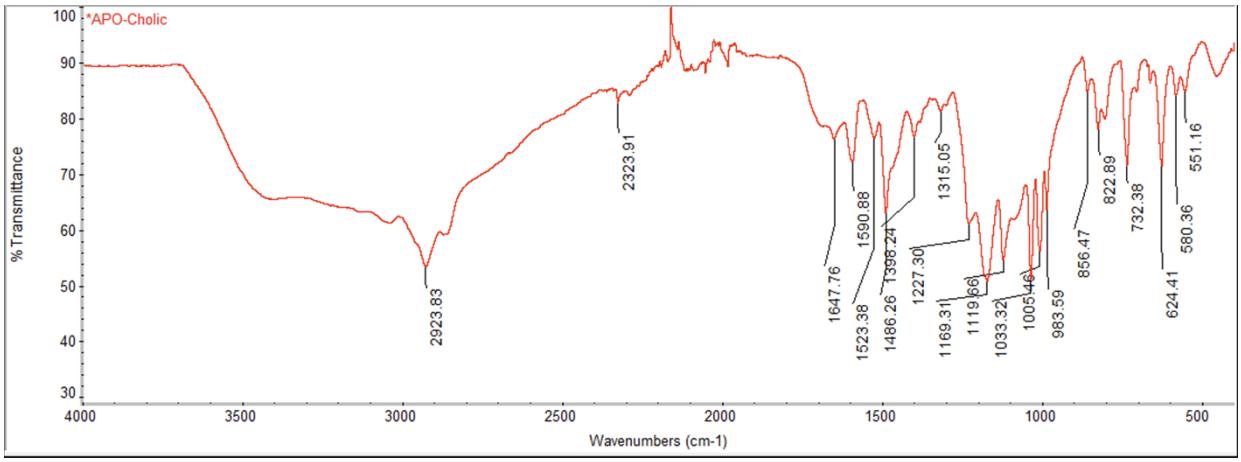

Figure s33. Fourier transform infrared spectroscopy (FTIR-ATR, Thermo Scientific Nicolet iS50) of $TPPS_3$-Deox [**2E**]. FTIR: γcm^{-1}: 2924 and 2854 (C-H stretch), 1523 (N-H in plane bend).

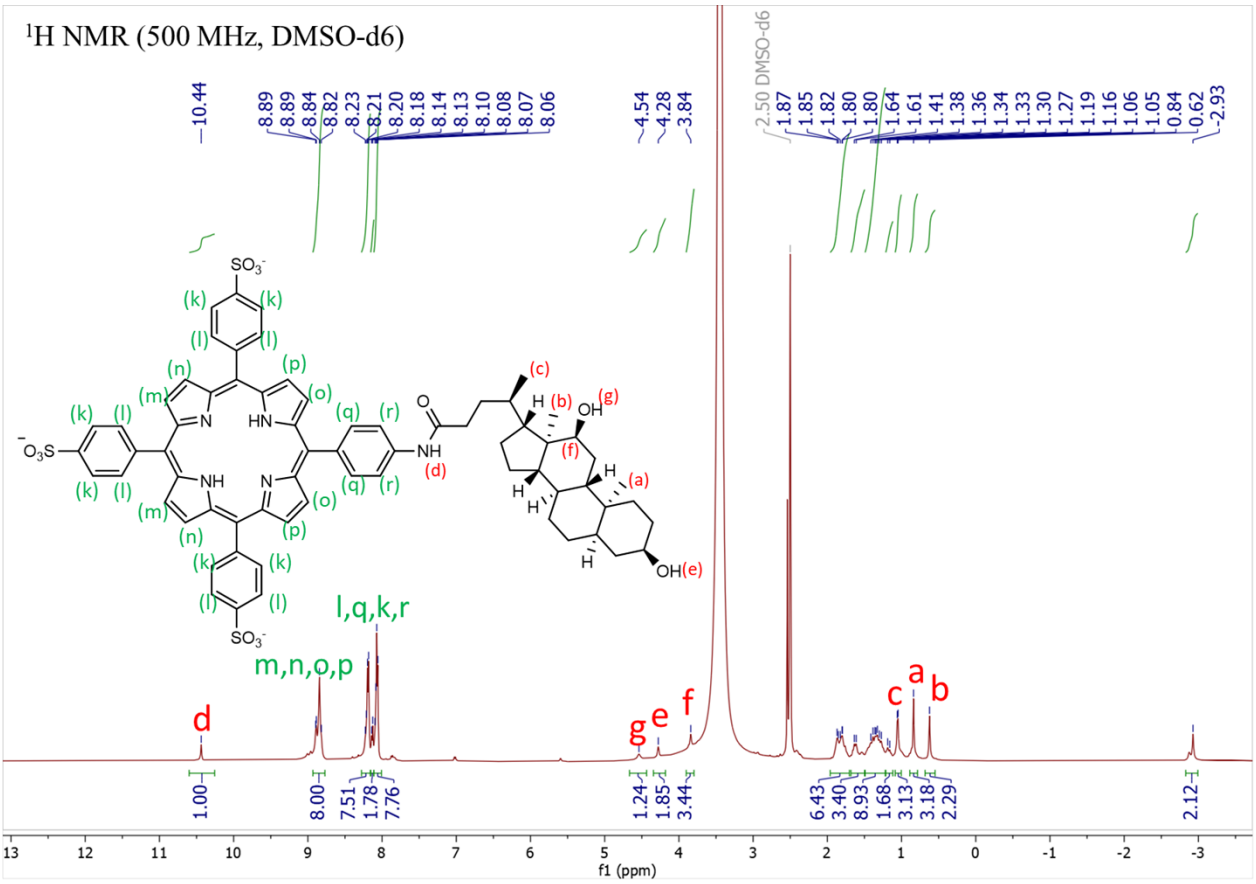

Figure s34. ^1H NMR spectrum of $TPPS_3$-Deox [**2E**] acquired on Bruker US 500 MHz system. ^1H NMR (500 MHz, DMSO-d_6) δ (ppm) 10.44 (s, 1H), 8.84 (m, 8H, β-pyrrole), 8.21 (m , J= 7.9 Hz, 6H), 8.13 (m, 2H), 8.07 (m 8H), 4.54 (b, 1H), 4.38 (b, 1H), 3.84 (b, 1H), 1.87 (m, 7H), 1.61 (m, 4H), 1.34 (m, 8H), 1.19 (m, 2H) 1.05 (d, 3H), 0.84 (s, 3H), 0.62 (s, 3H), -2.93 (s, 2H)

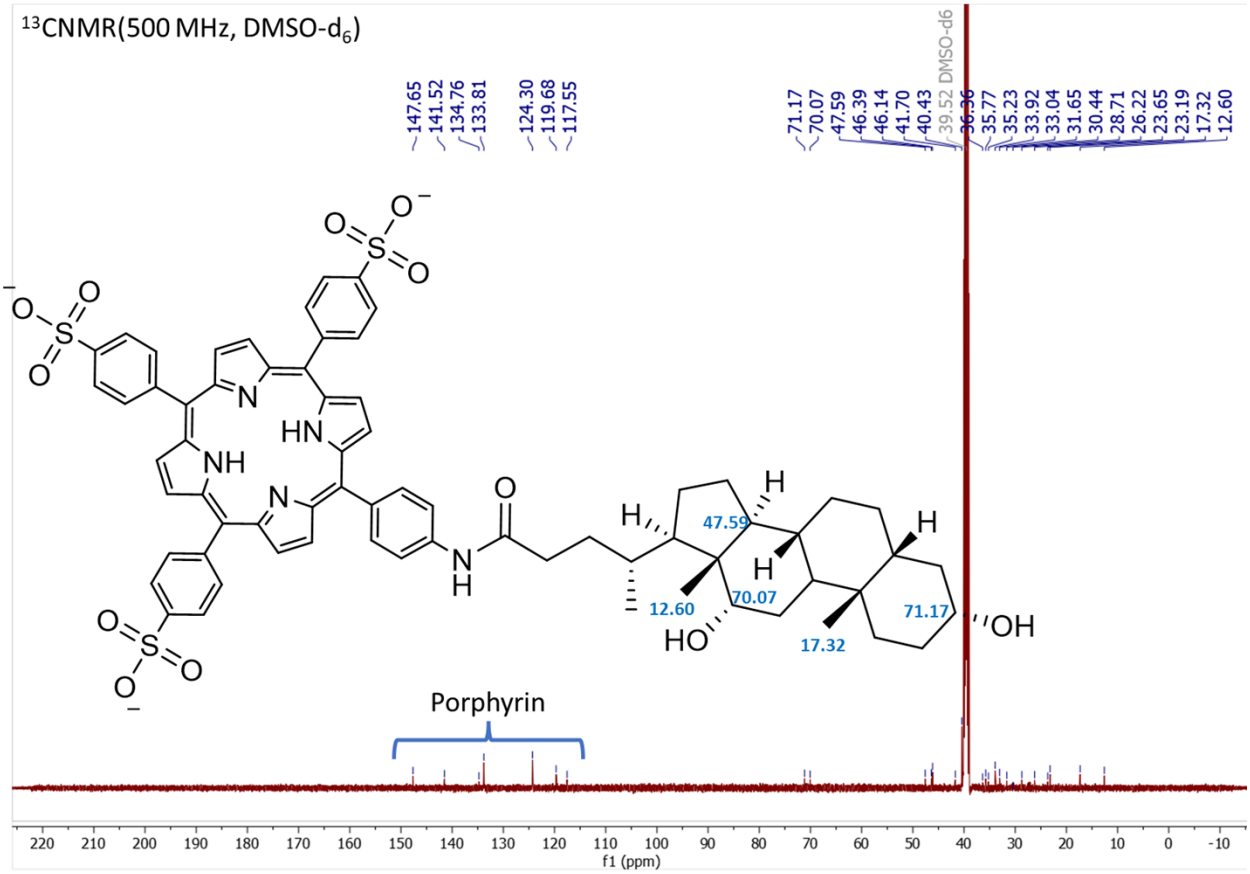

Figure s35. ^{13}C NMR spectrum of TPPS$_3$-Deox [**2E**] acquired on Bruker US 500 MHz system. ^{13}CNMR(500 MHz, DMSO-d$_6$) δ: 147.65, 141.52, 134.76, 133.81, 124.30, 119.68, 117.55 (45 C, tri-4-sulfonatophenyl)porphyrin), 71.17, 70.07, 47.59, 46.39, 46.14, 41.70, 40.43, 36.36, 35.77, 35.23, 33.92, 33.04, 31.65, 30.44, 28.71, 26.22, 23.65, 23.19, 17.32, 12.60 (23 C, deoxycholic acid).

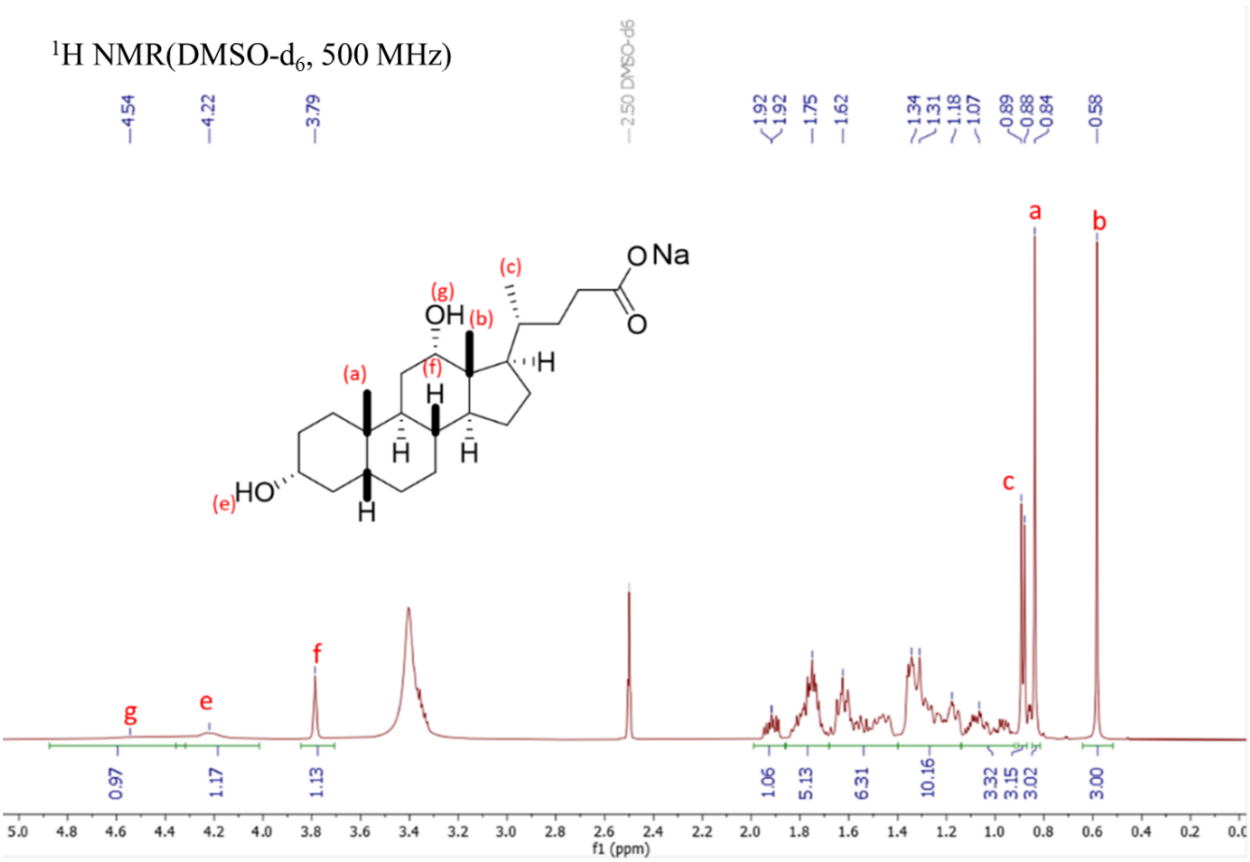

Figure s36. [1]H NMR spectrum of sodium deoxycholate acquired on Bruker US 500 MHz system. [1]H NMR (500 MHz, DMSO-d_6) δ (ppm) δ 4.54 (s, 1H), 4.22 (s, 1H), 3.79 (t, 1H), 1.92 (m, 1H), 1.75 (m, 5H), 1.62 (m, 6H), 1.31 (m, 10H), 1.07 (m, 3H), 0.88 (d, 3H), 0.84 (s, 3H), 0.58 (s, 3H).

.

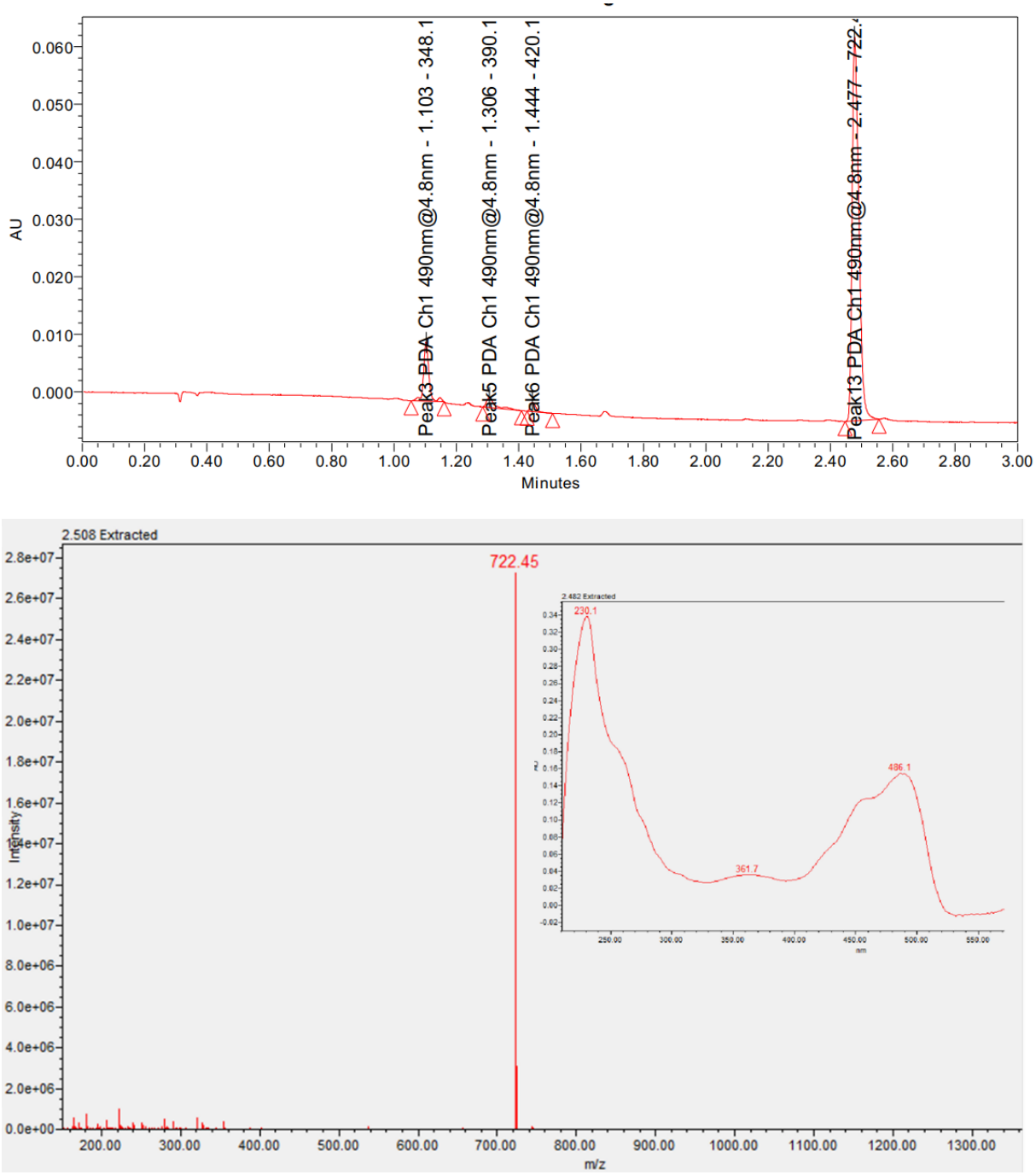

Figure s37. UHPLC-MS spectra of FITC-Deox [**3E**] recorded with Waters ACQUITY H-class UHPLC system with PDA detector recording at 490 nm and single quadrupole MS detector in positive mode 490 nm. Elution occurred at 2.471 minutes. MS (ESI) m/z calculated for $[M]^+$ $C_{44}H_{52}NO_8^+$: 722.37. Found: 722.45.

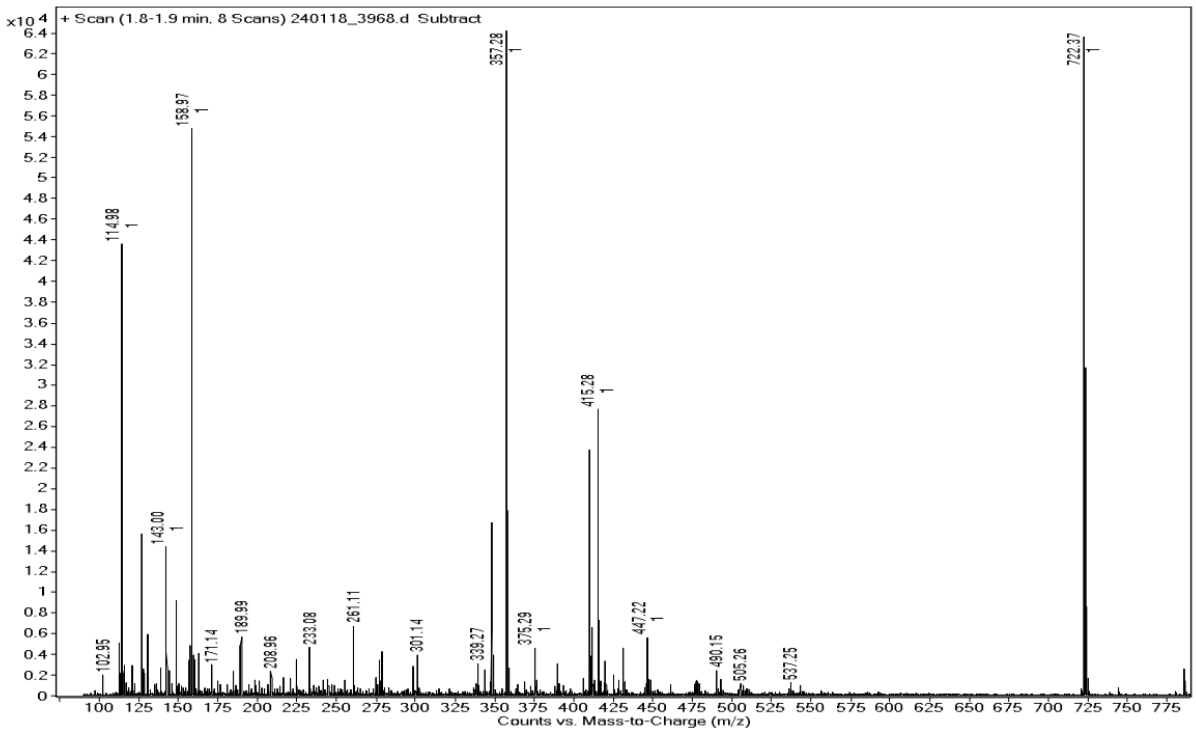

Predicted Isotope Match Table

Isotope	*m/z*	*Calc m/z*	Diff (mDa)	Abund (%)	Calc Abund (%)	+/-
1	722.3680	722.3687	-0.7	100.0	100.0	0.0
2	723.3711	723.3721	-1.0	48.4	48.9	0.5
3	724.3734	724.3751	-1.7	13.2	13.3	0.1
4	725.3759	725.3780	-2.1	2.5	2.6	0.1

Figure s38. Mass spectrum obtained for FITC-Deox [**3E**] with Agilent 6538 Q-TOF system in ESI MS positive mode. MS (ESI) m/z calculated for $[M]^+$ $C_{44}H_{52}NO_8^+$: 722.3687. Found: 722.3680.

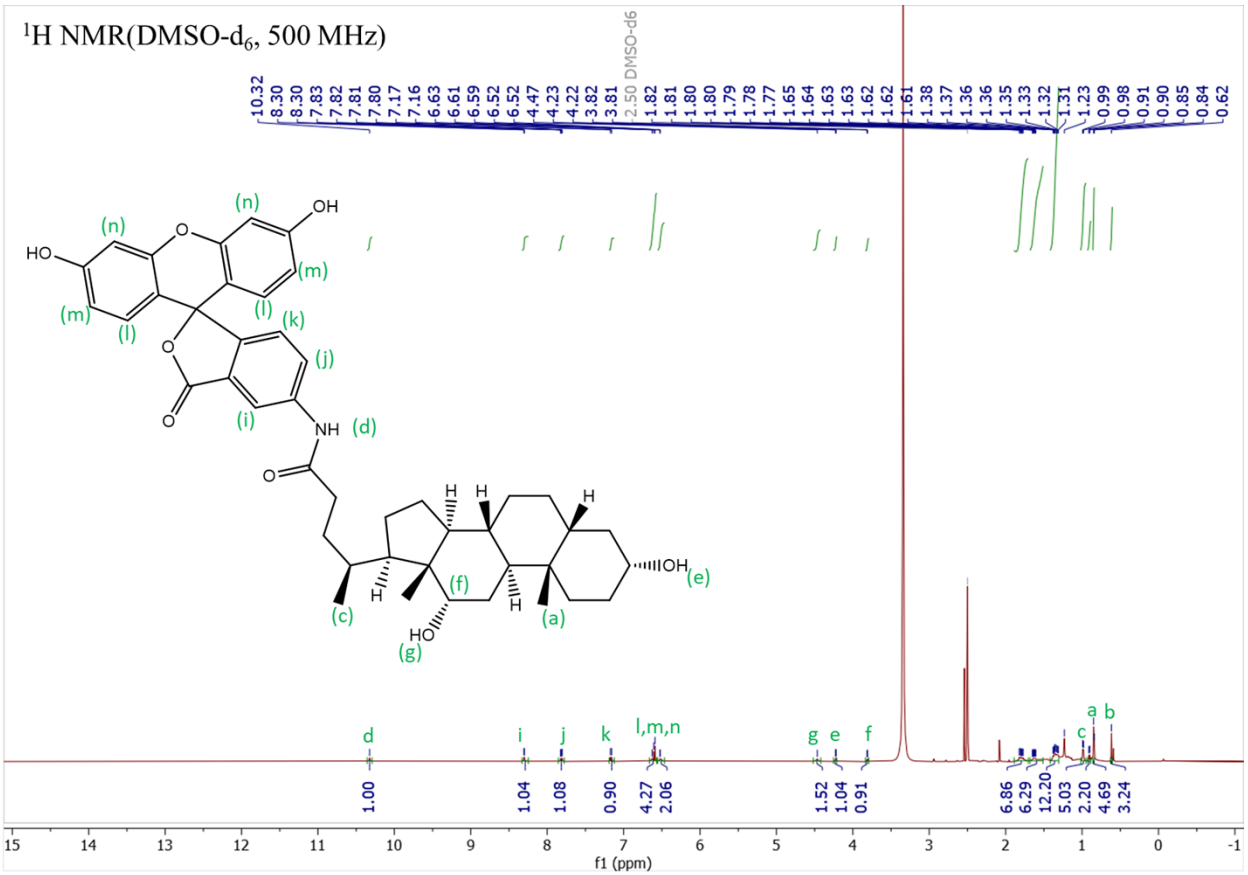

Figure s39. ^{1}H NMR spectrum of FITC-Deox [**3E**] acquired on Bruker US 500 MHz system. ^{1}H NMR (500 MHz, DMSO-d_6) δ (ppm) 10.32 (s, 1H), 7.81 (d, 1H), 7.16 (dd, 1H), 6.59 (m, 6H), 4.47 (s, 1H), 4.22 (d, 1H), 3.81 (m, 1H), 1.80 (m, 6H), 1.63 (m, 6H), 1.38 (m, 10H), 0.98 (d, 3H), 0.84 (s, 3H), 0.62 (s, 3H).

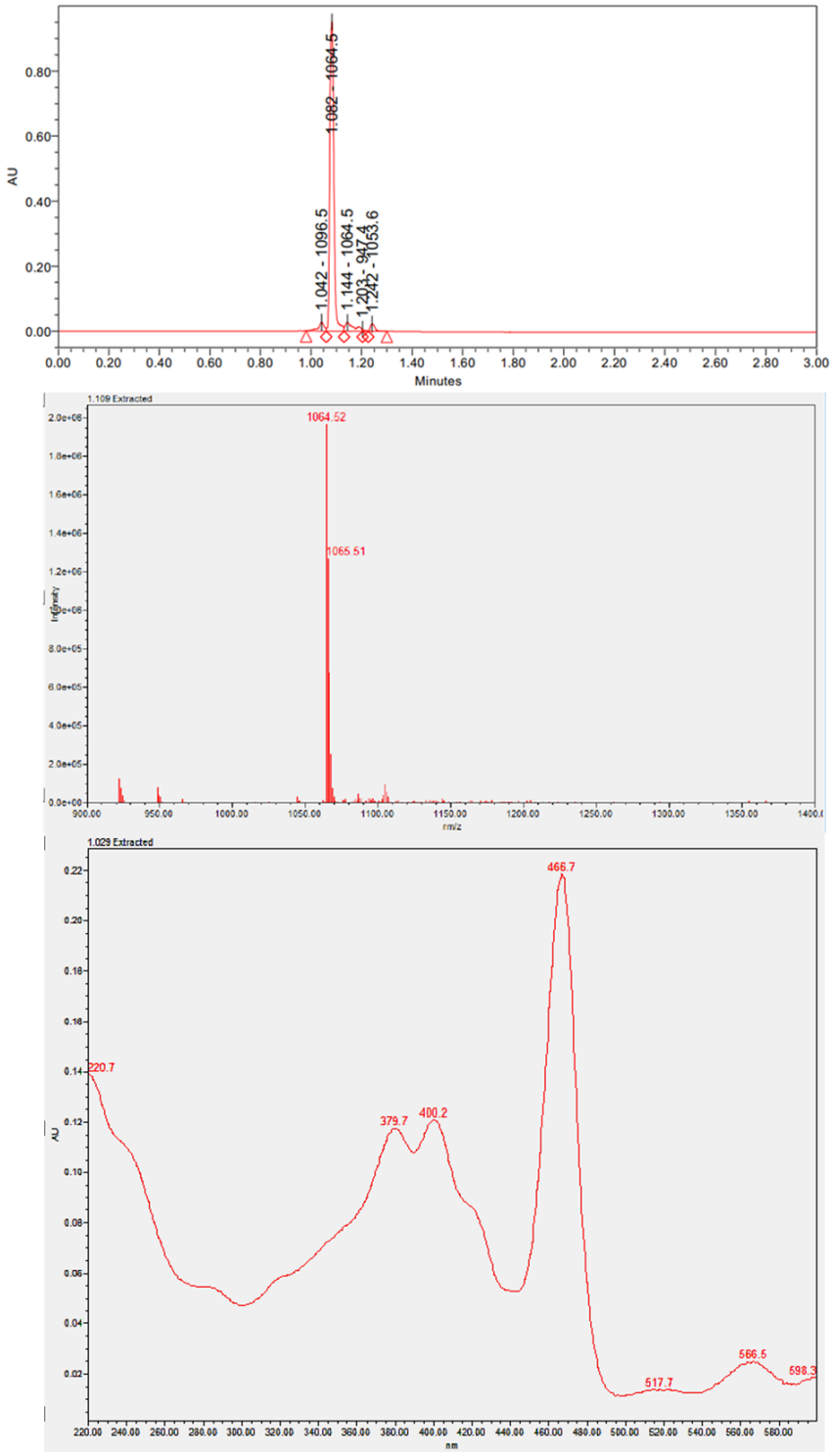

Figure s40. UHPLC-MS spectra of MITC-Hex [**1F**] recorded with Waters ACQUITY H-class UHPLC system with PDA detector recording at 467 nm and single quadrupole MS detector in positive mode. Elution occurred at 1.082 minutes. MS (ESI) m/z calcd for $[M]^+$ $C_{68}H_{67}MnN_5O_{12}S_3^+$: 1064.11. Found: 1064.52. Accompanied by spectral profile found for MITC-Hex.

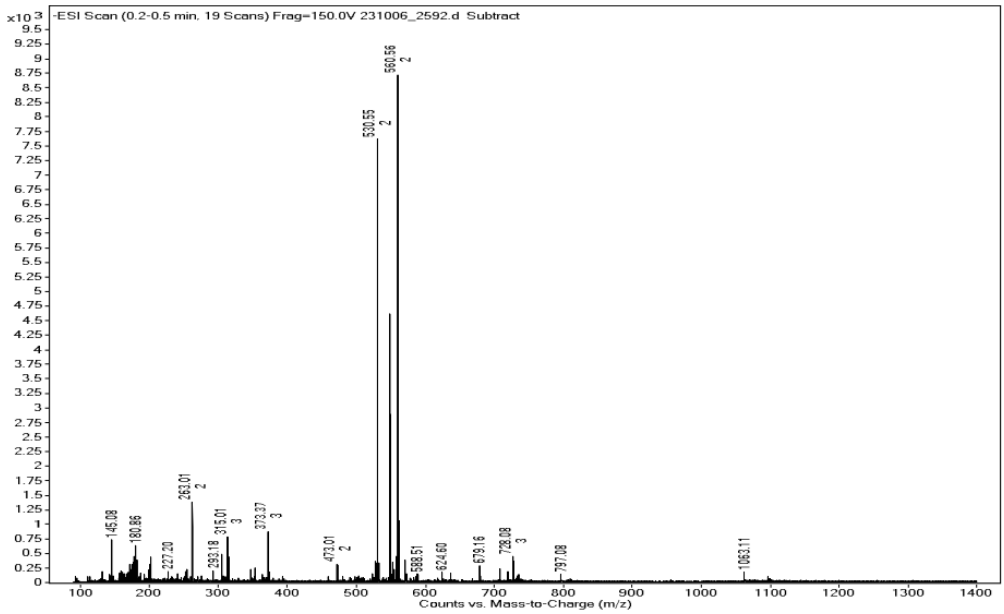

Target Ion Species

Ion Species	*m/z*	*Ionic Formula*
(M-2H)-2	530.5451	C51 H36 Mn N5 O12 S3

MFG Calculator Results

Target m/z	*Ionic Formula*	*Calc m/z*	*+/- (mDa)*	*+/- (ppm)*	*MFG Score*
530.5451	C51 H36 Mn N5 O12 S3	530.5457	-0.6	-1.1	99.27
530.5451	C50 H40 Mn N O16 S3	530.5450	0.1	0.2	98.99
530.5451	C52 H32 Mn N9 O8 S3	530.5464	-1.3	-2.5	97.58
530.5451	C56 H32 Mn N9 O3 S4	530.5451	0.0	0.0	97.53
530.5451	C63 H32 Mn N3 O5 S3	530.5448	0.3	0.6	97.49
530.5451	C55 H28 Mn N9 O8 S2	530.5447	0.4	0.8	96.98
530.5451	C64 H28 Mn N7 O S3	530.5454	-0.3	-0.6	96.49
530.5451	C55 H36 Mn N5 O7 S4	530.5445	0.6	1.1	96.15
530.5451	C54 H32 Mn N5 O12 S2	530.5440	1.1	2.1	96.03
530.5451	C59 H32 Mn N3 O10 S2	530.5460	-0.9	-1.7	95.60

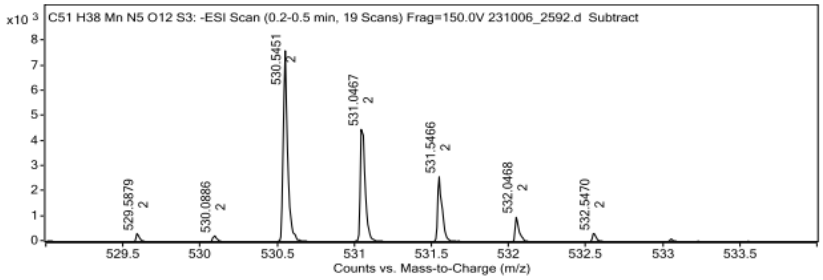

Predicted Isotope Match Table

Isotope	*m/z*	*Calc m/z*	Diff (mDa)	Abund (%)	Calc Abund (%)	+/-
1	530.5451	530.5457	-0.6	100.0	100.0	0.0
2	531.0467	531.0472	-0.5	62.5	60.2	-2.3
3	531.5466	531.5466	0.0	34.3	33.7	-0.6
4	532.0468	532.0470	-0.2	13.4	12.9	-0.5
5	532.5470	532.5469	0.1	4.4	4.3	-0.1
6	533.0459	533.0470	-1.1	1.4	1.2	-0.2

Figure s41. Mass spectrum obtained for MITC-Hex [**1F**] with Agilent 6538 Q-TOF system in ESI MS Negative mode. MS (ESI) m/z calculated for $[M\text{-}1H]^{1-}$ $C_{51}H_{38}MnN_5O_{12}S_3^-$: 1063.11. Found 1063.11. MS (ESI) m/z calculated for $[M_2\text{-}6H]^{4-}$ $((C_{51}H_{36}MnN_5O_{12}S_3)_2)^{4-}$: 530.5457. Found: 530.5451. MS (ESI) m/z calculated for $[M - 2H + acetate]^{2-}$ $(C_{53}H_{40}MnN_5O_{14}S_3)^{2-}$: 560.56. Found: 560.56.

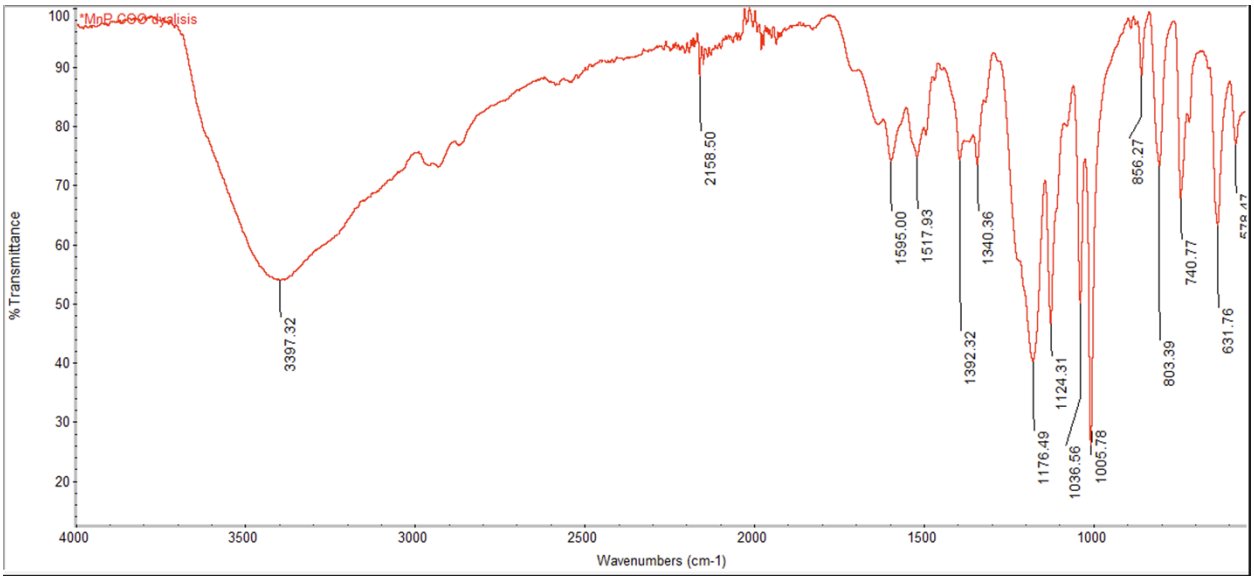

Figure s42. Fourier transform infrared spectroscopy (FTIR-ATR, Thermo Scientific Nicolet iS50) of MITC-Hex [**1F**]. FTIR: 1517 (N-H in plane bend).

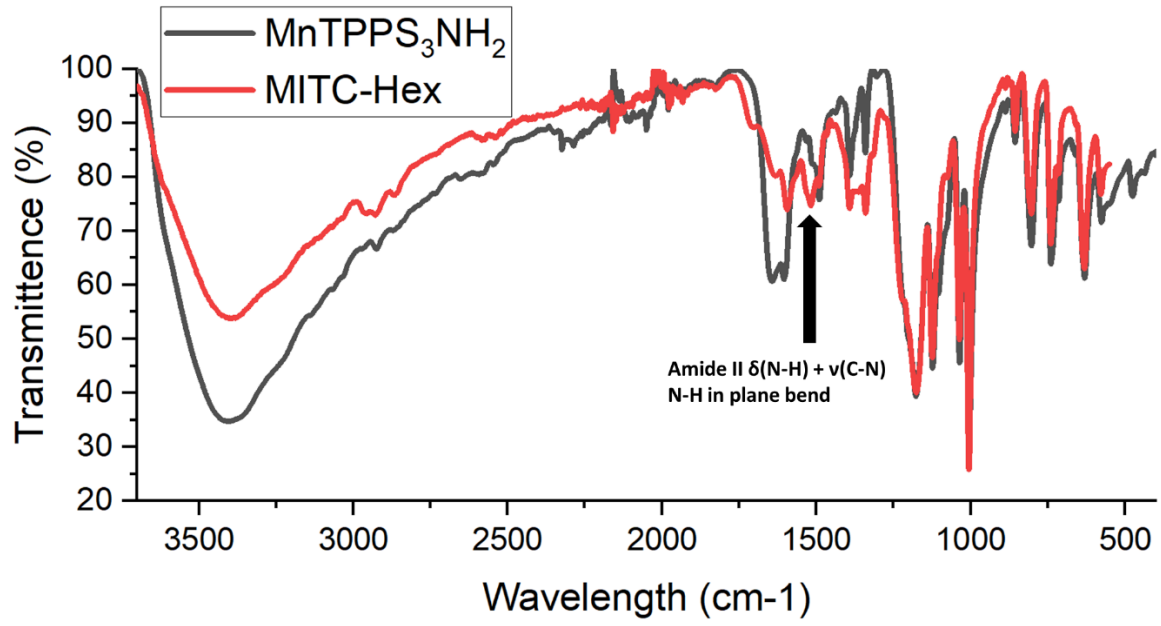

Figure s43. Fourier transform infrared spectroscopy (FTIR-ATR, Thermo Scientific Nicolet iS50) of MITC-Hex [**1F**] and $MnTPPS_3NH_2$ [**1B**] precursor. FTIR: γcm^{-1}: 1517 (N-H in plane bend).

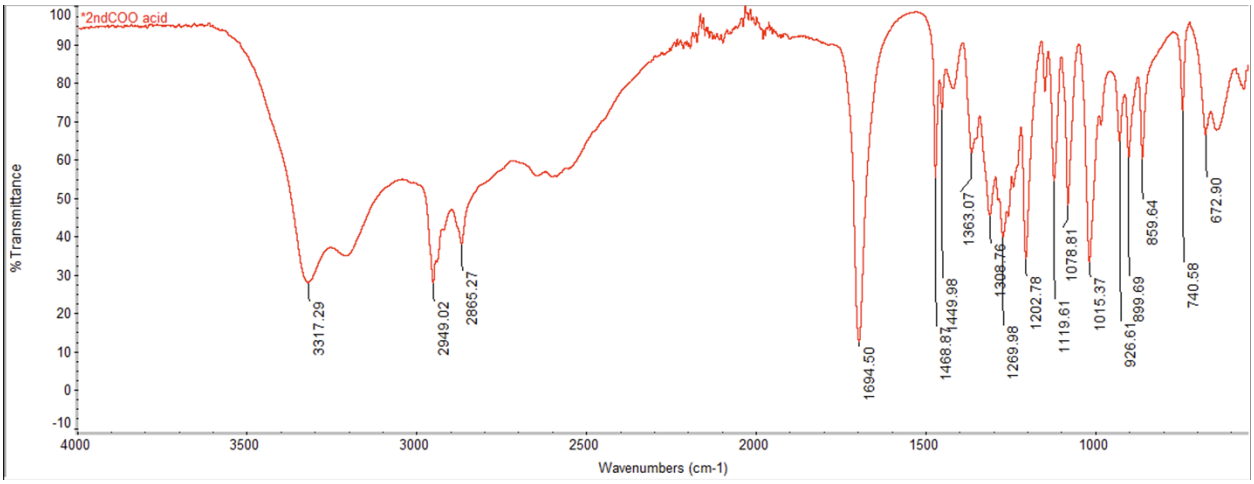

Figure s44. Fourier transform infrared spectroscopy (FTIR-ATR, Thermo Scientific Nicolet iS50) of 3,5-dihydroxycyclohexanecarboxylic acid.

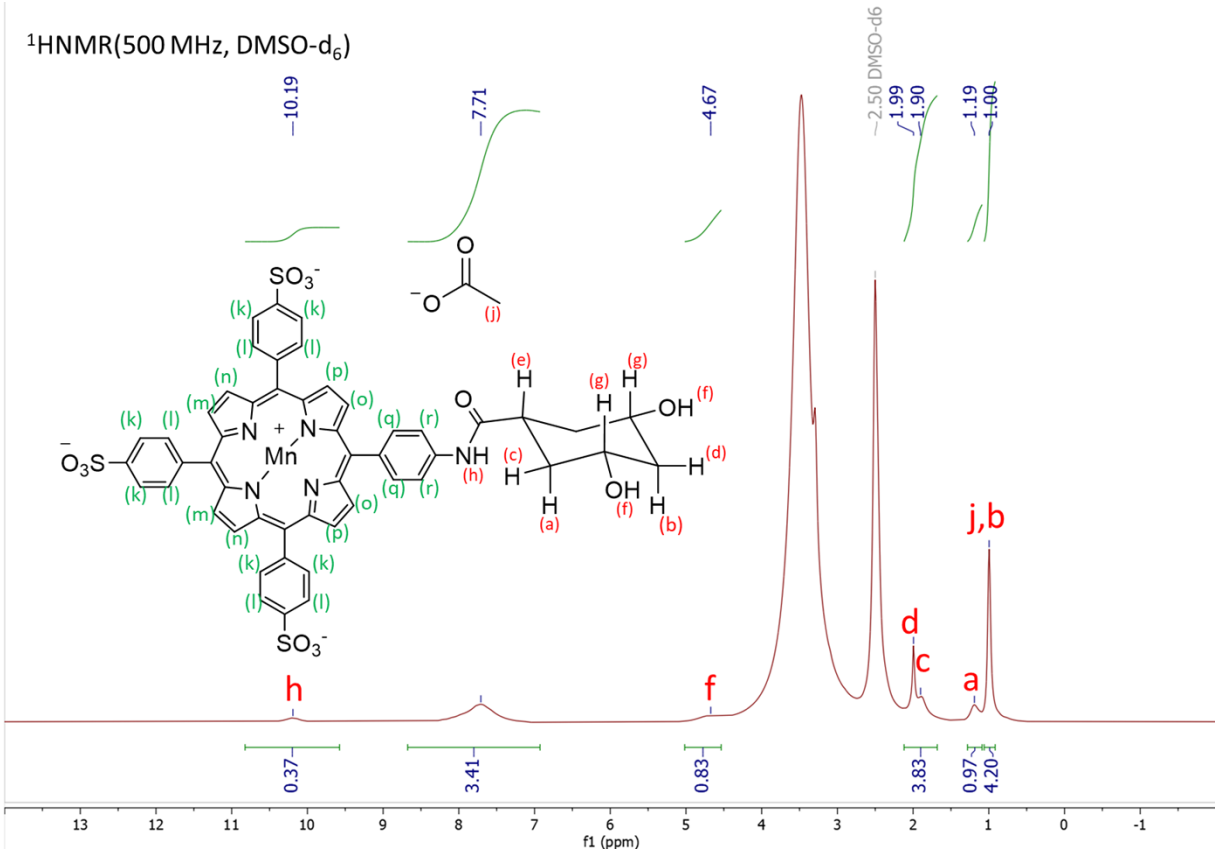

Figure s45 ^{1}H NMR spectrum of MITC-Hex [**1F**] acquired on Bruker US 500 MHz system. ^{1}HNMR(500 MHz, DMSO-d_6) δ: 10.19 (b, 1H), 7.71 (b, 16H), 4.67 (b, 2H), 1.99 to 1.90 (m, 3H), 1.19 (b, 1H), 1.00 (b, 3H). Paramagnetic Mn^{3+} broadened and supressed nearby proton signals.

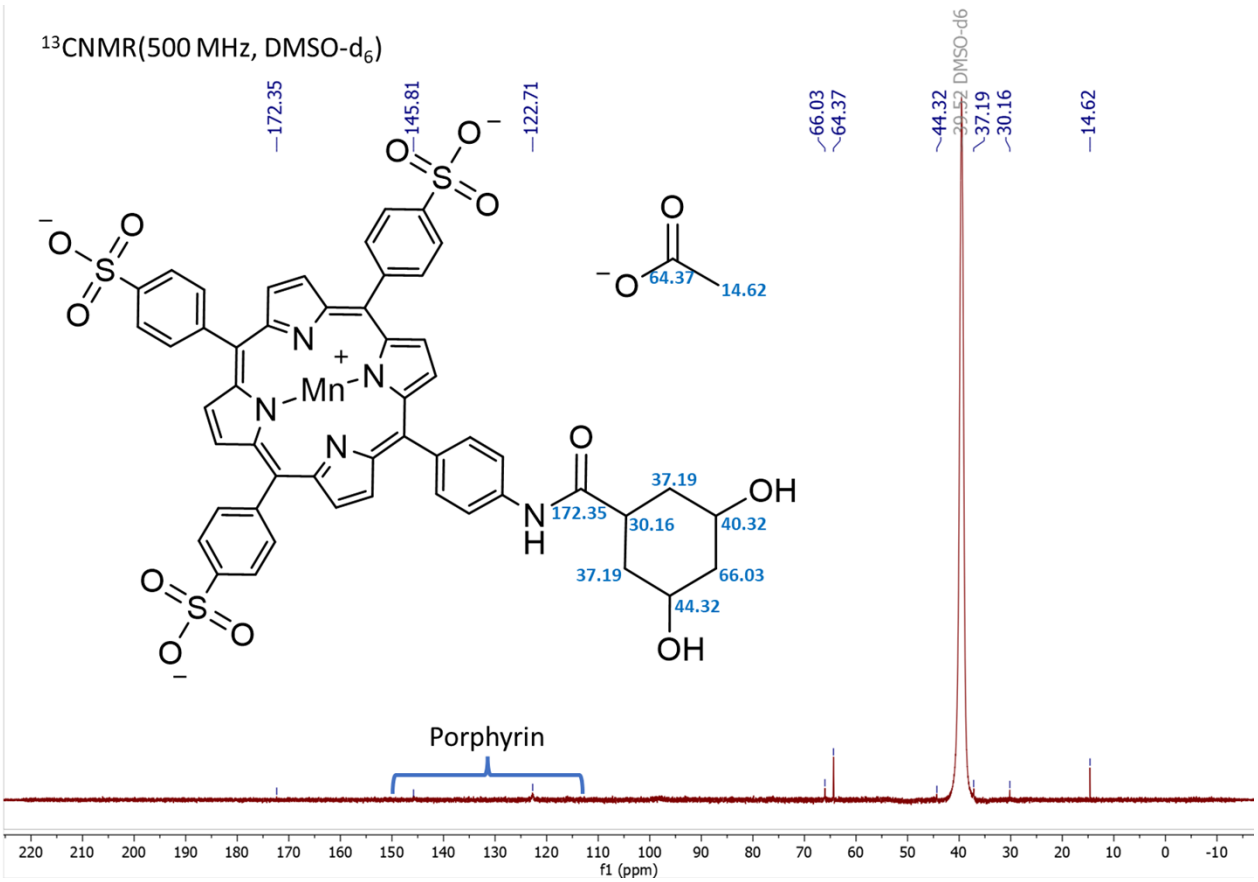

Figure s46. ^{13}C NMR spectrum of MITC-Hex [**1F**] acquired on Bruker US 500 MHz system. ^{13}CNMR(500 MHz, DMSO-d_6) δ: 172.35 (amide linkage) 145.81 122.71 (45 C, manganese tri-4-sulfonatophenyl)porphyrin), 66.03, 44.32, 37.19, 30.16 (6 C, cyclohexanediol), 64.37, 14.62 (2 C, Acetate) Paramagnetic Mn^{3+} broadened and supressed nearby carbon signals.

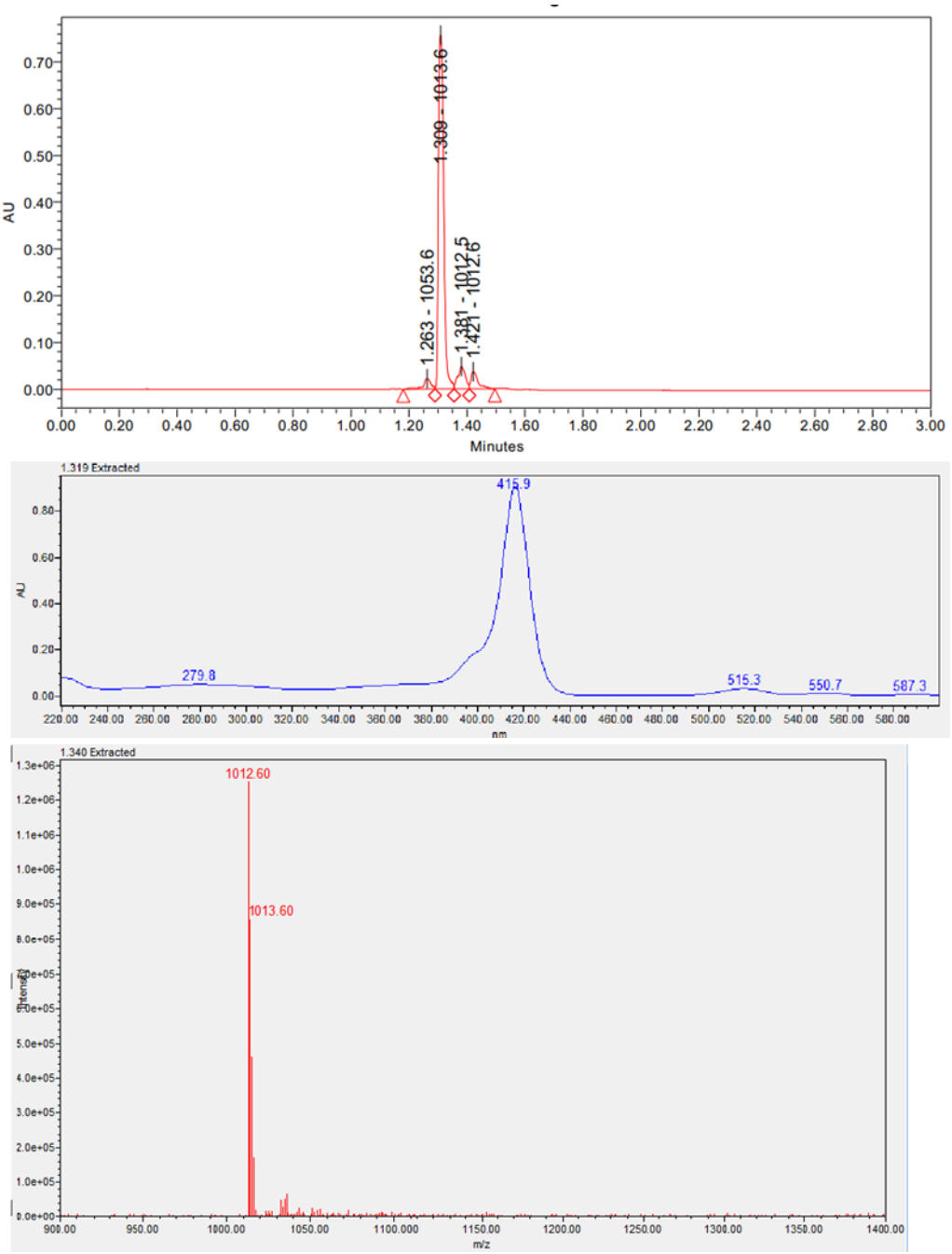

Figure s47. UHPLC-MS spectra of $TPPS_3$-Hex [**2F**] recorded with Waters ACQUITY H-class UHPLC system with PDA detector recording at 419 nm and single quadrupole MS detector in positive mode. Elution occurred at 1.309 minutes. Mass spectrum obtained by Waters ACQUITY H-class UHPLC system with PDA detector and single quadrupole MS detector in positive mode. MS (ESI) m/z calcd for $[M+H]^+$ $C_{51}H_{42}N_5O_{12}S_3^+$: 1012.20. Found: 1012.60.

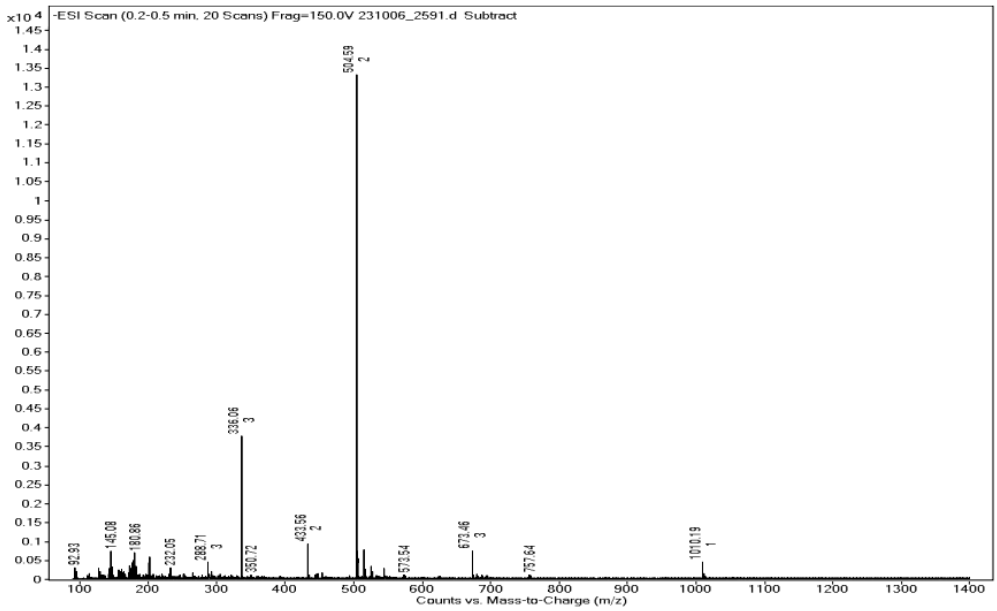

Target Ion Species

Ion Species	*m/z*	*Ionic Formula*
(M-2H)-2	504.5873	C51 H39 N5 O12 S3

MFG Calculator Results

Target m/z	*Ionic Formula*	*Calc m/z*	*+/- (mDa)*	*+/- (ppm)*	*DBE*	*MFG Score*
504.5873	C50 H43 N O16 S3	504.5877	-0.4	-0.8	29.0	98.68
504.5873	C54 H35 N5 O12 S2	504.5867	0.6	1.2	39.0	98.19
504.5873	C55 H31 N9 O8 S2	504.5874	-0.1	-0.2	44.0	97.64
504.5873	C51 H39 N5 O12 S3	504.5884	-1.1	-2.2	34.0	97.37
504.5873	C53 H39 N O16 S2	504.5861	1.2	2.4	34.0	96.78
504.5873	C46 H39 N7 O14 S3	504.5864	0.9	1.8	30.0	96.57
504.5873	C63 H35 N3 O5 S3	504.5875	-0.2	-0.4	47.0	96.10
504.5873	C55 H39 N5 O7 S4	504.5872	0.1	0.2	38.0	95.96
504.5873	C42 H39 N7 O19 S2	504.5877	-0.4	-0.8	26.0	95.88
504.5873	C56 H35 N9 O3 S4	504.5878	-0.5	-1.0	43.0	95.82

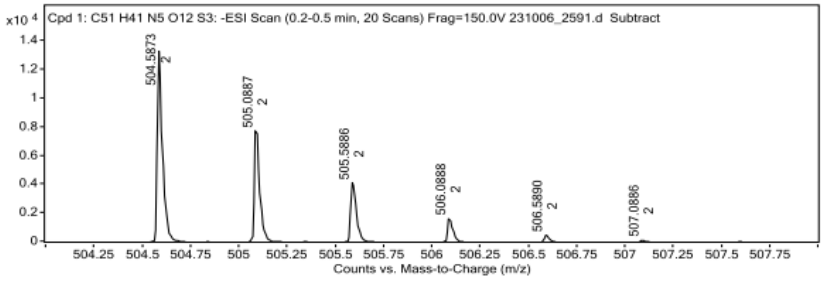

Predicted Isotope Match Table

Isotope	*m/z*	*Calc m/z*	Diff (mDa)	Abund (%)	Calc Abund (%)	+/-
1	504.5873	504.5884	-1.1	100.0	100.0	0.0
2	505.0887	505.0899	-1.2	60.5	60.3	-0.2
3	505.5886	505.5893	-0.7	31.8	33.7	1.9
4	506.0888	506.0897	-0.9	12.7	12.9	0.2
5	506.5890	506.5896	-0.6	3.9	4.3	0.4
6	507.0886	507.0898	-1.2	1.3	1.2	-0.1
7	507.5884	507.5899	-1.5	0.3	0.3	0.0

Figure s48. Mass spectrum obtained for $TPPS_3$-Hex [**2F**] with Agilent 6538 Q-TOF system in ESI MS Negative mode. MS (ESI) m/z calculated for $[M-2H]^{2-}$ $C_{51}H_{39}N_5O_{12}S_3^{2-}$: 504.5884. Found: 504.5873. Calcd for $[M-3H]^{3-}$ $C_{51}H_{38}N_5O_{12}S_3^{3-}$: 336.06. Found: 336.06. Calcd for $[M]^-$ $C_{51}H_{40}N_5O_{12}S_3^-$: 1010.18. Found: 1010.19.

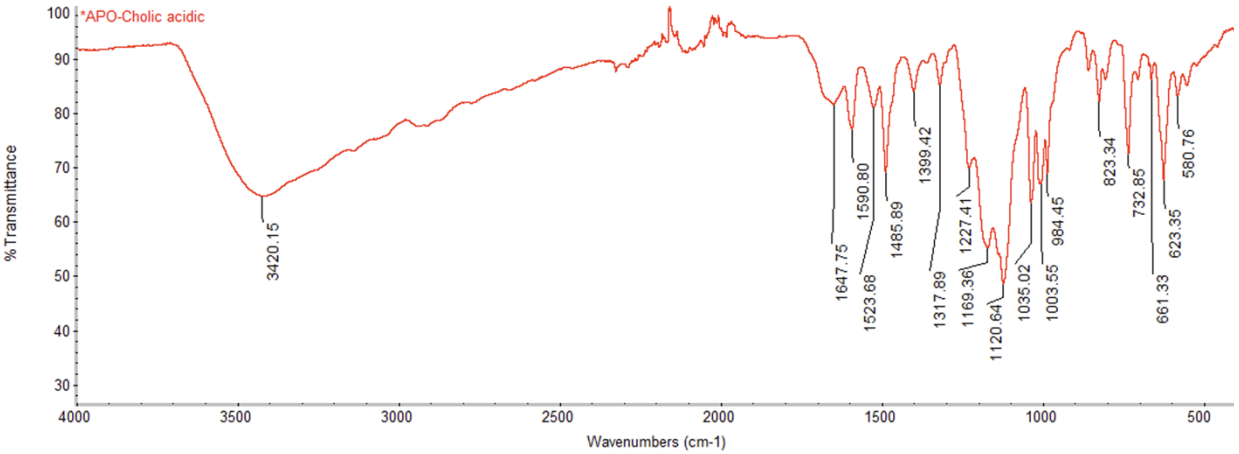

Figure s49. Fourier transform infrared spectroscopy (FTIR-ATR, Thermo Scientific Nicolet iS50) of $TPPS_3$-Hex [**2F**]. FTIR: γcm^{-1}: 1524 (N-H in plane bend).

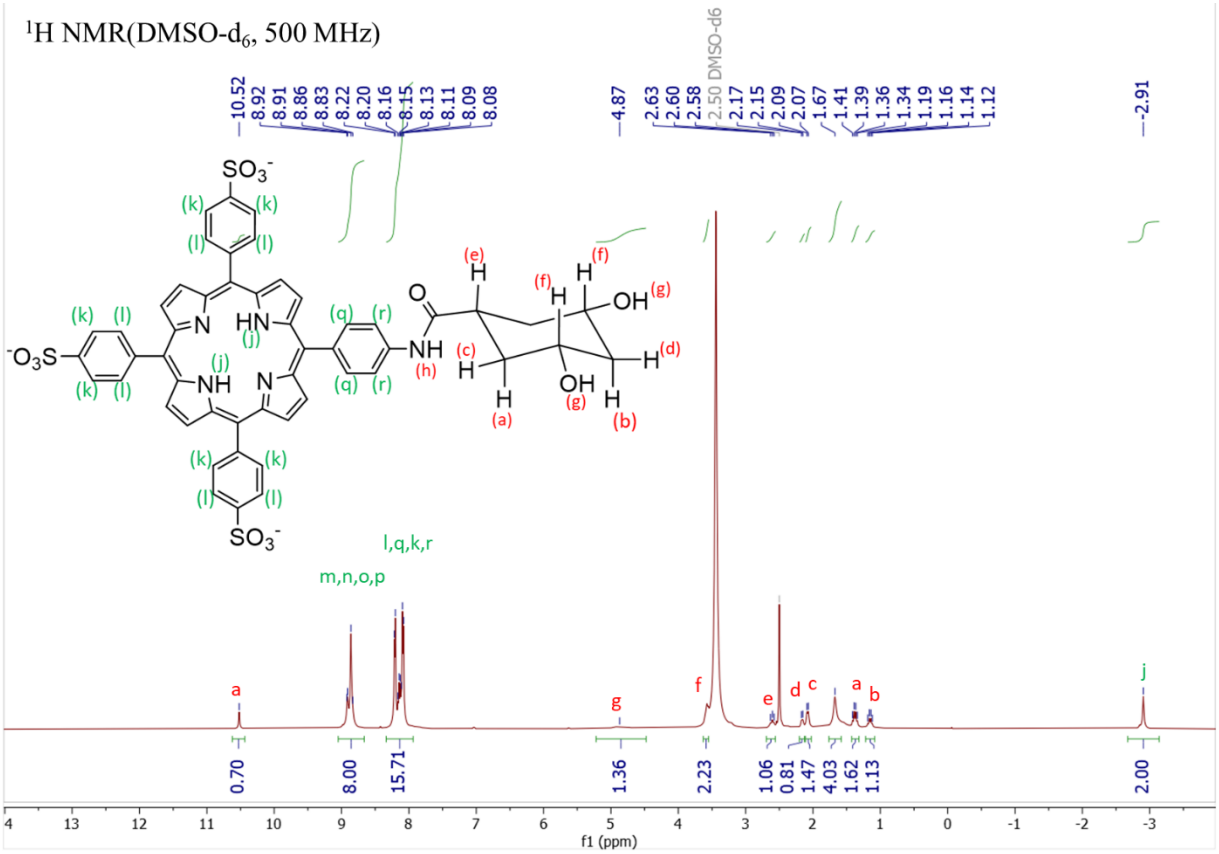

Figure s50. ^1H NMR spectrum of $TPPS_3$-Hex [**2F**] acquired on Bruker US 500 MHz system. ^1H NMR (500 MHz, DMSO-d_6) δ (ppm) 10.52 (s, 1H), 8.86 (m, 8H, β-pyrrole), 8.13 (m , 16H), 4.87 (s, 2H), 3.57 (m 2H), 2.60 (d, 1H), 2.16 (m, 1H), 2.08 (m, 2H), 1.37 (m, 2H), 1.15 (m, 1H), -2.91 (s, 2H). Signal at δ (ppm) 1.67 (b, 3H) associated with acetate coordinated to acidic porphyrin[15].

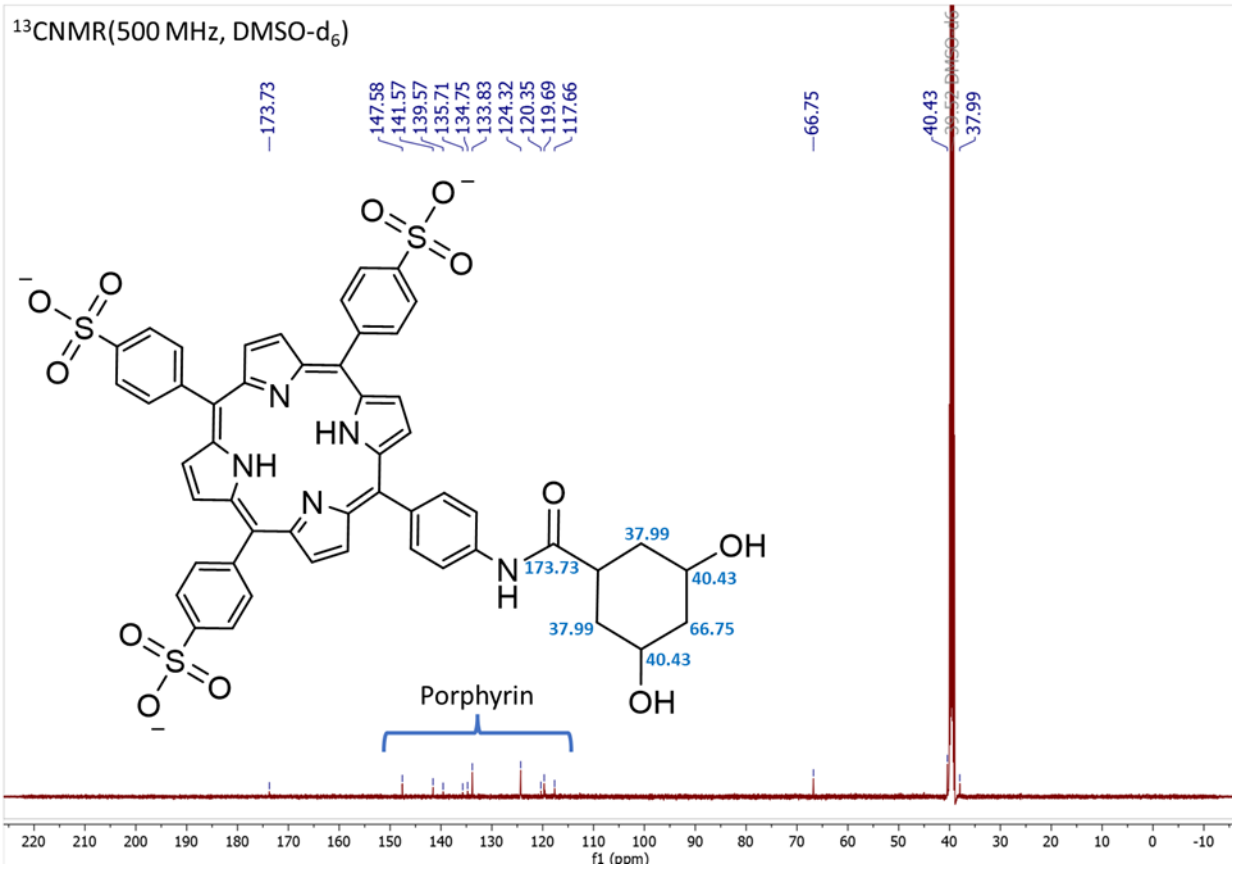

Figure s51. ^{13}C NMR spectrum of TPPS$_3$-Hex [**2F**] acquired on Bruker US 500 MHz system. ^{13}CNMR(500 MHz, DMSO-d$_6$) δ: 173.73, 147.58, 141.57, 139.57, 135.71, 134.75, 133.83, 124.32, 120.35, 119.69, 117.66 (45 C, tri-4-sulfonatophenyl)porphyrin), 66.75, 40.43, 37.99 (6 C, cyclohexanediol).

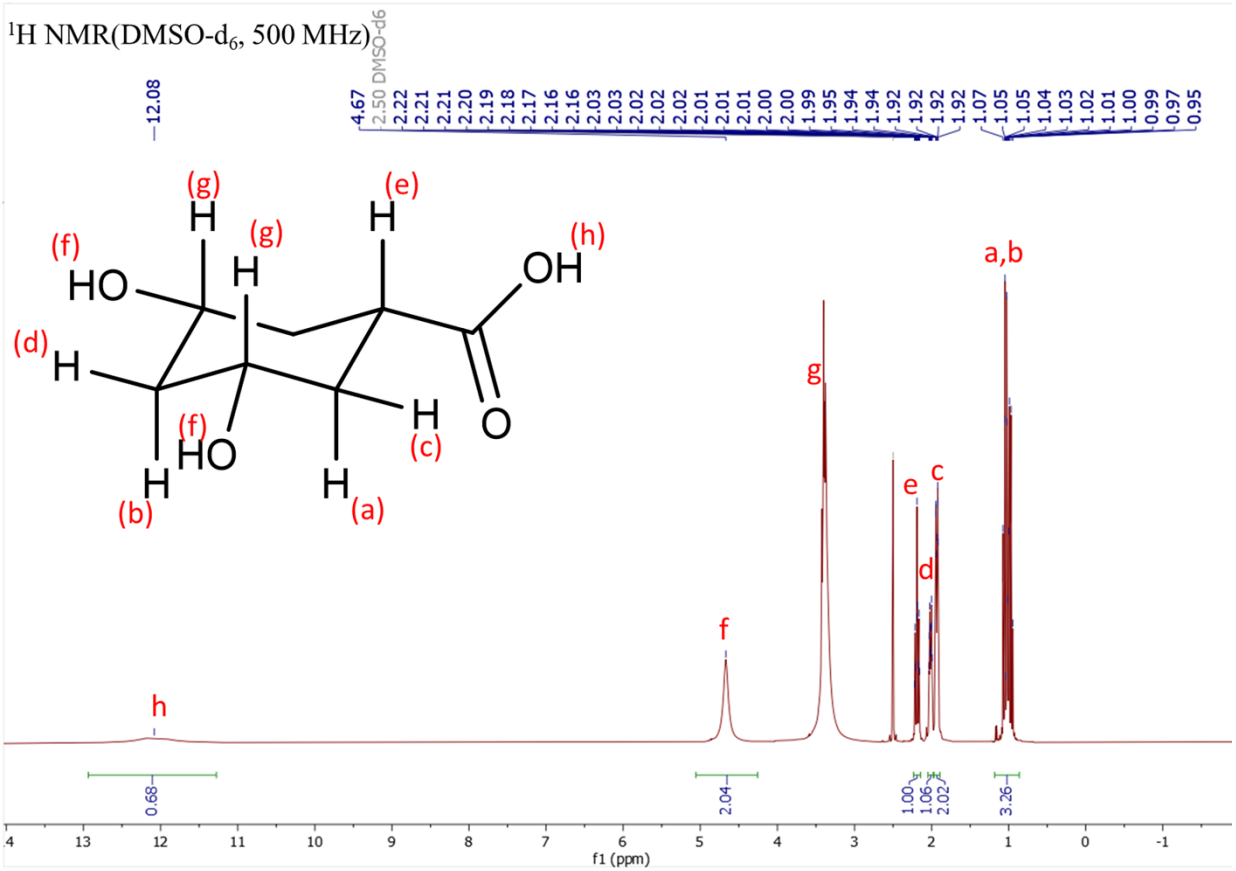

Figure s52. [1]H NMR spectrum of 3,5-dihydroxycyclohexanecarboxylic acid acquired on Bruker US 500 MHz system. [1]H NMR (500 MHz, DMSO-d_6) δ (ppm) δ 12.08 (s, 1H), 4.67 (s, 1H), 2.19 (tt, 1H), 2.01 (m, 1H), 1.93 (m, 2H), 1.01 (m, 3H).

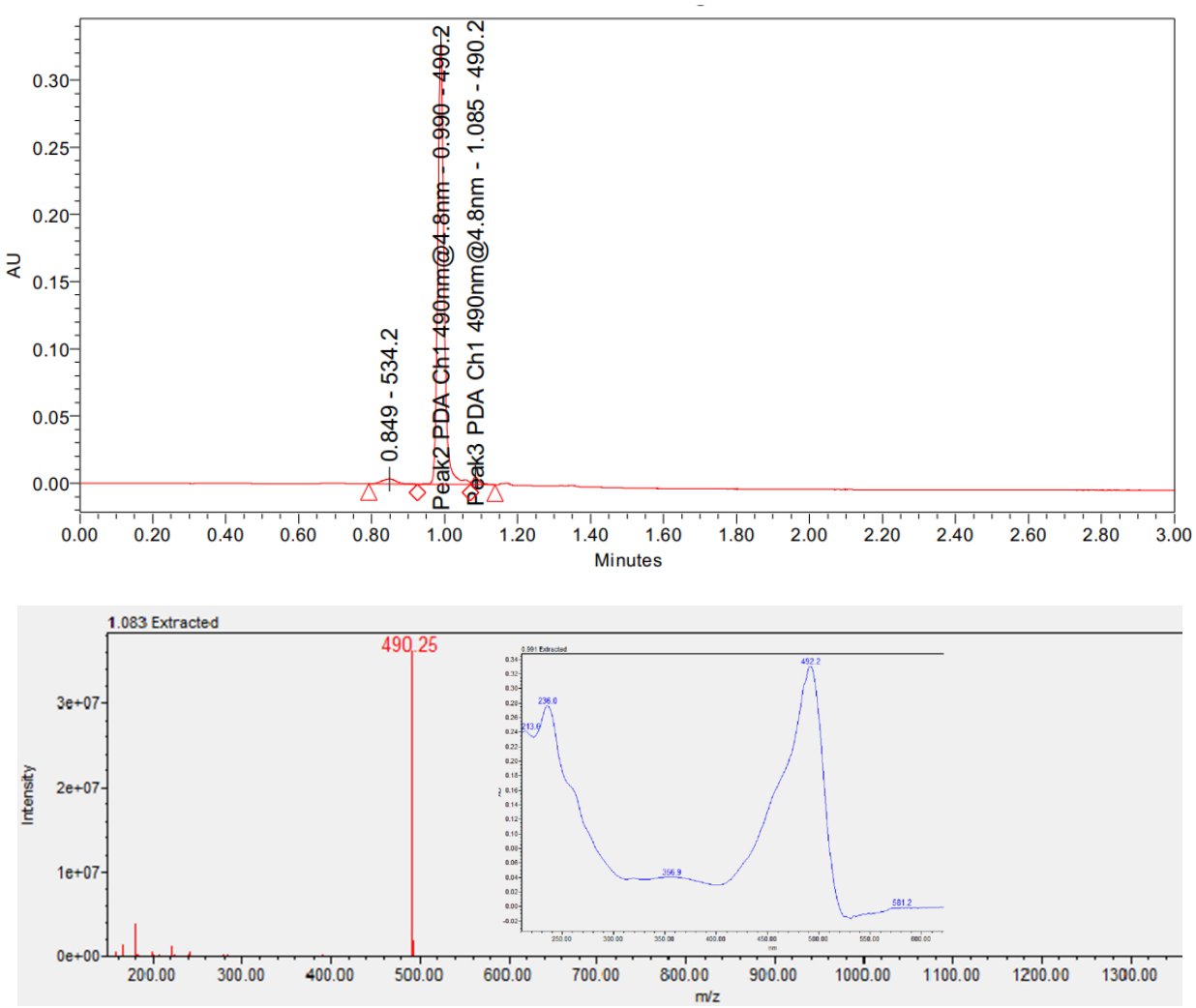

Figure s53. UHPLC-MS spectra of FITC-Hex [**3F**] recorded with Waters ACQUITY H-class UHPLC system with PDA detector recording at 490 nm and single quadrupole MS detector in positive mode. Elution occurred at 0.990 minutes. MS (ESI) m/z calculated for $[M]^+$ $C_{27}H_{24}NO_8^+$: 490.15. Found: 490.25. Possible carbamate product at 0.8498 with 534 mz.

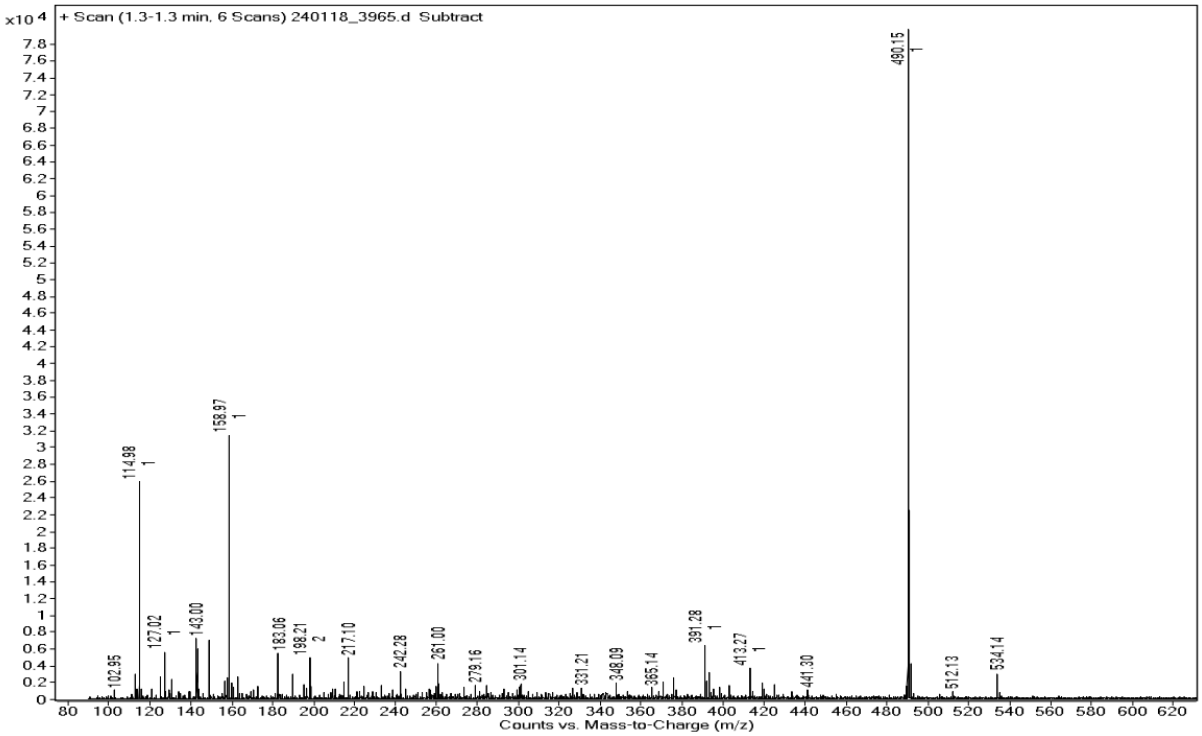

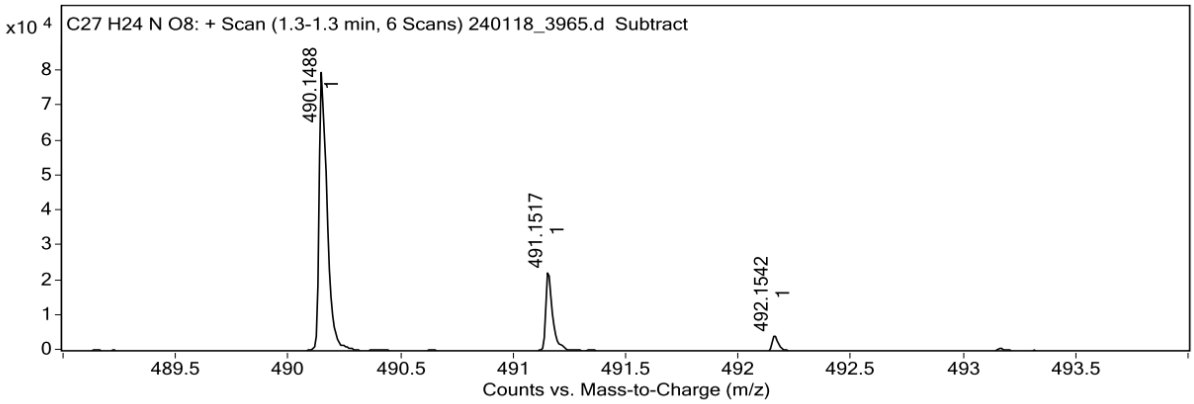

Predicted Isotope Match Table

Isotope	*m/z*	*Calc m/z*	Diff (mDa)	Abund (%)	Calc Abund (%)	+/-
1	490.1488	490.1496	-0.8	100.0	100.0	0.0
2	491.1517	491.1530	-1.3	29.0	30.1	1.1
3	492.1542	492.1556	-1.4	5.5	6.0	0.5

Figure s54. Mass spectrum obtained for FITC-Hex [**3F**] with Agilent 6538 Q-TOF system in ESI MS positive mode. MS (ESI) m/z calculated for $[M]^+$ $C_{44}H_{52}NO_8^+$: 490.1496. Found: 490.1488.

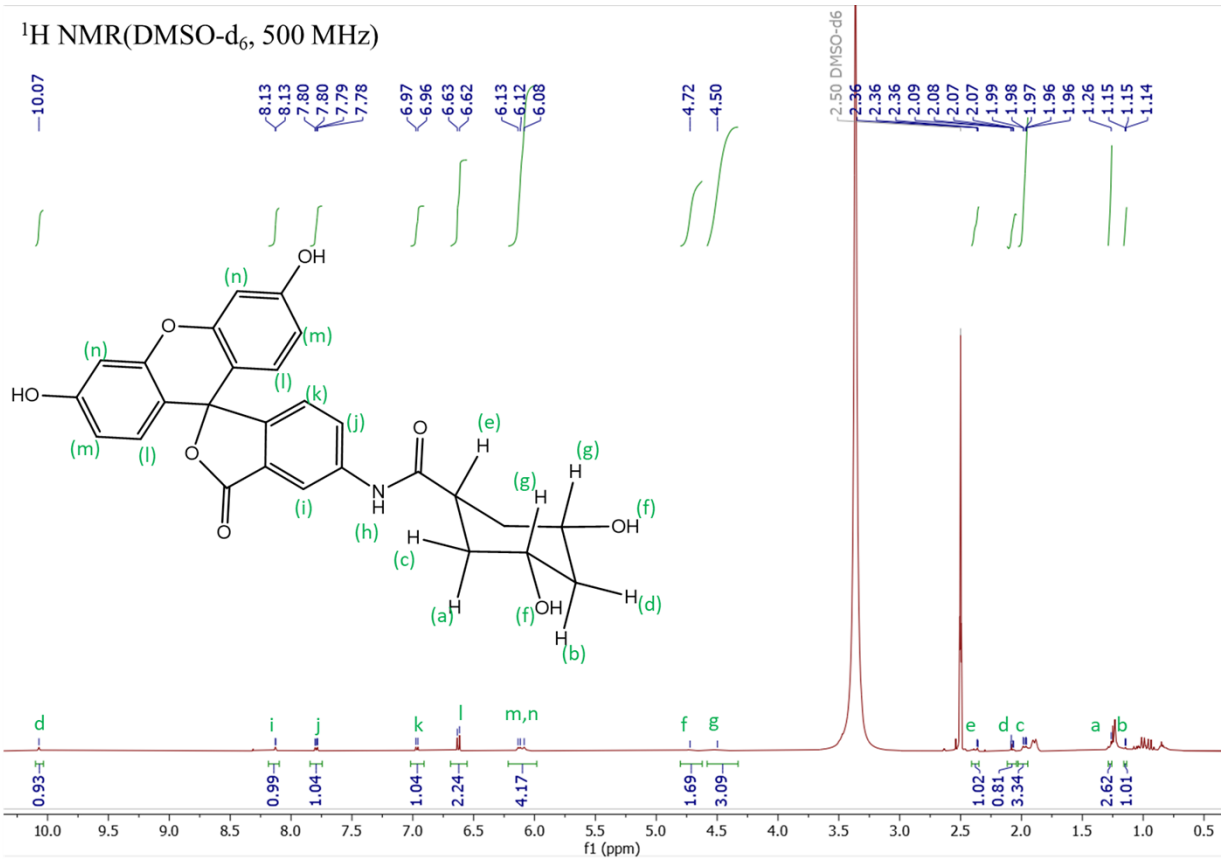

Figure s55. ^{1}H NMR spectrum of FITC-Hex [**3F**] acquired on Bruker US 500 MHz system. ^{1}H NMR (500 MHz, DMSO-d_6) δ (ppm) 10.32 (s, 1H), 8.13 (d, 1H), 7.8 (dd, 1H), 6.96 (d, 1H), 6.62 (dd, 2H), 6.12 (m, 4H), 4.72 (b, 1H), 4.50 (b, 2H), 2.36 (m, 1H), 2.06 (m, 1H), 1.98 (m, 2H), 1.26 (m, 2H), 1.15ff (m, 1H)

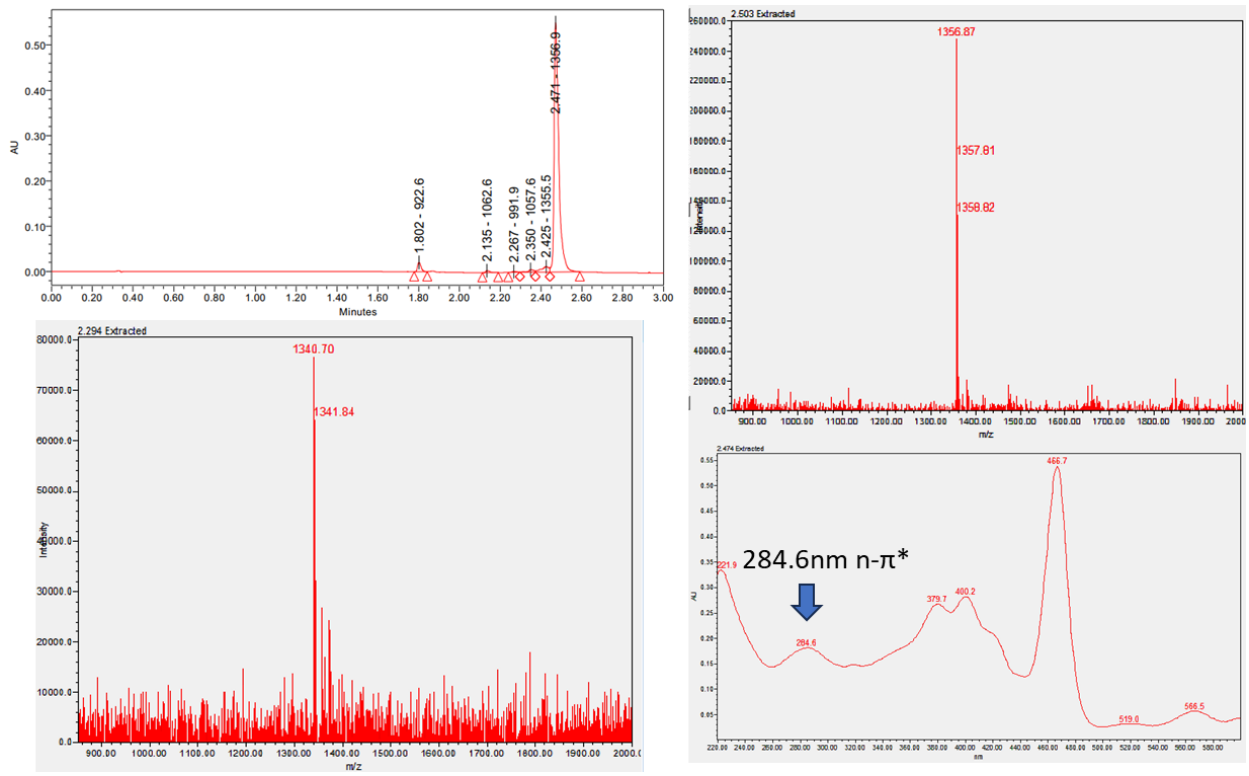

Figure s56. UHPLC-MS spectra of MITC-S-Deox [**1G**] recorded with Waters ACQUITY H-class UHPLC system with PDA detector recording at 467 nm and single quadrupole MS detector in positive mode. Elution occurred at 2.471 (supposed to be 2.117) minutes. MS (ESI) m/z calcd for $[M]^+$ $C_{69}H_{67}MnN_5O_{13}S_4^+$: 1356.30. Found: 1356.87. Trace signal for the carbamate MITC-O-Deox [**1H**] at MS (ESI) m/z calcd for $[M]^+$ $C_{69}H_{67}MnN_5O_{14}S_3^+$: 1340.32. Found: 1340.70. UV-Vis found unique peak at 284.6nm associated with n-π* transitions of aryl-NH thiocarbamates [7–9].

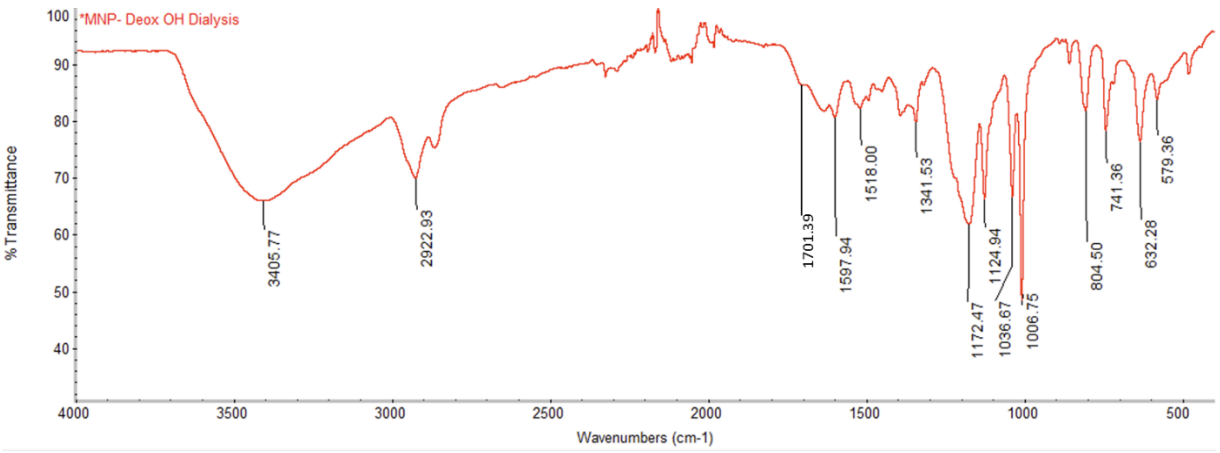

Figure s57. Fourier transform infrared spectroscopy (FTIR-ATR, Thermo Scientific Nicolet iS50) of MITC-S-Deox [**1G**]. FTIR: 1701 cm^{-1} (C=O stretching)[11] FTIR: 1519 cm^{-1} (N-H in plane bend)[10].

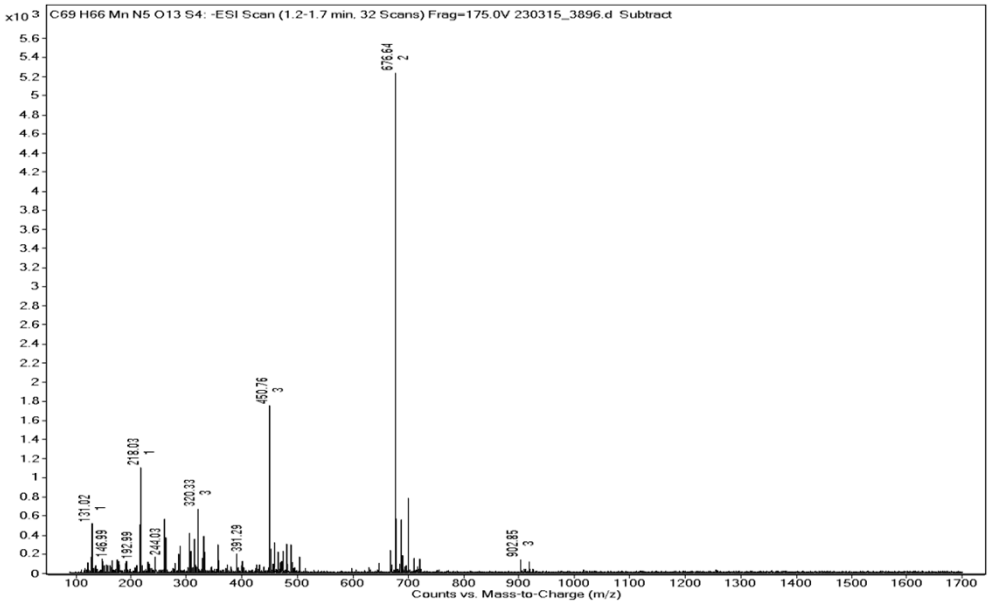

Target Ion Species

Ion Species	*m/z*	*Ionic Formula*
(M-2H)-2	676.6392	C69 H64 Mn N5 O13 S4

MFG Calculator Results

Target m/z	*Ionic Formula*	*Calc m/z*	*+/- (mDa)*	*+/- (ppm)*	*MFG Score*
676.6392	C70 H60 Mn N9 O9 S4	676.6394	-0.2	-0.3	98.82
676.6392	C71 H66 Mn N2 O14 S4	676.6394	-0.2	-0.3	98.63
676.6392	C72 H62 Mn N6 O10 S4	676.6401	-0.9	-1.3	98.39
676.6392	C69 H64 Mn N5 O13 S4	676.6387	0.5	0.7	97.74
676.6392	C84 H58 Mn N4 O3 S4	676.6392	0.0	0.0	97.27
676.6392	C73 H58 Mn N10 O6 S4	676.6408	-1.6	-2.4	96.86
676.6392	C86 H60 Mn N O4 S4	676.6398	-0.6	-0.9	96.62
676.6392	C83 H62 Mn O7 S4	676.6385	0.7	1.0	96.57
676.6392	C74 H64 Mn N3 O11 S4	676.6408	-1.6	-2.4	96.47
676.6392	C82 H56 Mn N7 O2 S4	676.6385	0.7	1.0	96.44

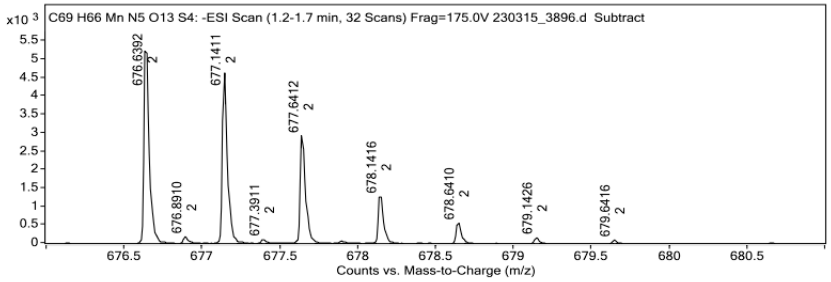

Predicted Isotope Match Table

Isotope	*m/z*	*Calc m/z*	Diff (mDa)	Abund (%)	Calc Abund (%)	+/-
1	676.6392	676.6387	0.5	100.0	100.0	0.0
2	677.1411	677.1403	0.8	82.8	80.8	-2.0
3	677.6412	677.6400	1.2	53.4	52.8	-0.6
4	678.1416	678.1403	1.3	24.5	25.0	0.5
5	678.6410	678.6403	0.7	10.3	9.9	-0.4

Figure s58. Mass spectrum obtained for MITC-S-Deox [**1G**] with Agilent 6538 Q-TOF system in ESI MS Negative mode. MS (ESI) m/z calculated for $[M_2\text{-}6H]^{4-}$ $((C_{69}H_{64}MnN_5O_{13}S_4)_2)^{4-}$: 676.6387 Found: 676.6392. MS (ESI) m/z calculated for $[M_2\text{-}8H]^{6-}$ $((C_{69}H_{63}MnN_5O_{13}S_4)_2)^{6-}$: 450.76. Found: 450.76. Is consistent with dimers formed by sulfonatophenyl metalloporphyrins. Carbamate product MITC-O-Deox [**1H**] could be found at MS (ESI) m/z calculated for $[M_2\text{-}6H]^{4-}$ $((C_{69}H_{66}MnN_5O_{14}S_3)^2)^{4-}$: 669.66. Found: 669.66.

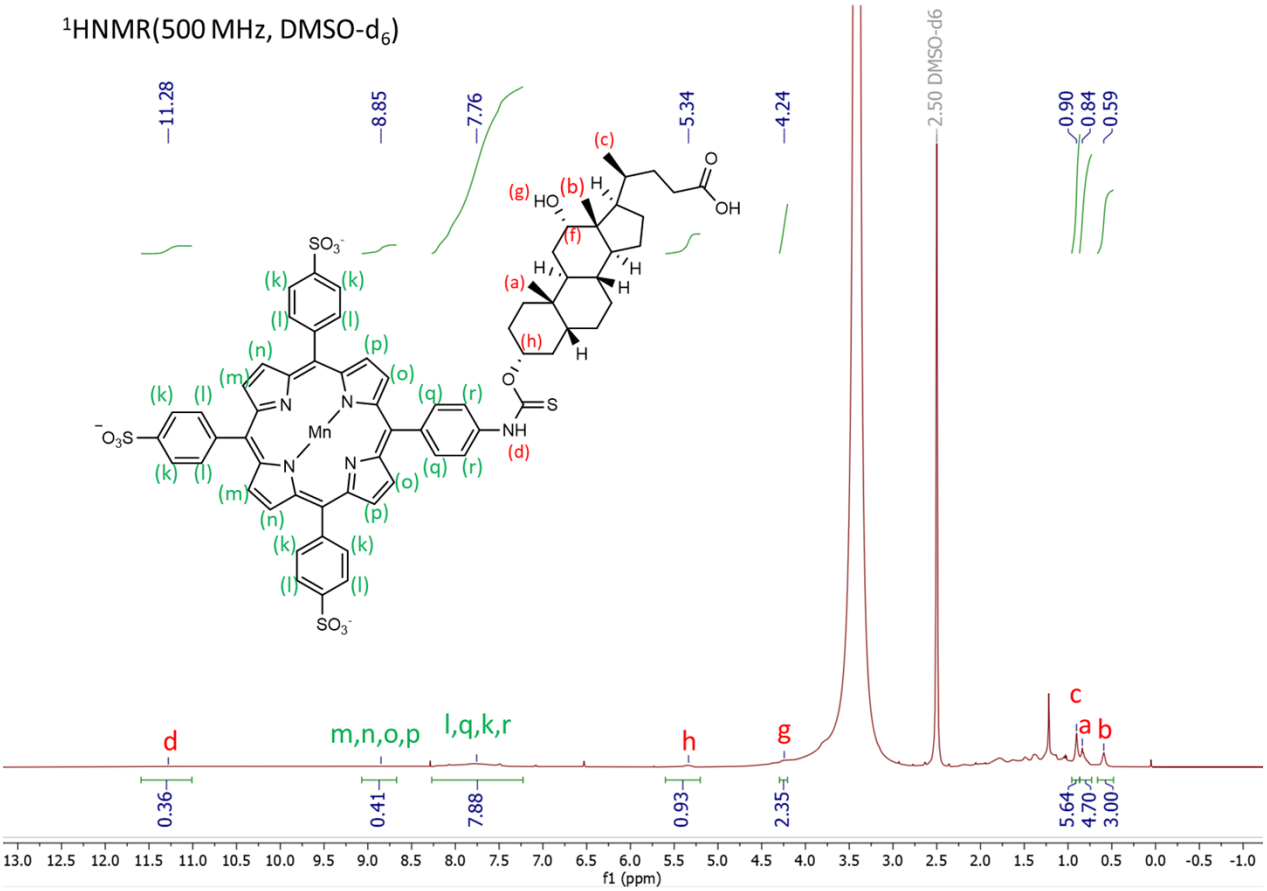

Figure s59. ^{1}H NMR spectrum of MITC-S-Deox [**1G**] acquired on Bruker US 500 MHz system. ^{1}HNMR(500 MHz, DMSO-d_6) δ: 11.28 (b, 1H), 8.85 (b, 8H), 7.76 (b, 16H), 5.34 (b, 1H), 4.24 (b, 1H), 0.90 (b, 3H), 0.94 (b, 3H), 0.59 (b, 3H). Signal associated with N-aryl thiocarbamate at δ (ppm) 11.28 [12,13]. Paramagnetic Mn^{3+} broadened and supressed nearby proton signals.

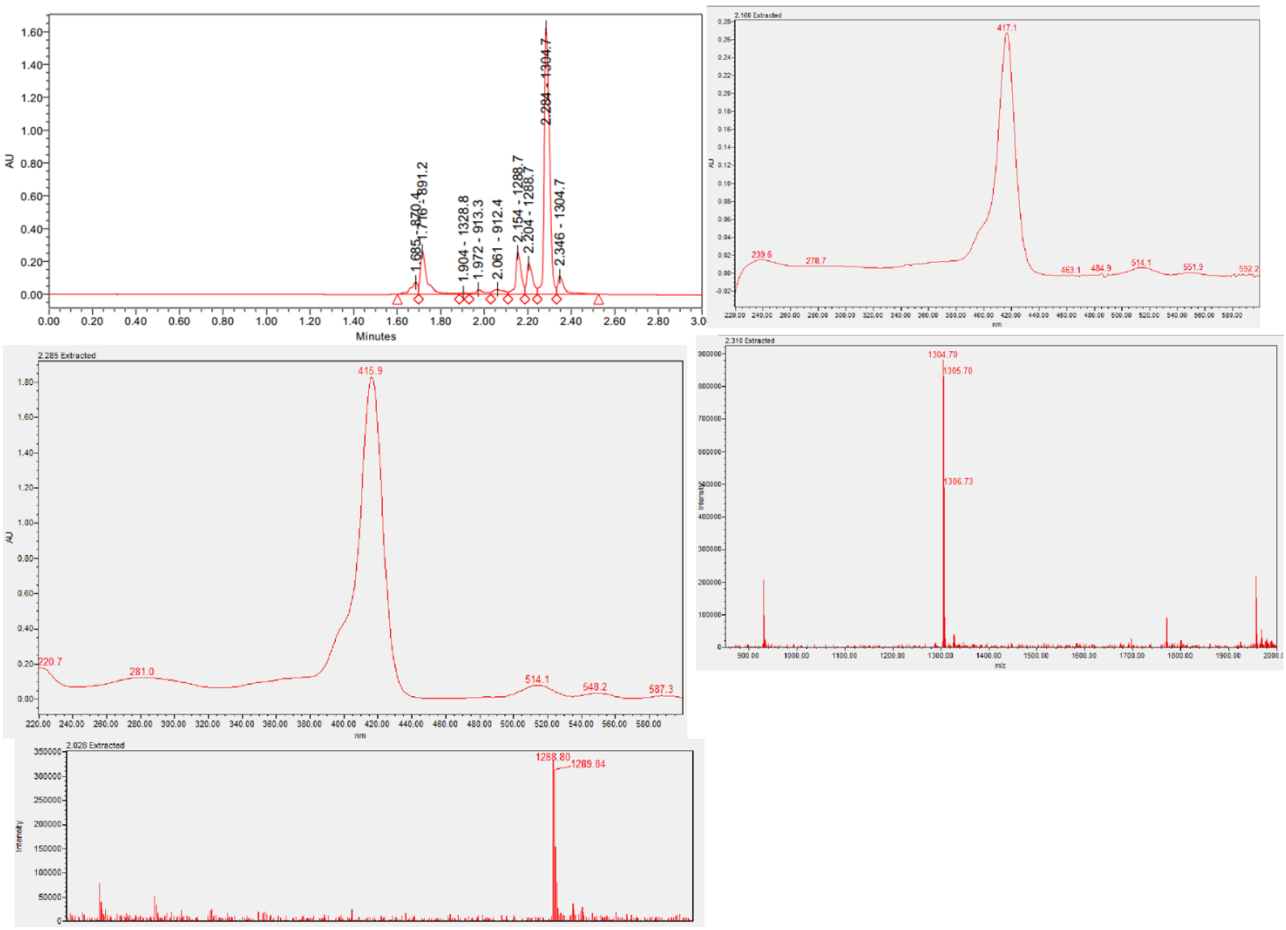

`**Figure s60.** Mass Spectrum obtained for $TPPS_3$-S-Deox [**2G**] with a Waters ACQUITY H-class UHPLC system with PDA detector and single quadrupole MS detector in positive mode. MS (ESI) m/z calcd for $[M+H]^+$ $C_{69}H_{70}N_5O_{13}S_4^+$: 1304.38. Found: 1304.70. eluting at 2.284 minutes λ_{max}= 419 nm. Eluted at 2.284 minutes. Carbamate product $TPPS_3$-O-Deox [**2H**] found at 2.154 minutes with m/z calcd for $[M+H]^+$ $C_{69}H_{70}N_5O_{14}S_3^+$: 1288.41. Found: 1222.80.

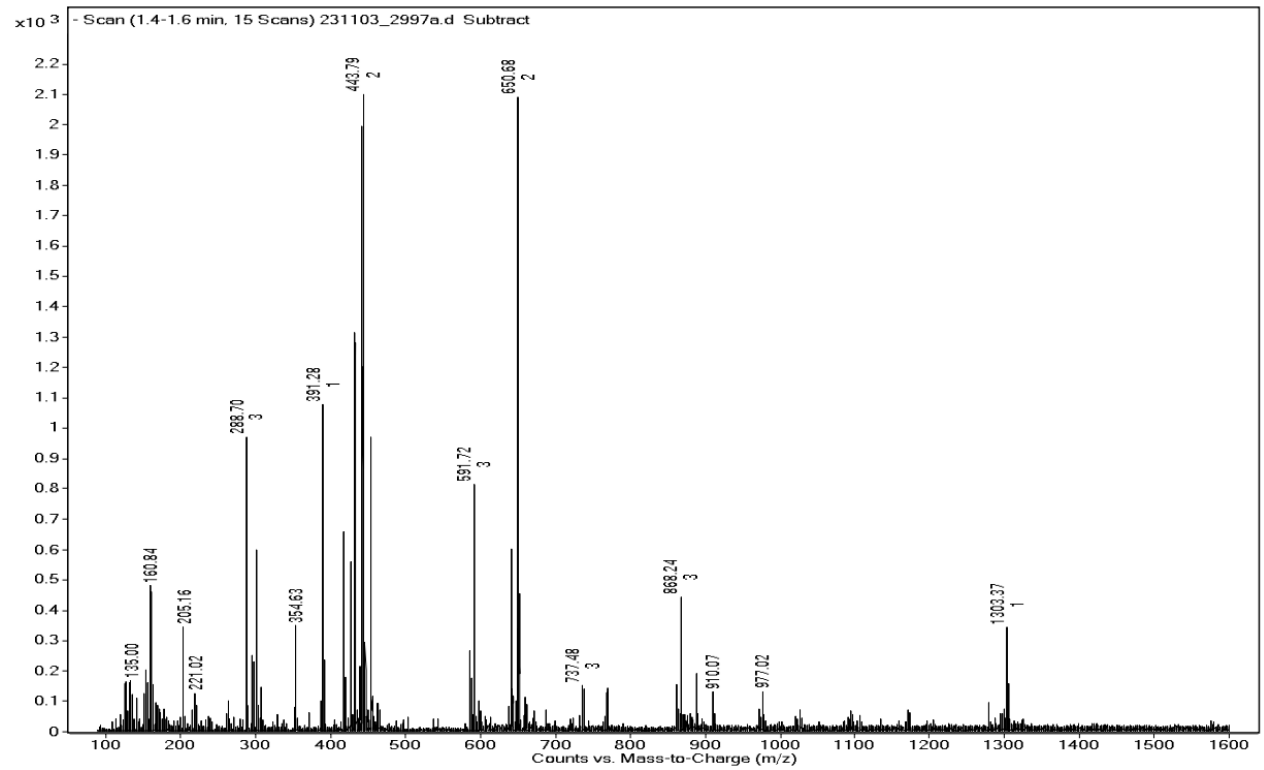

Predicted Isotope Match Table

Isotope	*m/z*	*Calc m/z*	Diff (mDa)	Abund (%)	Calc Abund (%)	+/-
1	650.6807	650.6815	-0.8	100.0	100.0	0.0
2	651.1825	651.1830	-0.5	76.4	80.9	4.5
3	651.6820	651.6827	-0.7	51.0	52.9	1.9
4	652.1829	652.1830	-0.1	22.2	25.0	2.8

Figure s61. Mass Spectrum obtained for $TPPS_3$-S-Deox [**2G**] with an Agilent 6538 Q-TOF system in ESI MS Negative mode. MS (ESI) m/z calcd for $[M-2H]^{2-}$ $C_{69}H_{67}N_5O_{13}S_4^{2-}$: 650.6815. Found: 650.6807. Calcd for $[M-3H]^{3-}$ $C_{52}H_{38}N_5O_{13}S_4^{3-}$: 356.05. Found: 356.05. Calcd for $[M]^-$ $C_{52}H_{40}N_5O_{13}S_4^-$: 1070.15. Found: 1070.15.

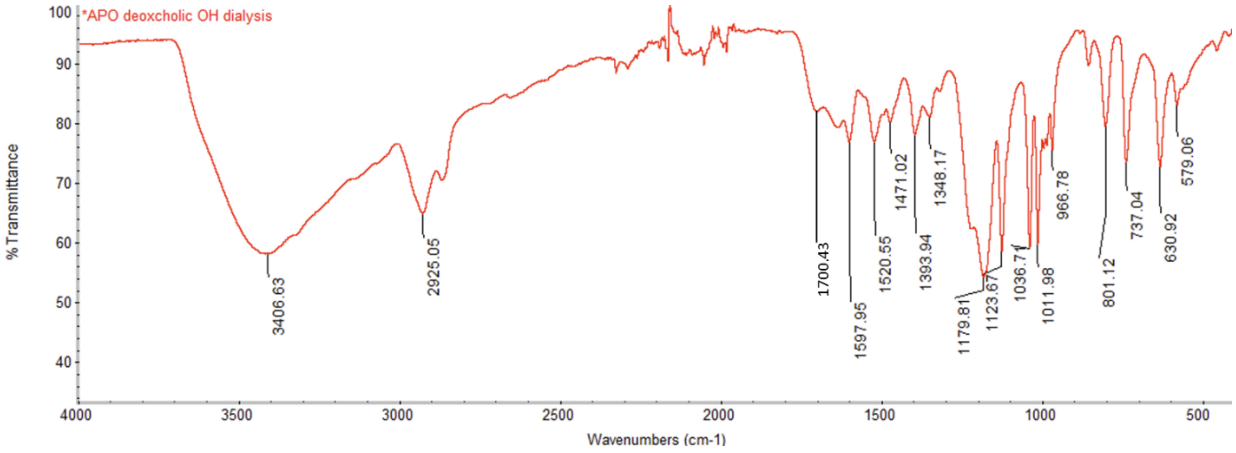

Figure s62. Fourier transform infrared spectroscopy (FTIR-ATR, Thermo Scientific Nicolet iS50) of $TPPS_3$-S-Deox [**2G**]. FTIR: 1700 cm^{-1} (C=O stretching)[11] 1520 cm^{-1} (N-H in plane bend)[10].

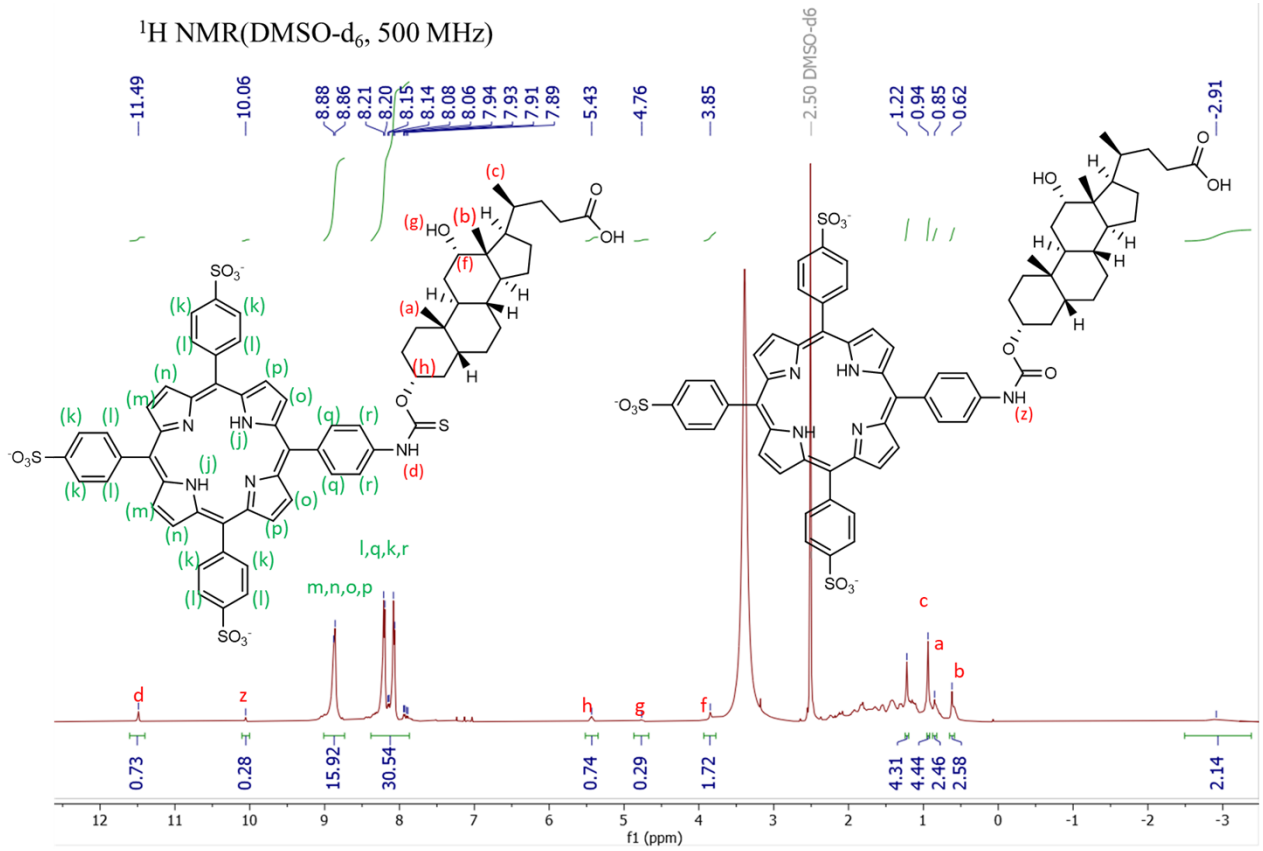

Figure s63. ^{1}H NMR spectrum of $TPPS_3$-S-Deox [**2G**] acquired on Bruker US 500 MHz system. ^{1}H NMR (500 MHz, DMSO-d_6) δ (ppm) 11.49 (b, 1H), 8.86 (m, 8H, β-pyrrole), 8.20 (m , J= 7.9 Hz, 8H), 8.06 (m 8H), 5.43 (s, 1H), 4.76 (d, 1H), 3.85 (t, 1H), 1.87 (m, 6H), 0.94 (d, 3H), 0.85 (s, 3H), 0.62 (s, 3H), -2.91 (s, 2H). Signal associated with N-aryl thiocarbamate at δ (ppm) 11.49 [12]. Signal associated with N-aryl carbamate from $TPPS_3$-O-Deox [**2H**] at δ (ppm) 10.06 (s, 1H).

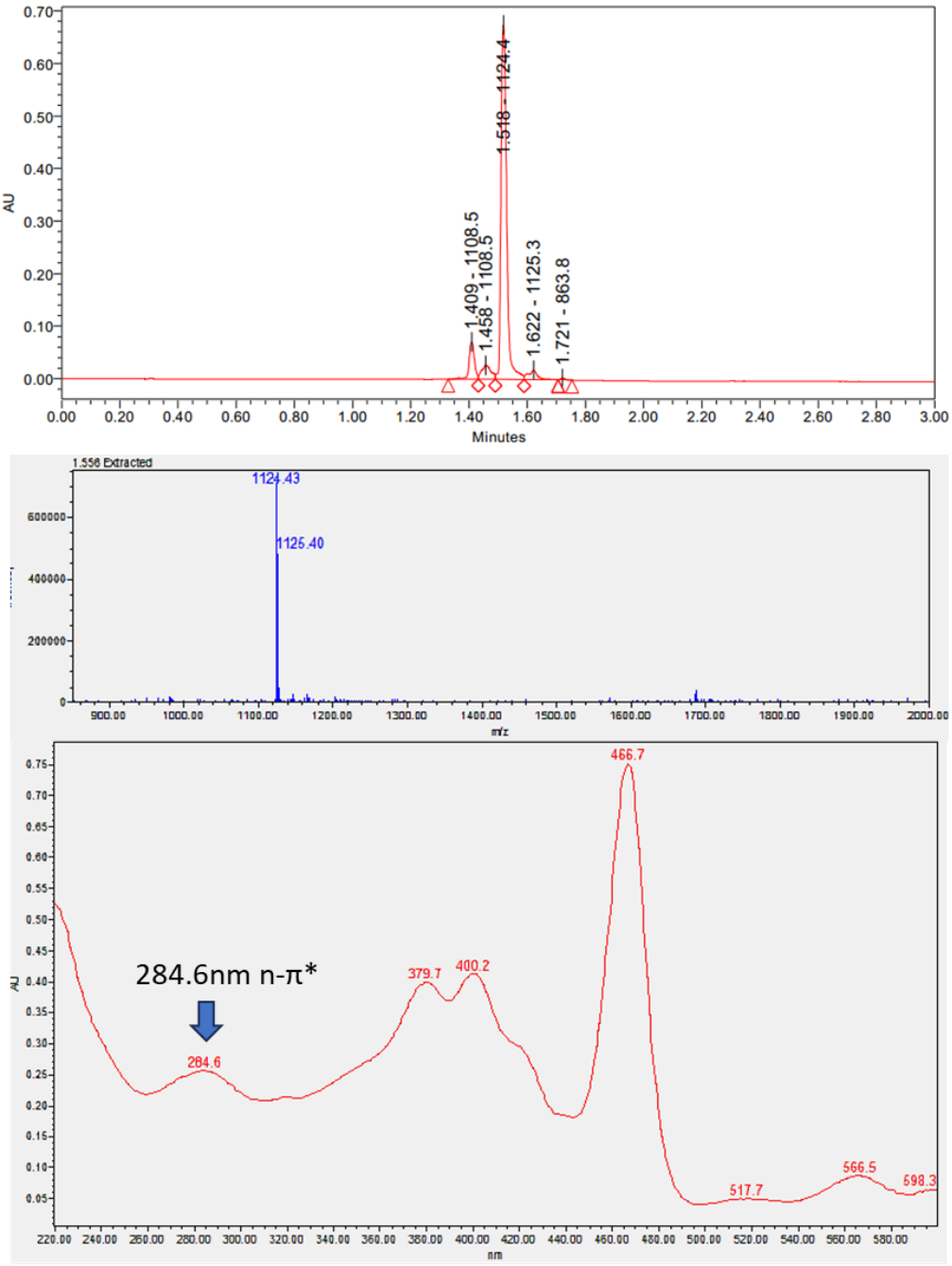

Figure s64. UHPLC-MS spectra of MITC-S-Hex [**1I**] recorded with Waters ACQUITY H-class UHPLC system with PDA detector recording at 467 nm and single quadrupole MS detector in positive mode. Elution occurred at 1.518 minutes. MS (ESI) m/z calcd for $[M]^+$ $C_{52}H_{39}MnN_5O_{13}S_4^+$: 1124.08. Found: 1124.43. Trace signal for carbamate [**1J**] at 1.409 minutes. MS (ESI) m/z calcd for $[M]^+$ $C_{52}H_{39}MnN_5O_{14}S_3^+$: 1108.10. Found: 1108.54. UV-Vis found unique peak at 284.6nm associated with n-π* transitions of aryl-NH thiocarbamates [7–9].

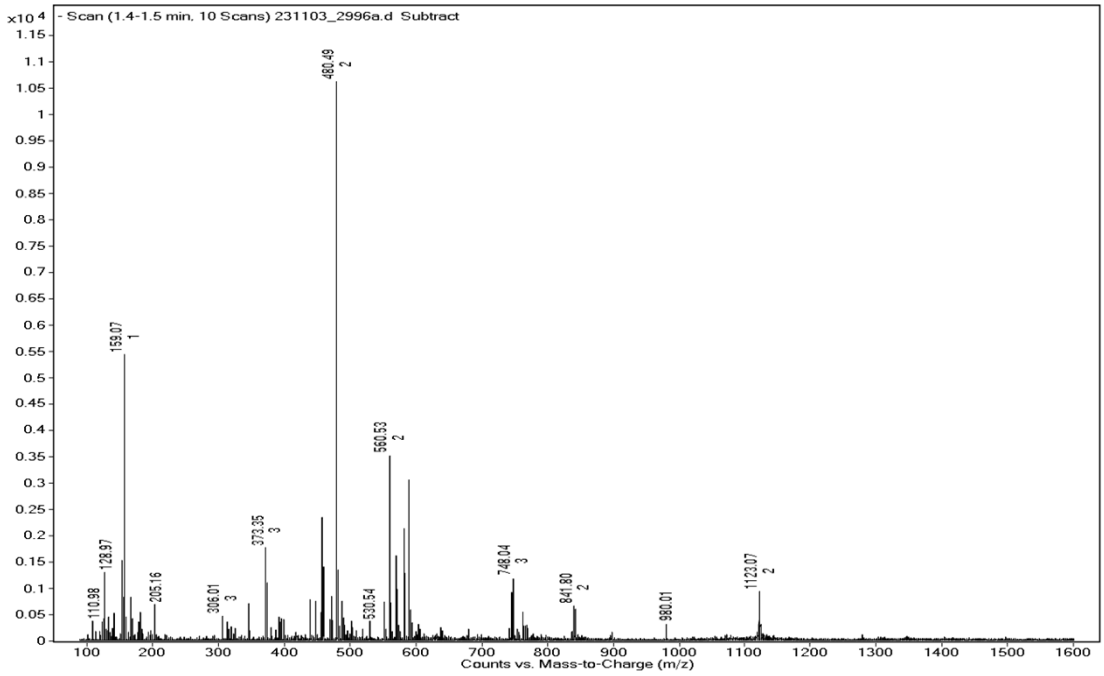

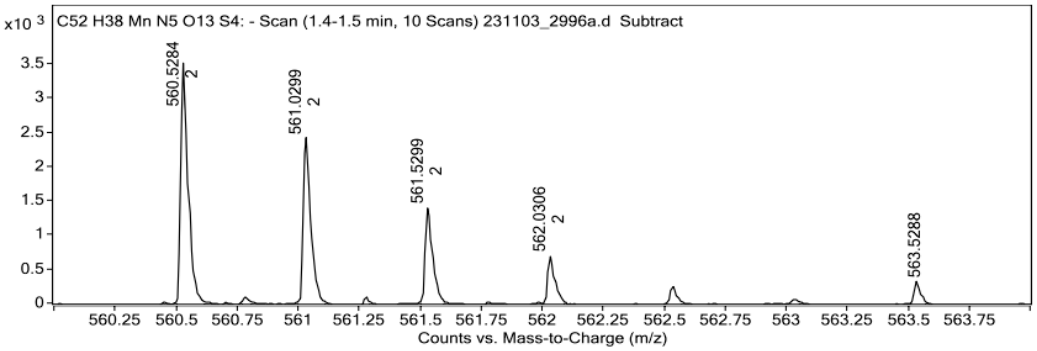

Predicted Isotope Match Table

Isotope	*m/z*	*Calc m/z*	Diff (mDa)	Abund (%)	Calc Abund (%)	+/-
1	560.5284	560.5292	-0.8	100.0	100.0	0.0
2	561.0299	561.0307	-0.8	69.6	62.1	-7.5
3	561.5299	561.5298	0.1	41.4	39.6	-1.8
4	562.0306	562.0302	0.4	20.3	16.4	-3.9
5	562.5304	562.5299	0.5	7.7	6.1	-1.6
6	563.0301	563.0299	0.2	2.3	1.9	-0.4
7	563.5288	563.5298	-1.0	9.5	0.5	-9.0
8	564.0311	564.0299	1.2	4.6	0.1	-4.5
9	564.5328	564.5300	2.8	5.1	0.0	-5.1

Figure s65. Mass Spectrum obtained for MITC-S-Hex [**1I**] with an Agilent 6538 Q-TOF system in ESI MS Negative mode. MS (ESI) m/z calcd for $[M\text{-}H]^-$ $C_{52}H_{38}MnN_5O_{13}S_4^-$: 1123.07 Found: 1123.07. MS (ESI) m/z calcd for $[M_2\text{-}6H]^{4-}$ $((C_{52}H_{36}MnN_5O_{13}S_4)_2)^{4-}$: 560.5292 Found: 560.5284 MS (ESI) m/z calculated for $[M_2\text{-}8H]^{6-}$ $((C_{52}H_{35}MnN_5O_{13}S_4)_2)^{6-}$: 373.35. Found: 373.35. Is consistent with dimers formed by sulfonatophenyl metalloporphyrins. MS (ESI) m/z calculated for $[M_2\text{-}3H]^{3-}$ $((C_{52}H_{36}N_5O_{13}S_4Mn)_2+H)^{3-}$: Found 748.04. MS (ESI) m/z calculated for $[M_2\text{-}4H]^{3-}$ $((C_{52}H_{36}N_5O_{13}S_4Mn)_2)^{3-}$: Calculated 748.04. Found 748.04. Carbamate product MITC-O-Hex [**1J**] could be found at MS (ESI) m/z calculated for $[M - 3H]^{-2}$ $(C_{52}H_{36}MnH_5O_{14}S_3)^{2-}$: calculated 552.5406, found 552.5395.

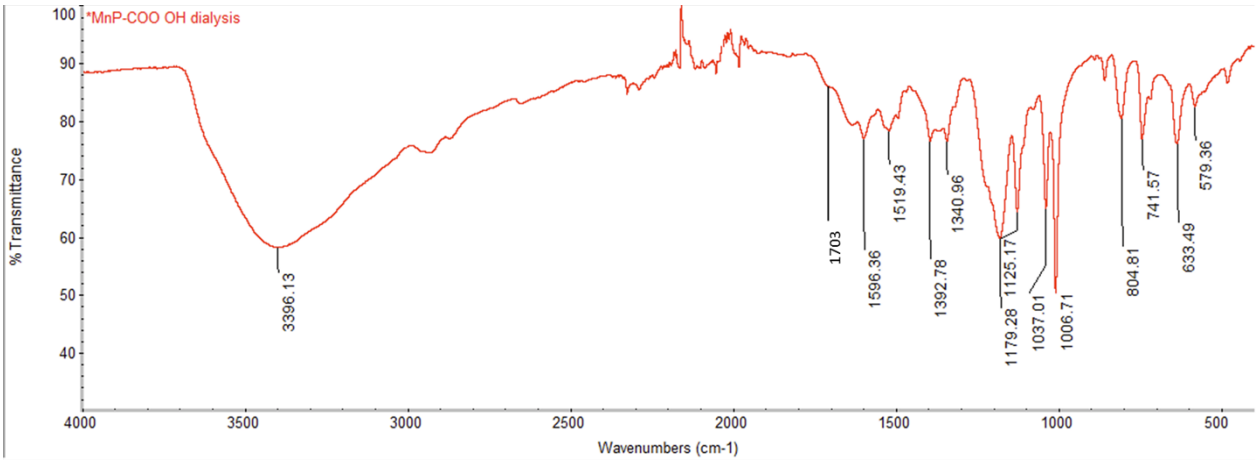

Figure s66. Fourier transform infrared spectroscopy (FTIR-ATR, Thermo Scientific Nicolet iS50) of MITC-S-Hex [**1I**]. FTIR: Shoulder to approximately 1703 cm^{-1} (C=O stretching)[11] 1519 cm^{-1} (N-H in plane bend)[10].

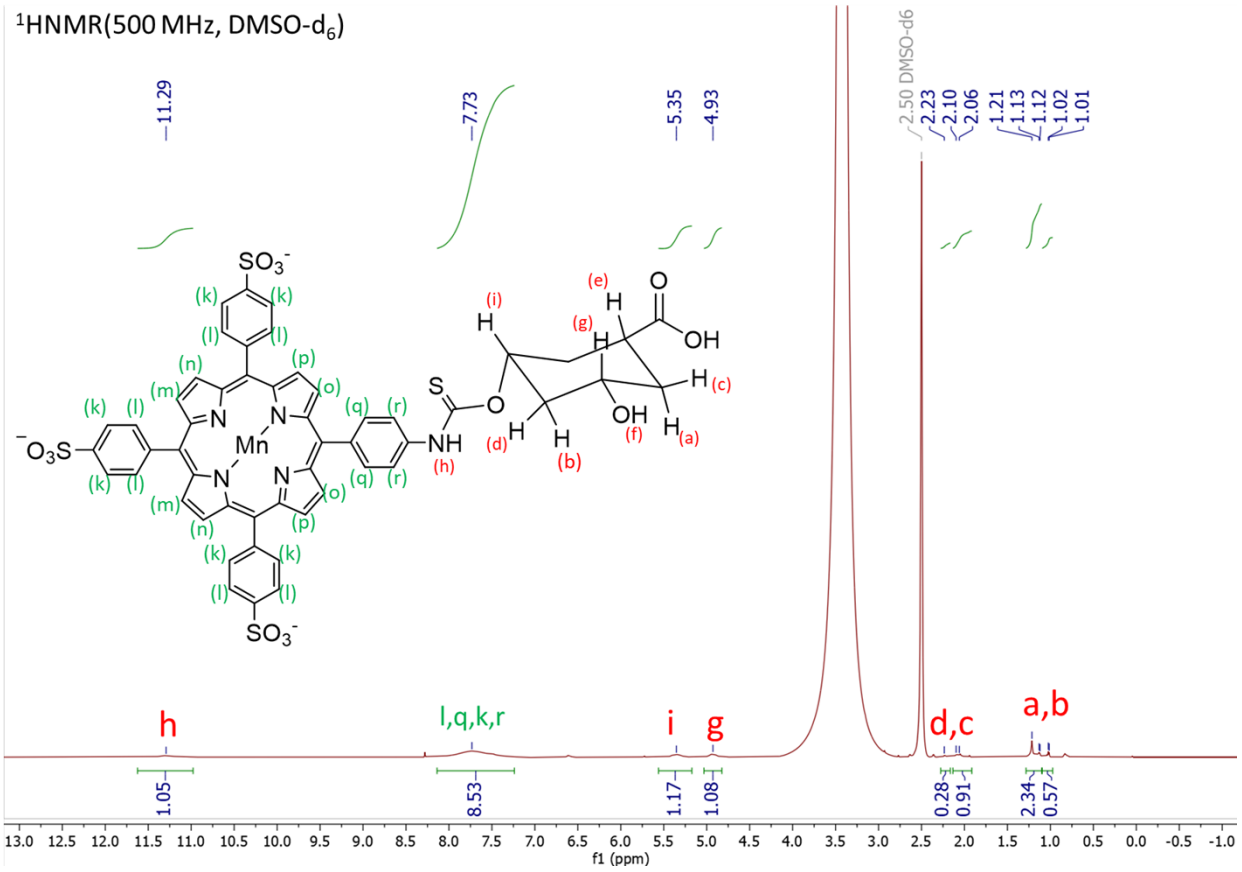

Figure s67. ^{1}H NMR spectrum of MITC-S-Hex [**1I**] acquired on Bruker US 500 MHz system. ^{1}HNMR(500 MHz, DMSO-d_6) δ: 11.29 (b, 1H), 7.73k (b, 16H), 5.35 (b, 1H) 4.93 (b, 1H), 2.23 to 2.06 (m, 3H), 1.21(b, 1H), 1.12 (b, 1H) 1.01 (b, 1H) Signal associated with N-aryl thiocarbamate at δ (ppm) 11.29 [12,13]. Paramagnetic Mn^{3+} broadened and supressed nearby proton signals.

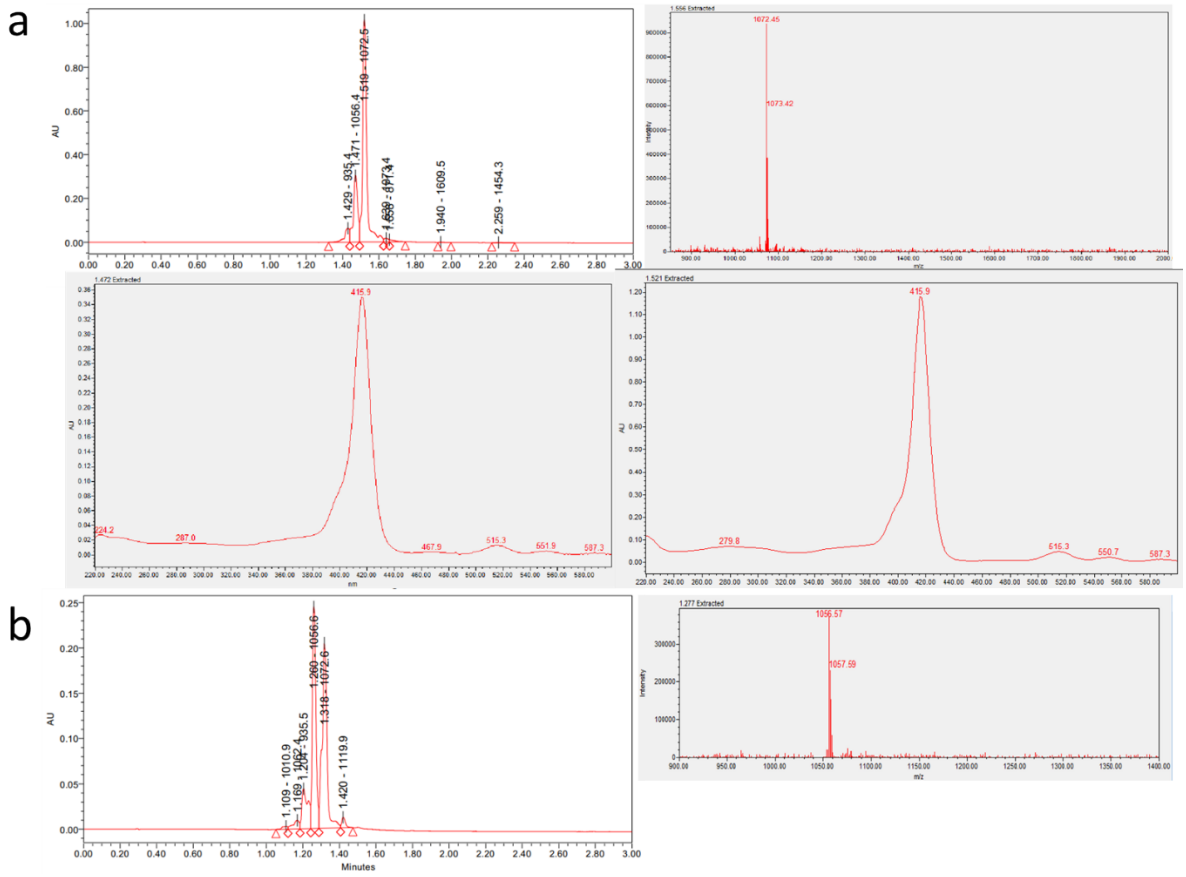

Figure s68. (a) Mass Spectrum obtained for $TPPS_3$-S-Hex [**2I**] with a Waters ACQUITY H-class UHPLC system with PDA detector and single quadrupole MS detector in positive mode. Eluting at 1.519 minutes MS (ESI) m/z calcd for $[M+H]^+$ $C_{52}H_{42}N_5O_{13}S_4^+$: 1072.17. Found: 1072.45. Carbamate side product $TPPS_3$-O-Hex [**2J**] eluting at 1.471 minutes. MS (ESI) m/z calcd for $[M+H]^+$ $C_{52}H_{42}N_5O_{14}S_3^+$: 1056.19. Found: 1056.57. (b) Proportion of carbamate product [**2J**] at 1.260 minutes increases with time relative to $TPPS_3$-S-Hex at 1.318 minutes, as shown with product from reaction stopped at 72 hr.

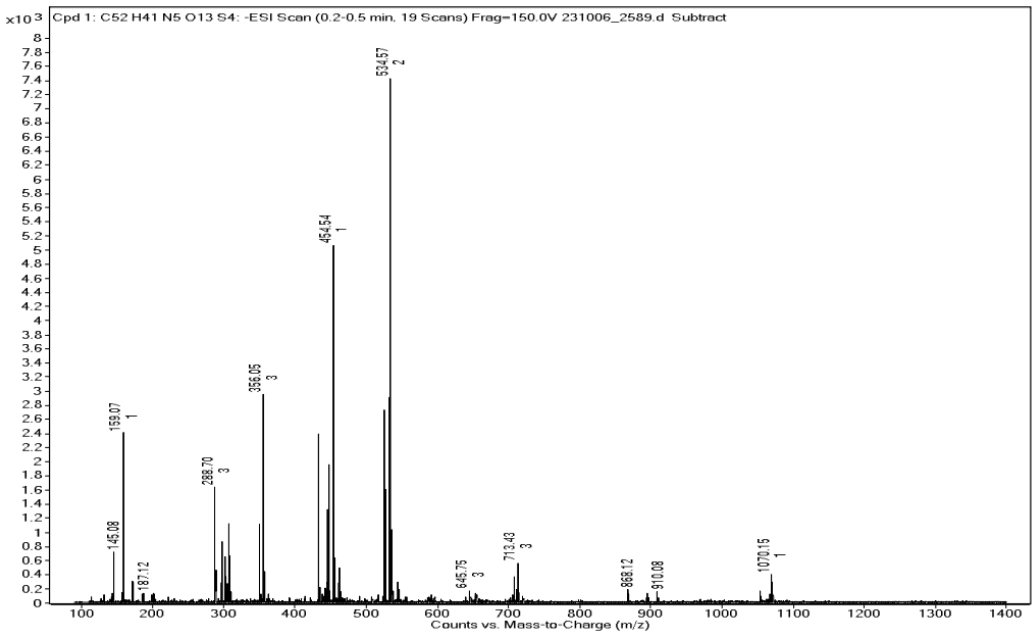

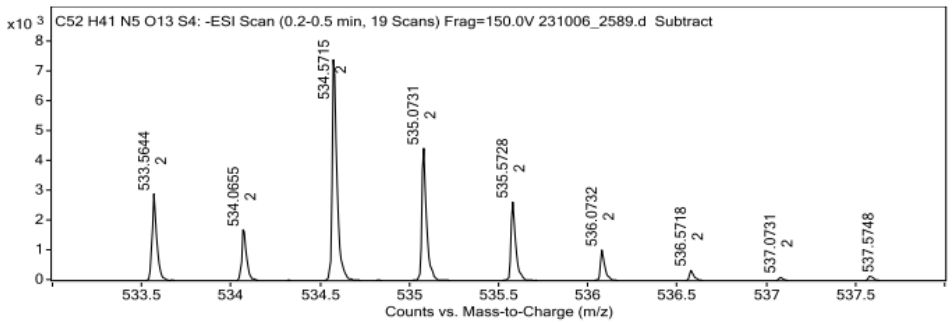

Predicted Isotope Match Table

Isotope	*m/z*	*Calc m/z*	Diff (mDa)	Abund (%)	Calc Abund (%)	+/-
1	534.5715	534.5719	-0.4	100.0	100.0	0.0
2	535.0731	535.0734	-0.3	57.4	62.2	4.8
3	535.5728	535.5725	0.3	34.2	39.6	5.4
4	536.0732	536.0729	0.3	13.4	16.5	3.1
5	536.5718	536.5726	-0.8	4.7	6.1	1.4
6	537.0731	537.0726	0.5	1.7	1.9	0.2

Figure s69. Mass Spectrum obtained for $TPPS_3$-S-Hex [**2I**] with an Agilent 6538 Q-TOF system in ESI MS Negative mode. MS (ESI) m/z calcd for $[M\text{-}2H]^{2-}$ $C_{52}H_{39}N_5O_{13}S_4^{2-}$: 534.5719. Found: 534.5715. Calcd for $[M\text{-}3H]^{3-}$ $C_{52}H_{38}N_5O_{13}S_4^{3-}$: 356.05. Found: 356.05. Calcd for $[M]^-$ $C_{52}H_{40}N_5O_{13}S_4^-$: 1070.15. Found: 1070.15.

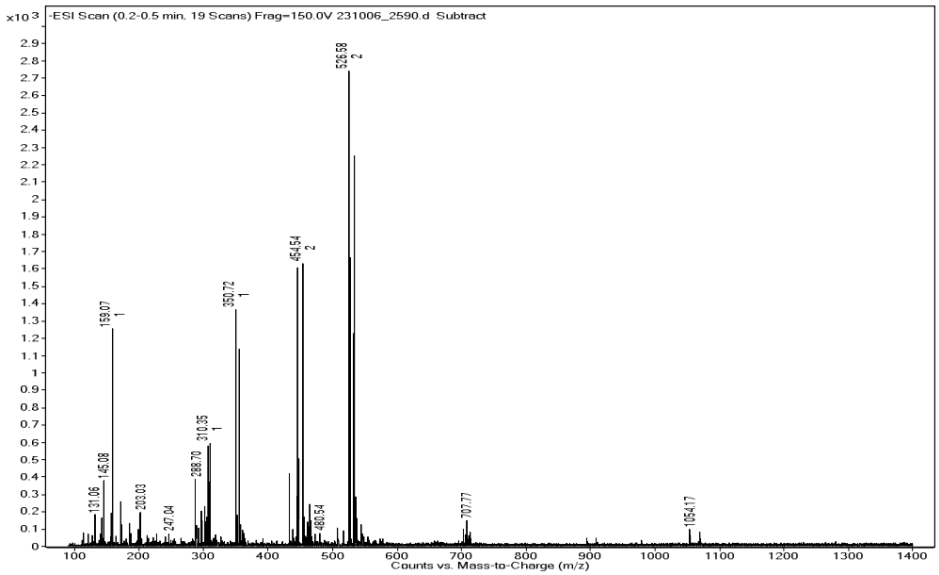

Predicted Isotope Match Table

Isotope	*m/z*	*Calc m/z*	Diff (mDa)	Abund (%)	Calc Abund (%)	+/-
1	526.5835	526.5833	0.2	100.0	100.0	0.0
2	527.0852	527.0849	0.3	60.2	61.4	1.2
3	527.5844	527.5843	0.1	31.4	34.8	3.4
4	528.0849	528.0847	0.2	13.9	13.6	-0.3
5	528.5841	528.5846	-0.5	4.7	4.5	-0.2
6	529.0828	529.0848	-2.0	1.3	1.3	0.0

Figure s70. Mass Spectrum obtained for carbamate $TPPS_3$-O-Hex [**2J**] with Agilent 6538 Q-TOF system in ESI MS Negative mode. m/z calcd for $[M\text{-}2H]^{2-}$ $C_{52}H_{39}N_5O_{14}S_3^{2-}$: 526.5833. Found: 526.5835. Calcd for $[M\text{-}3H]^{3-}$ $C_{52}H_{38}N_5O_{14}S_3^{3-}$: 350.72. Found: 350.72. Calcd for $[M]^-$ $C_{52}H_{40}N_5O_{14}S_3^-$: 1054.17. Found: 1054.17.

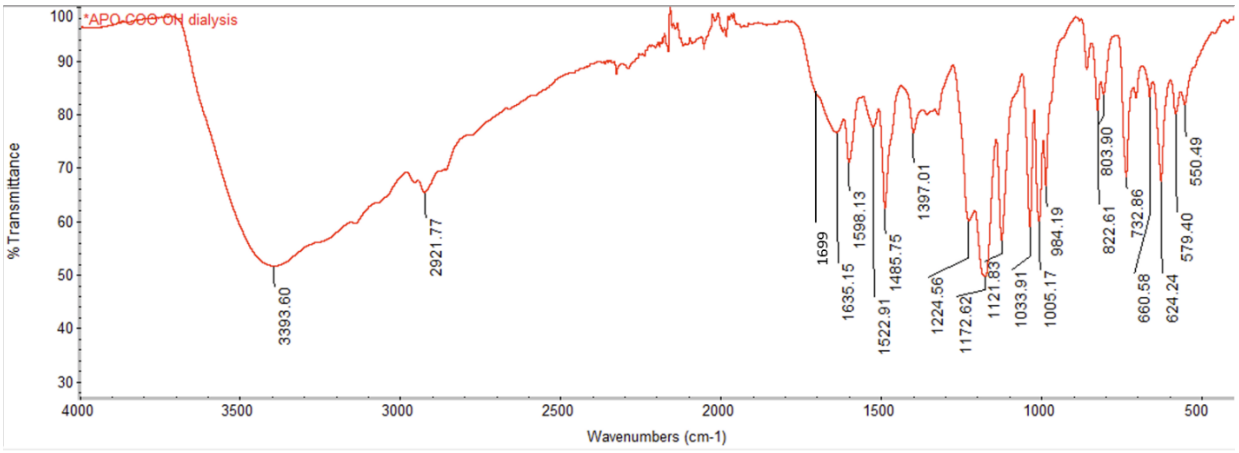

Figure s71. Fourier transform infrared spectroscopy (FTIR-ATR, Thermo Scientific Nicolet iS50) of $TPPS_3$-S-Hex [**2I**]. FTIR: Shoulder extending to approximately 1699 cm^{-1} (C=O stretching)[13] 1523 cm^{-1} (N-H in plane bend)[10].

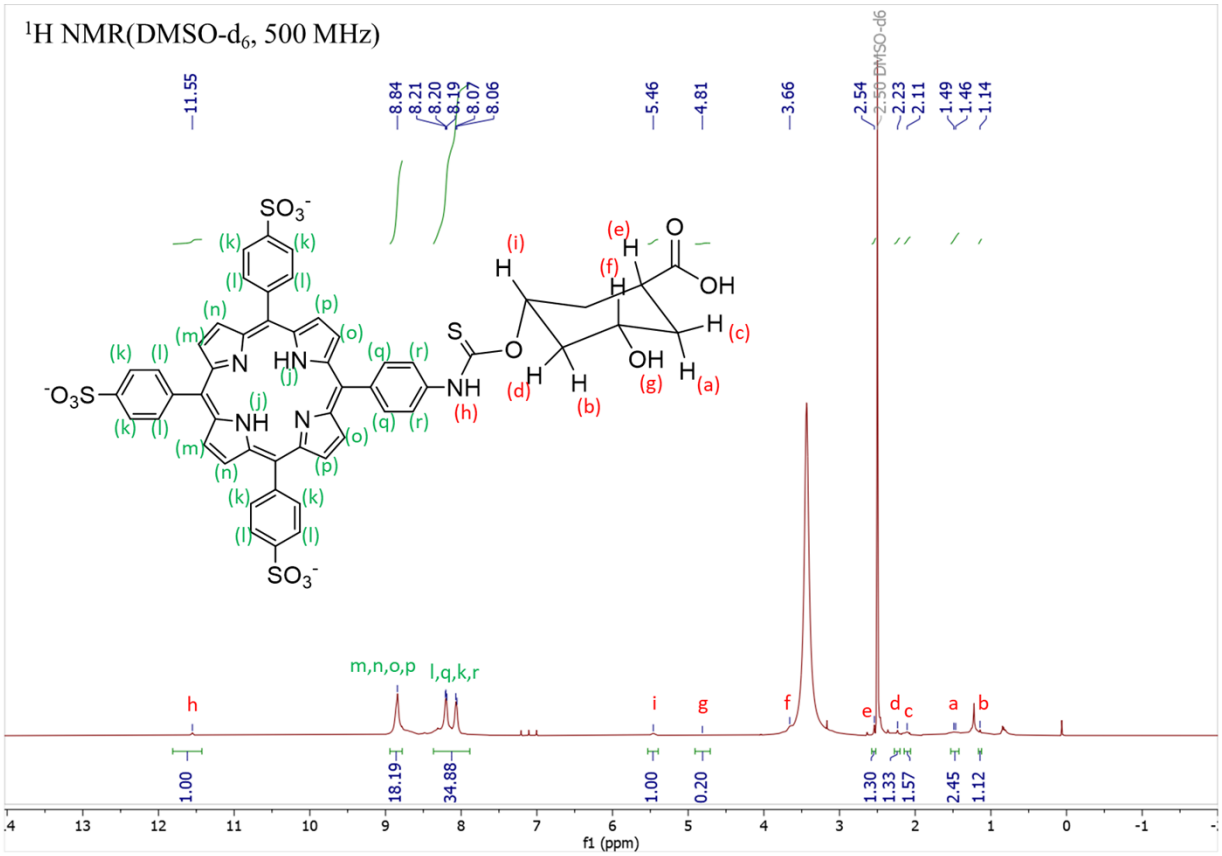

Figure s72. ^1H NMR spectrum of $TPPS_3$-S-Hex [**2I**] acquired on Bruker US 500 MHz system. ^1H NMR (500 MHz, DMSO-d_6) δ (ppm) 11.55 (b, 1H), 8.84 (m, 8H, β-pyrrole), 8.20 (m , 16H), 5.46 (s, 1H), 4.81 (m 1H), 3.66 (d, 1H), 2.54 (m, 1H), 2.23 (m, 2H), 2.11 (m, 2H), 1.49 (m, 2H), 1.14 (m, 1H). Signal associated with N-aryl thiocarbamate at δ (ppm) 11.55 [12,13].

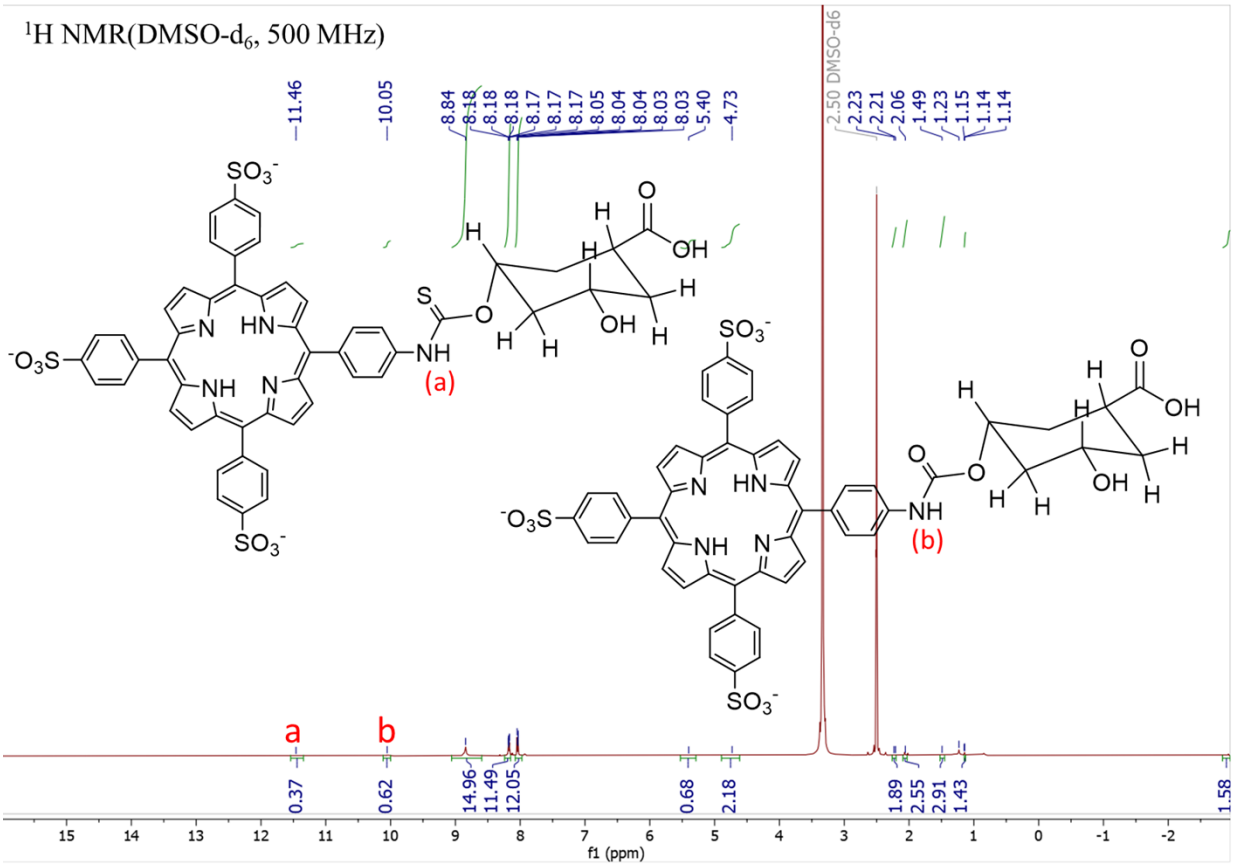

Figure s73. ^{1}H NMR spectrum of crude TPPS$_3$-O-Hex [**2J**] with some TPPS$_3$-S-Hex [**2I**] acquired on Bruker US 500 MHz system. ^{1}H NMR (500 MHz, DMSO-d$_6$). Signal associated with carbamate nitrogen from TPPS$_3$-O-Deox [**2H**] at δ (ppm) 10.05 (s, 1H).

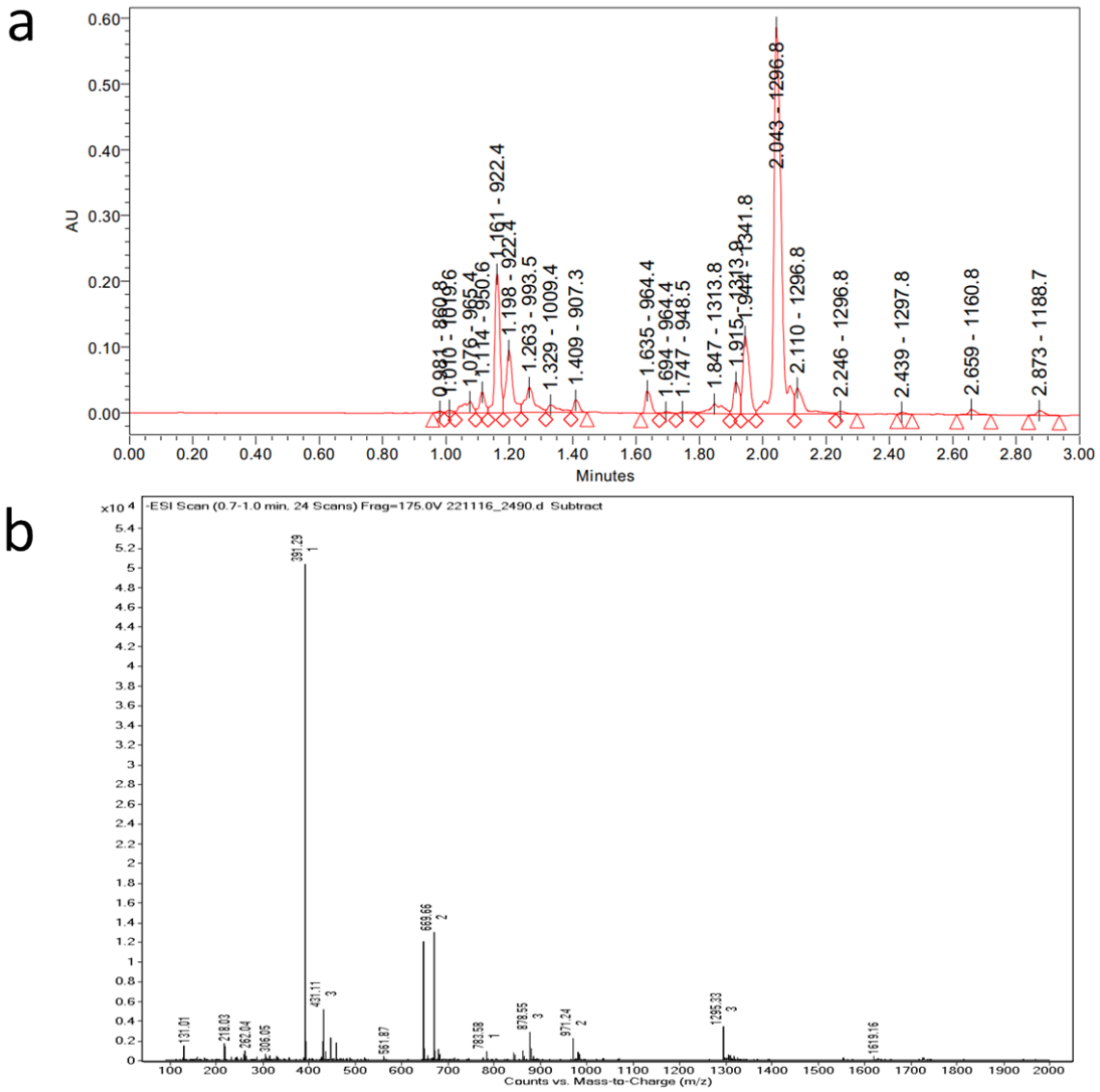

Figure s74. a) UHPLC-MS spectra of deoxycholic acid reaction with the Thiocarbamate MITC-S-Deox [**1G**] in the presence of base, producing the amide product MITC-Deox [**1E**] and leaving behind the more stable carbamate MITC-O-Deox [**1H**] at 1.944 min, MS (ESI) m/z calculated for $[M]^+$ $((C_{69}H_{67}MnN_5O_{14}S_3))^+$: 1340.32. Found: 1341.8. d) Agilent 6538 Q-TOF system in ESI MS negative mode where MITC-O-Deox [**1H**] could be found at MS (ESI) m/z calculated for $[M2-6H]^{4-}$ $((C_{69}H_{66}MnN_5O_{14}S_3)_2)^{4-}$: 669.66. Found: 669.66.

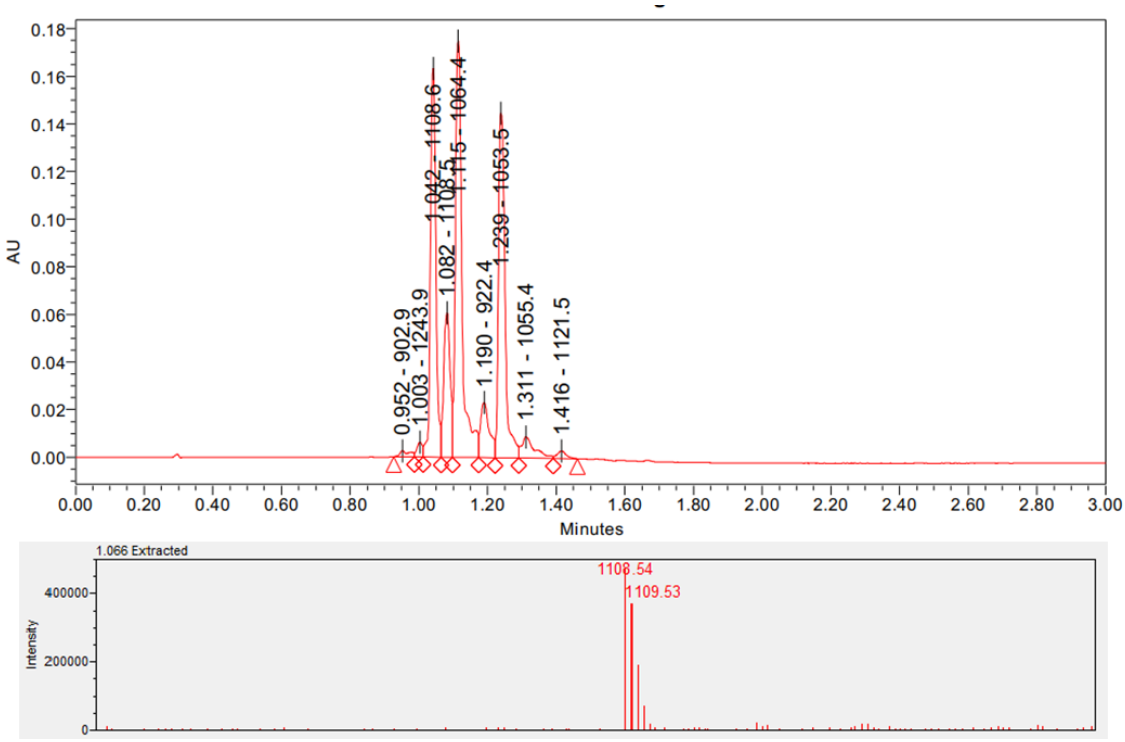

Figure s75. UHPLC-MS spectra of 3,5-dihydroxycyclohexanecarboxylic acid reaction with the thiocarbamate MITC-S-Hex [**1I**] in the presence of base producing the amide product MITC-Hex [**1F**] (1.115 minutes) leaving behind the stable carbamate MITC-O-Hex [**1J**] at 1.042 minutes.

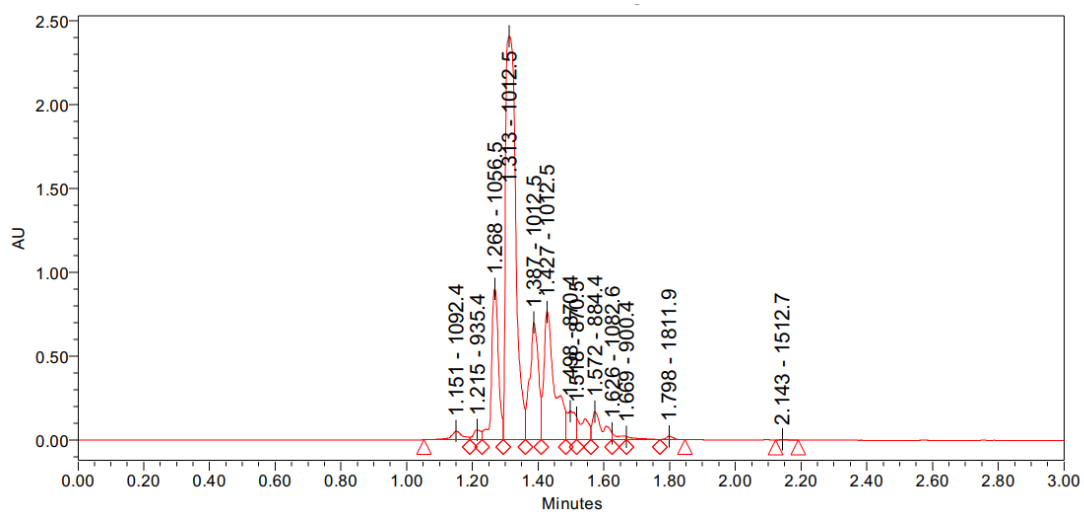

Figure s76. UHPLC-MS spectra of reaction between 3,5-dihydroxycyclohexanecarboxylic acid and the thiocarbamate $TPPS_3$-S-Hex [**2I**] in the presence of base producing the amide product $TPPS_3$-Hex [**2F**] (1.313 minutes), leaving behind the stable carbamate $TPPS_3$-O-Hex [**2J**] (1.268 minutes).

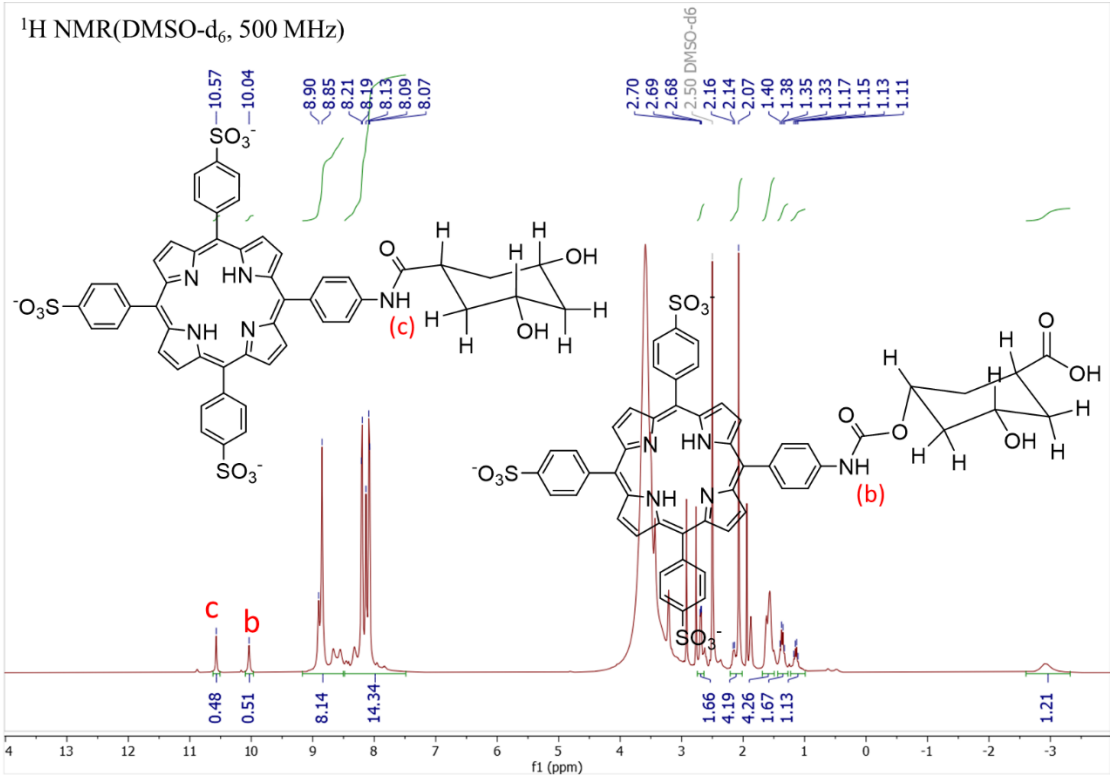

Figure s77. ^{1}H NMR spectrum of crude $TPPS_3$-Hex [**2F**] obtained from reaction of $TPPS_3$-S-Hex [**2I**] acquired on Bruker US 500 MHz system. ^{1}H NMR (500 MHz, DMSO-d_6) peak associated with $TPPS_3$-Hex found at at δ (ppm) 10.57 (s, 1H) while signal associated with carbamate nitrogen proton from $TPPS_3$-O-Hex [**2J**] is found at δ (ppm) 10.05 (s, 1H).